AD-A092 316 OHIO STATE UNIV COLUMBUS ELECTROSCIENCE LAB F/G 20/14
AIRBORNE ANTENNA PATTERN CODE USER'S MANUAL.(U)
SEP 80 W D BURNSIDE, T CHU F30602-79-C-0068
UNCLASSIFIED ESL-711679-2 RADC-TR-80-302 NL

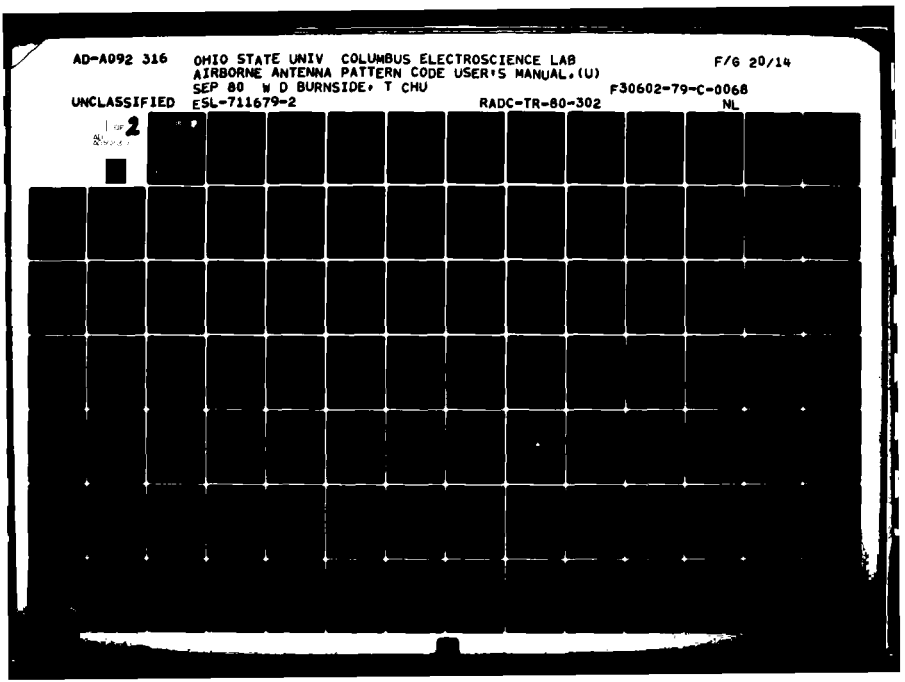

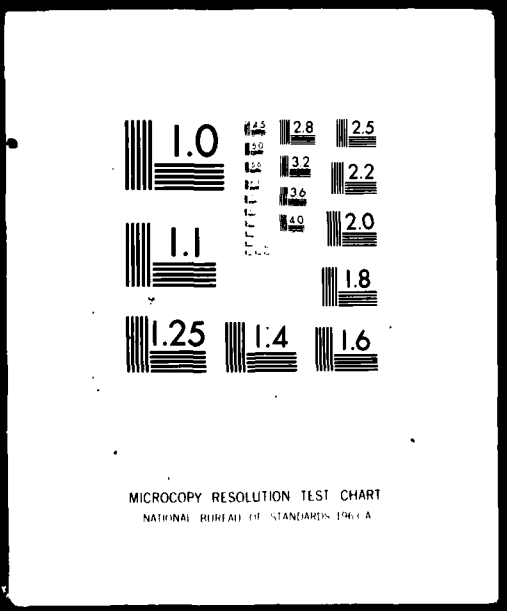

RADC-TR-80-302
Interim Report
September 1980

LEVEL II

12

AIRBORNE ANTENNA PATTERN CODE USER'S MANUAL

The Ohio State University ElectroScience Laboratory

W. D. Burnside
T. Chu

ROME AIR DEVELOPMENT CENTER
Air Force Systems Command
Griffiss Air Force Base, New York 13441

This report has been reviewed by the RADC Public Affairs Office (PA) and is releasable to the National Technical Information Service (NTIS). At NTIS it will be releasable to the general public, including foreign nations.

RADC-TR-80-302 has been reviewed and is approved for publication.

APPROVED: Stuart H. Talbot

STUART H. TALBOT
Project Engineer

APPROVED: Hugh M Miller

HUGH M. MILLER, Colonel, USAF
Chief, Communications and Control Division

FOR THE COMMANDER: John P. Huss

JOHN P. HUSS
Acting Chief, Plans Office

SUBJECT TO EXPORT CONTROL LAWS

This document contains information for manufacturing or using munitions of war. Export of the information contained herein, or release to foreign nationals within the United States, without first obtaining an export license, is a violation of the International Traffic in Arms Regulations. Such violation is subject to a penalty of up to 2 years imprisonment and a fine of $100,000 under 22 U.S.C 2778.

Include this notice with any reproduced portion of this document.

If your address has changed or if you wish to be removed from the RADC mailing list, or if the addressee is no longer employed by your organization, please notify RADC (DCCR) Griffiss AFB NY 13441. This will assist us in maintaining a current mailing list.

Do not return this copy. Retain or destroy.

UNCLASSIFIED

SECURITY CLASSIFICATION OF THIS PAGE (When Data Entered)

REPORT DOCUMENTATION PAGE

READ INSTRUCTIONS BEFORE COMPLETING FORM

1. REPORT NUMBER: RADC-TR-80-302	2. GOVT ACCESSION NO.: AD-A092 316
3. RECIPIENT'S CATALOG NUMBER:	
4. TITLE (and Subtitle): AIRBORNE ANTENNA PATTERN CODE USER'S MANUAL	5. TYPE OF REPORT & PERIOD COVERED: Interim Report
	6. PERFORMING ORG. REPORT NUMBER: ESL-711679-2
7. AUTHOR(s): W. D. Burnside T. Chu	8. CONTRACT OR GRANT NUMBER(s): F30602-79-C-0068
9. PERFORMING ORGANIZATION NAME AND ADDRESS: The Ohio State University ElectroScience Laboratory, Department of Electrical Engineering, Columbus OH 43212	10. PROGRAM ELEMENT, PROJECT, TASK AREA & WORK UNIT NUMBERS: 62702F 45196308
11. CONTROLLING OFFICE NAME AND ADDRESS: Rome Air Development Center (DCCR) Griffiss AFB NY 13441	12. REPORT DATE: September 1980
	13. NUMBER OF PAGES: 108
14. MONITORING AGENCY NAME & ADDRESS (if different from Controlling Office): Same	15. SECURITY CLASS. (of this report): UNCLASSIFIED
	15a. DECLASSIFICATION/DOWNGRADING SCHEDULE: N/A

16. DISTRIBUTION STATEMENT (of this Report)

Approved for public release; distribution unlimited.

17. DISTRIBUTION STATEMENT (of the abstract entered in Block 20, if different from Report)

Same

18. SUPPLEMENTARY NOTES

RADC Project Engineer: Stuart H. Talbot (DCCR)

19. KEY WORDS (Continue on reverse side if necessary and identify by block number)

High frequency analysis
Geometrical theory of diffraction
Electromagnetic radiation
Cylinder structures
Airborne antenna patterns
Experimental verification
Computer code manual
Roll plane model
Elevation plane model

20. ABSTRACT (Continue on reverse side if necessary and identify by block number)

This report describes the use of a computer code to analyze antenna mounted on aircraft fuselage. Ram jet configurations can be handled as a special case by this code. The pattern can be taken in terms of an arbitrary conical cut. The organization of the code, definition of input and output data, multiple finite plate approach to simulate the structures on aircraft and various examples are presented. The analysis is based on the geometrical theory of diffraction, and various computed

DD FORM 1 JAN 73 1473 EDITION OF 1 NOV 65 IS OBSOLETE

UNCLASSIFIED (Cont'd)

SECURITY CLASSIFICATION OF THIS PAGE (When Data Entered)

Item 20 (Cont'd)

patterns are compared with experimental results.

ACKNOWLEDGMENT

Since this user's manual will be used on two contracts (N62269-78-C-0379 with NADC and F30602-79-C-0068 with RADC), except for the examples used to exercise the code, it was decided to share the expense of this report between the two projects. This allows us to put the examples appropriate to both contracts in a single report which makes it more versatile for all concerned.

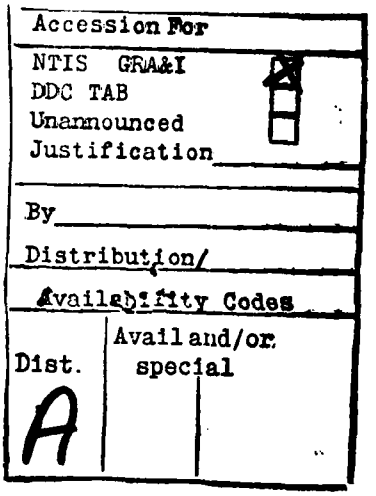

TABLE OF CONTENTS

I. INTRODUCTION

In order to investigate the radiation patterns of antennas in a complex environment such as on an aircraft the following Fortran IV computer code has been developed. The computer code is used to compute the near zone radiated fields for antennas mounted on an elliptic cylinder and in the presence of a set of finite flat plates. The analysis applied in the development of the code is based on the geometrical theory of diffraction (GTD)[1,2].

The code allows the user to simulate a wide variety of complex electromagnetic radiation problems using the cylinder/plates model. For example, the elliptic cylinder can be used to simulate the fuselage or jet intake of an aircraft; whereas, the plates are used to represent the wings, stabilizers, stores, etc. Alternatively, the antenna could be mounted directly on a ship mast. In this case the mast could be approximated by the elliptic cylinder with the other ship structures simulated by flat plates. Note that the plates can be attached to the cylinder and/or to other plates. In fact, the plates can be connected together to form a box. In terms of special sections in the input data set, antennas mounted on missile configurations will be discussed. The T-tail effect and mutual coupling effect of antenna arrays mounted on nearly flat fuselage are also illustrated by examples.

As with any ray optical solution such as this GTD code, there is a limit to the number of interactions included in the field computation. In this case, the code includes the source, reflected, diffracted, reflected/reflected, reflected/diffracted, and diffracted/reflected. In addition, the user can request the code to add various diffracted/diffracted terms. This implies that the code can handle structures for which the energy does not significantly bounce back-and-forth across the target. In any event, the code automatically shadows all terms, such that if a higher-order interaction should have been included the resulting pattern will contain a discontinuity. These higher-order

terms are normally negligible and can only affect the pattern in rather small sectors. However, if they are significant in some region, the amplitude of the jump is associated with the radiation level of the missing higher-order term. Consequently when the solution fails because of a lack of higher-order terms, it tends to indicate its failure.

The code has the flexibility to handle arbitrary pattern cuts. In addition, an arbitrary antenna type can be analyzed provided the current distribution across the aperture is known. This is done by approximating the distribution by a set of magnetic current elements mounted on the cylinder surface. The magnetic current elements have a cosine distribution along the magnetic current direction and are uniform in the orthogonal direction. The code can, also, treat a monopole or monopole arrays; however, length of each element cannot exceed a quarter wavelength.

The mutual coupling effect for monopole arrays mounted on fuselage can be handled by thin-wire theory[10], if the region near the array is nearly flat. For engineering purposes, image theory can be applied to calculate the relative current distributions as equivalent dipole arrays. The relative current value on each dipole is then taken to be part of the input data for each monopole source specification. The final pattern is the superposition of the contributions from each individual monopole.

The limitations associated with the computer code result from the basic nature of the analyses. The solution is derived using the GTD, which is a high frequency approach. In terms of the scattering from plate structures this means that each plate should have edges at least a wavelength long. In terms of the cylinder structure its major and minor radii should be at least a wavelength in extent. In addition, each antenna element should be at least a wavelength from all edges. In many cases, the wavelength limit can be reduced to a quarter wavelength for engineering purposes.

The present form of the computer code is not large in terms of computer storage and executes a pattern for a single antenna element very efficiently. The present code requires approximately 200 K bytes of storage. It will run a pattern cut of 360 points for a simple aircraft model with one antenna element in approximately 30 seconds on a CDC-6600 computer.

This user's manual is designed to give an overall view of the operation of the computer code, to instruct a user in how to use it to model structures, and to show the validity of the code by comparing various computed results against measured data whenever available. Section II describes an overall view of the organization of the program. The definition of the input is given in Section III. How to apply the capabilities of this input data to a practical structure is briefly discussed in Section IV. This includes a clarification of the subtle points of interpreting the input data. The representation of the output is discussed in Section V. Various sample problems are presented in Section VI and VII to illustrate the operation, versatility, and validity of the code.

II. PRINCIPLES OF OPERATION

The analytical modeling of complex scattering shapes in order to predict the radiation patterns of antennas has been accomplished by the use of the Geometrical Theory of Diffraction (GTD)[1,2]. This is a high frequency technique that allows a complicated structure to be approximated by basic shapes representing canonical problems in the GTD. These shapes include flat and curved wedges and convex curved surfaces. The GTD is a ray optical technique and it therefore allows one to gain some physical insight into the various scattering and diffraction mechanisms involved. Consequently, one is able to quickly seek out the dominant or significant scattering and diffraction mechanism for a given geometrical configuration. This, in turn, leads to an

accurate engineering solution to practical antenna problems. This approach has been used successfully in the past to model aircraft shapes[3,4,5,6] and ship-like structures[7,8,9].

This section briefly describes the basic operation of this code for the analysis of airborne antenna patterns. The present version of the code allows analysis of structures that can be modeled by concave flat plate structures, and an elliptic cylinder all of which are built up from the basic canonical structures. These shapes allow one to model a wide variety of structures in the UHF range and above where the scattering structures are large in terms of a wavelength. The general rule is that the lower frequency limit of this solution is dictated by the spacings between the various scattering centers and their overall size. In practice this means that the smallest dimensions should be on the order of a wavelength. This can often be relaxed to approximately a quarter-wavelength.

The positive time convention $e^{j\omega t}$ has been used in this scattering code. Also, the radiation patterns are assumed to be in the near field. All of the structures in this code are assumed to be perfectly conducting and the surrounding medium is free space.

As mentioned above, the GTD approach is ideal for a general high frequency study of aircraft antennas in that only the most basic structural features of an otherwise very complicated structure need to be modeled. This is because ray optical techniques are used to determine components of the field incident on and diffracted by various structures. Components of the diffracted fields are found using the GTD solutions in terms of the individual rays which are summed with the geometrical optics terms at the field point. The rays from a given scatterer tend to interact with other structures causing various higher-order terms. In this way one can trace out the various possible combinations of rays that interact between scatterers and determine and include only the dominant terms. Thus, one need only be concerned with the important scattering components and neglect all other higher-

order terms. This method leads to accurate and efficient computer codes that can be systematically written and tested.

Complex problems are built up from similar components in terms of a modular computer code. This modular approach is illustrated in the block diagram of the main program shown in Table I. The code is broken up into many subroutines that represent different scattered field components, ray tracing methods, and shadowing routines. As can be seen from the flow chart, the code is structured so that all of one type of scattered field is computed at one time for the complete pattern cut so that the amount of core swapping is minimized thereby reducing overlaying and increasing efficiency. This also is an important feature that allows the code to be used on small computers that are not large enough to accept the entire code at one time. The code can be broken into smaller overlay segments which will individually fit in the machine. The results are, then, superimposed in the main program as the various segments are executed.

The subroutines for each of the scattered field components are all structured in the same basic way. First, the ray path is traced backward from the chosen observation point to a particular scatterer and subsequently to the source using either the laws of reflection or diffraction. Each ray path, assuming one is possible, is then checked to see if it is shadowed by any structure along the complete ray path. If it is shadowed the field is not computed and the code proceeds to the nex atterer or observation point. If the path is not interrupted the scattered field is computed using the appropriate GTD solutions. The fields are then superimposed in the main program. This shadowing process is often speeded up by making various decisions based on bounds associated with the geometry of the structure. This type of knowledge is used wherever possible.

The shadowing of rays is a very important part of the GTD Scattering code. It is obvious that this approach should lead to various discontinuities in the resulting pattern. However, the GTD diffraction coefficients are designed to smooth out the discontinuities in the fields such that a continuous field is obtained. When a scattered field is not included in the result, the lack of its presence is apparent. This can be used to advantage in analyzing complicated problems. Obviously in a complex problem not all the possible scattered fields can be included. In the GTD code the importance of the neglected terms are determined by the size of the so-called gliches or jumps in the pattern trace. If the gliches are small no additional terms are needed for a good engineering solution. If the gliches are large it may be necessary to include more terms in the solution. In any case the user has a gauge with which he can examine the accuracy of the results and is not falsely led into believing a result is correct when in fact there could be an error.

The brief discussion of the operation of this code given above should help the user get a feel for the overall code so he might better understand the code's capabilities and interpret its results. The code is designed, however, so that the general user can run the code without knowing all the details of its operation. Yet, he must become familiar with the input/output details which will be discussed in the next three sections.

TABLE I

BLOCK DIAGRAM OF THE MAIN PROGRAM

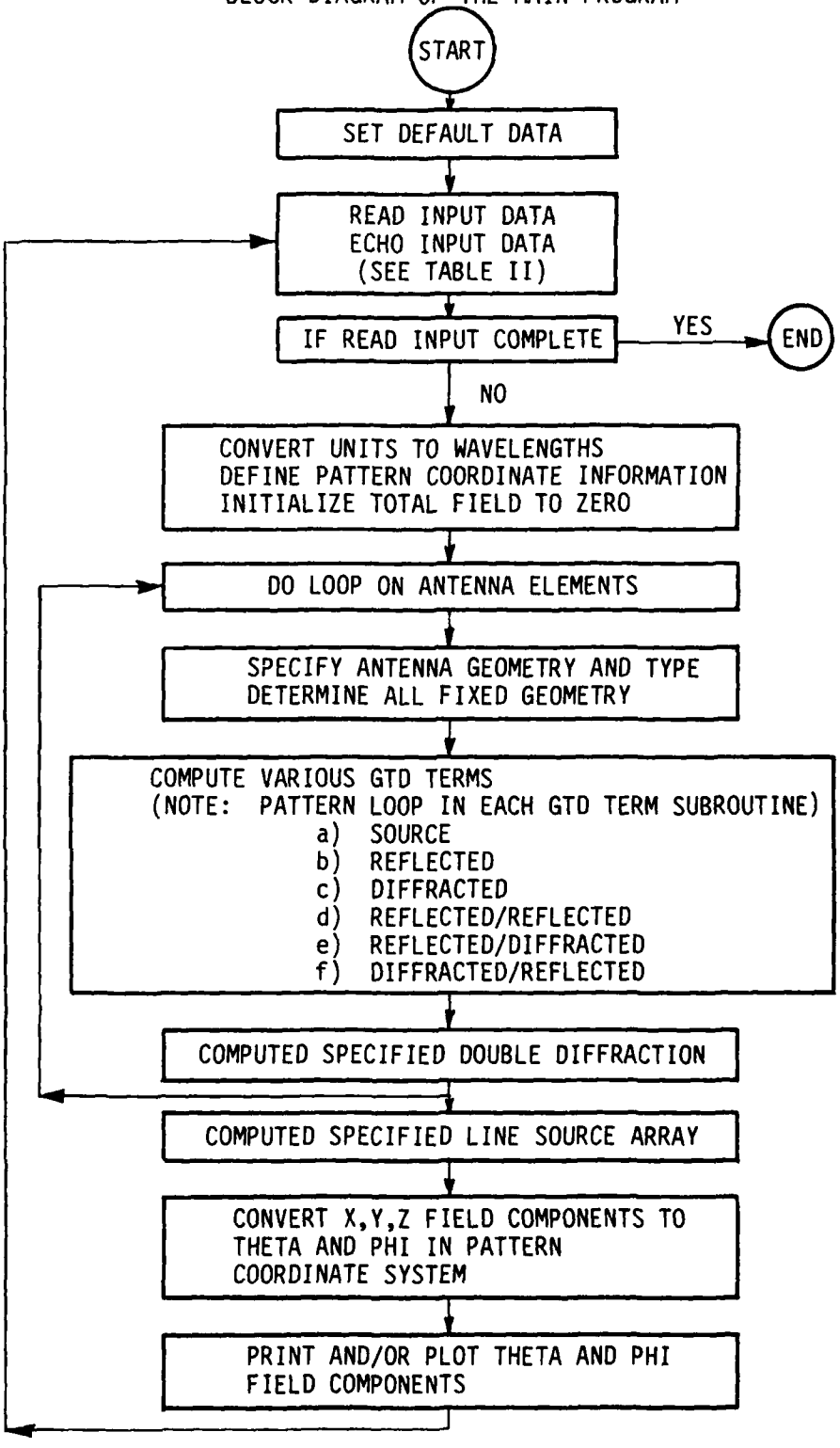

III. DEFINITION OF INPUT DATA

The method used to input data into the computer code is presently based on a command word system. This is especially convenient when more than one problem is to be analyzed during a computer run. The code stores the previous input data such that one need only input that data which needs to be changed from the previous execution. Also, there is a default list of data so for any given problem the amount of data that needs to be input has been shortened. The organization of the input data is illustrated in Table II.

In this system, all linear dimensions may be specified in either meters, inches, or feet and all angular dimensions are in degrees. All the dimensions are eventually referred to a fixed cartesian coordinate system used as a common reference for the source and structures. There is, however, a geometry definition coordinate system that may be defined using the "RT:" command. This command enables the user to rotate and translate the coordinate system to be used to input any selected data set into the best coordinate system for that particular geometry. Once the "RT:" command is used all the input following the command will be in that rotated and translated coordinate system until the "RT:" command is called again. The only exception to this is that the cylinder will always be in the reference coordinate system. See below for more details. There is also a separate coordinate system that can be used to define a pattern coordinate system. This is discussed in more detail in Section III-C in terms of the "PD:" command.

It is felt that the maximum usefulness of the computer code can be achieved using it on an interactive computer system. As a consequence, all input data are defined in free format such that the operator need only put commas between the various inputs. This allows the user on an interactive terminal to avoid the problems associated with typing in the field length associated with a fixed format. This method also

is useful on batch processing computers. Note that all read statements are made on unit #5, i.e., READ (5,*), where the "*" symbol refers to free format. Other machines, however, may have different symbols representing free format.

In all the following discussions associated with logical variables a "T" will imply true, and an "F" will imply false. The complete words true and false need not be input since most compilers just consider the first character in determining the state of the logical variable.

The following list defines in detail each command word and the variables associated with them. Section VI will give specific examples using this input method. Note that the program halts execution by sensing the end-of-file mark associated with the input data set.

TABLE II

BLOCK DIAGRAM OF THE INPUT DATA
ORGANIZATION FOR THE COMPUTER CODE

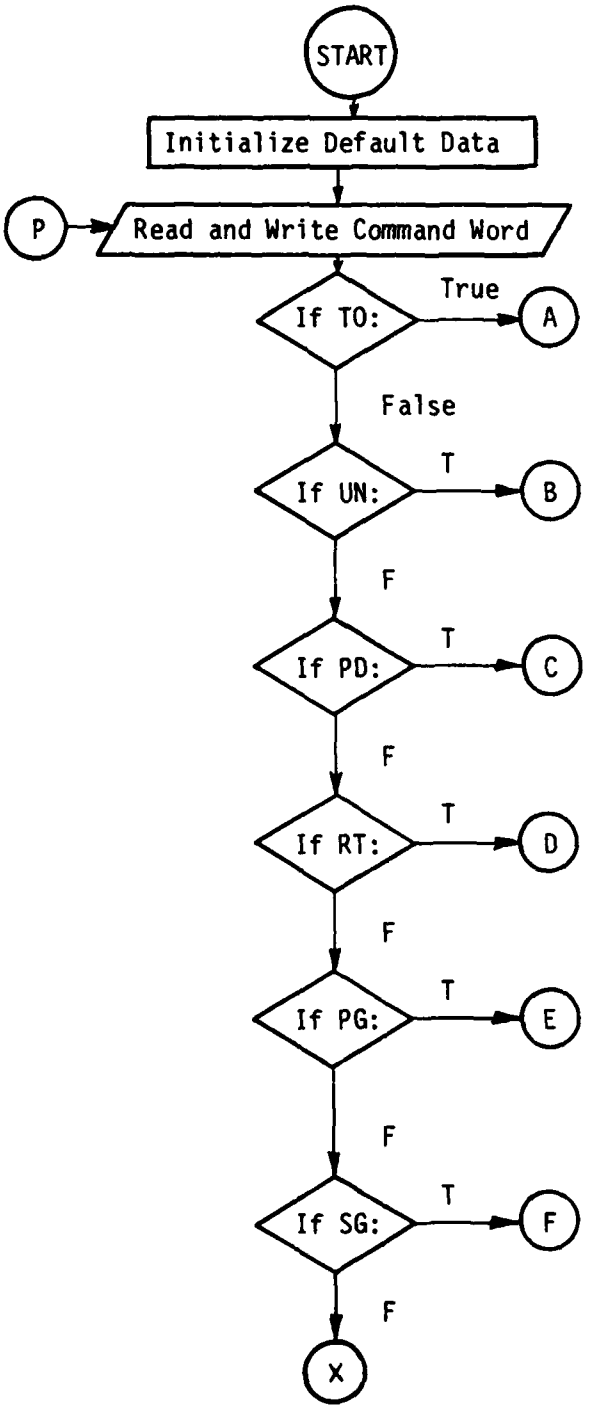

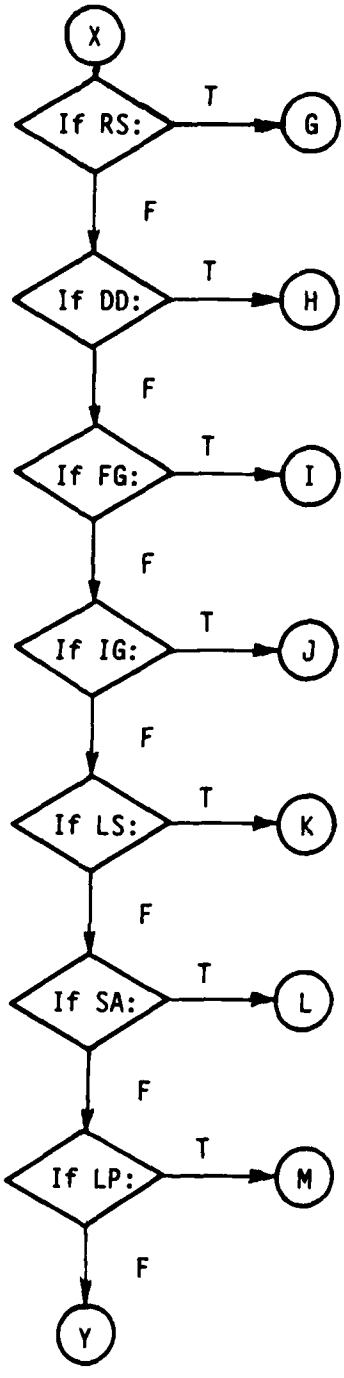
X
If RS:
T
G
F
If DD:
T
H
F
If FG:
T
I
F
If IG:
T
J
F
If LS:
T
K
F
If SA:
T
L
F
If LP:
T
M
F
Y

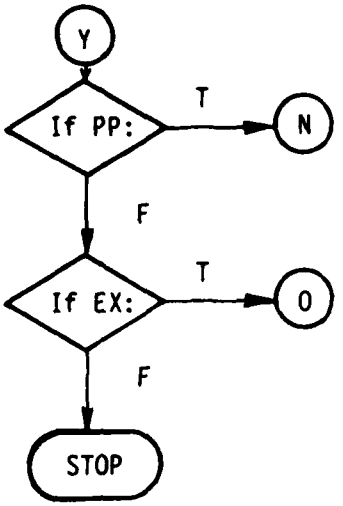
Y
If PP:
T
N
F
If EX:
T
O
F
STOP

A. Command TO:

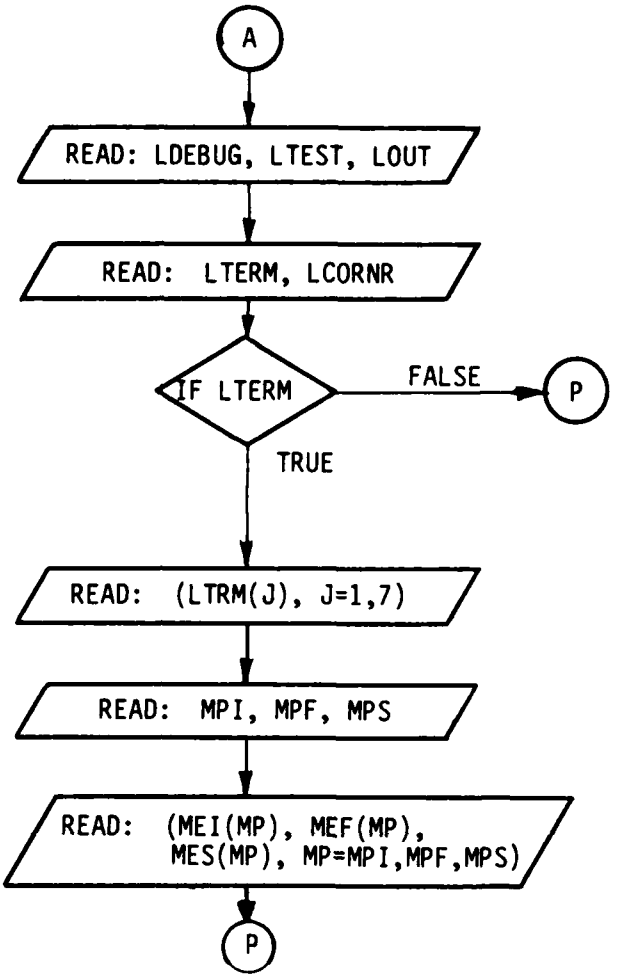

This command enables the user to obtain an extended output of various intermediate quantities in the computer code. This is useful in testing the program or in analyzing the contributions from various scattering mechanisms in terms of the total solution.

1. READ: LDEBUG, LTEST, LOUT

a) LDEBUG: This is a logical variable defined by T or F. It is used to debug the program if errors are suspected within the program. If set true, the program prints out data on unit #6 associated with each of its internal operations. These data can, then, be compared with previous data which are known to be correct. It is, also,

used to insure initial operation of the code. Only one pattern angle is considered. (normally set false)

b) LTEST: This a logical variable defined by T or F. It is used to test the input/output associated with each subroutine. The data written out on unit #6 are associated with the data in the window of the subroutine. They are written out each time the subroutine is called. It is, also, used to insure initial operation of the code. Only one pattern angle is considered. (normally set false)

c) LOUT: This is a logical variable defined by T or F. It is used to output data on unit #6 associated with the main program. It,also, is used to initially insure proper operation. It can be used to examine the various components of the pattern. (normally set false)

2. READ: LTERM, LCORNR

a) LTERM: This is a logical variable defined by T or F. It is used to tell the code whether or not individual terms are desired during the computation. (normally set false)

b) LCORNR: This is a logical variable defined by T or F. It is used to tell the code whether or not corner diffraction is desired during the computation. (normally set true)

3. READ: (LTRM(J), J=1,7)

a) LTRM(J): These are logical variables defined by T or F to specify a set of individual scattering components that are to be inlcuded in the scattered field computation. The components are defined by the following number designations.

J=1: source field
J=2: single reflected field
J=3: single diffracted field
J=4: double reflected field
J=5: reflected-diffracted field
J=6: diffracted-reflected field
J=7: double diffracted field

4. READ: MPI, MPF, MPS

a) MPI,MPF,MPS: These are integer variables to define plates used in computation, where
MPI = initial plate
MPF = final plate
MPS = increment in plates going from initial to final plate

Note: MPI=1, MPF=3, and MPS=2 implies plates 1 and 3 are included in the computation.

5. READ: (MEI(MP), MEF(MP), MES(MP), MP=MPI,MPF,MPS)

a) MEI(MP),MEF(MP),MES(MP): These are dimensioned integer variables to define the edges on the MPth plate used in the computation, where

MEI(MP) = initial edge on plate MP

MEF(MP) = final edge on plate MP

MES(MP) = increment in edges going from MEI(MP) to MEF(MP)

B. COMMAND UN:

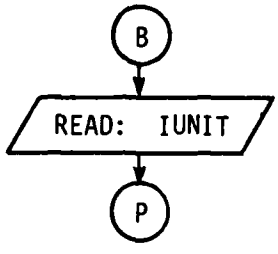

This command enables the user to specify the units used for all following linear dimensions in input data list.

1. READ: IUNIT

A) IUNIT: This is an integer variable that defines the units. If

$$\text{IUNIT} = \begin{cases} 1 \rightarrow \text{meters} \\ 2 \rightarrow \text{feet} \\ 3 \rightarrow \text{inches} \end{cases}$$

C. COMMAND PD:

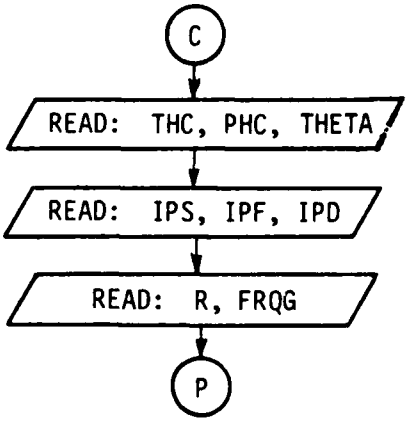

This command enables the user to define the pattern axis of rotation, the angular range, range from origin to receiver, and the frequency for the desired conical pattern.

This set of data is associated with the conical pattern desired during execution of the program. The pattern axis is defined by the spherical angles (THC, PHC) as illustrated in Figure 1. These angles define a radial vector direction which points in the direction of the pattern axis of rotation. These angles actually set-up a new coordinate system in relation to the original fixed coordinates. The new cartesian coordinates defined by the subscript "p" are found by first rotating about the z-axis the angle PHC and, then, about the y_p-axis the angle THC. The pattern is, then, taken in the "p" coordinate system in terms of spherical angles. The theta angle of the pattern taken about the z_p-axis is defined by THETA. The phi angle is defined by the next read statement. In the present form the program will, then, compute any conical pattern in that THETA is used as the conical pattern angle about the z_p-axis for the complete pattern calculation.

As an aid in setting up the "p" coordinate system the following set of equations give the relationships between (THC, PHC) and the x_p, y_p, z_p-axes. Note that the "p" axes are defined as radial vector directions in a spherical coordinate system:

$$\hat{x}_p = \cos(PHC)\sin(THC+90^o)\hat{x}+\sin(PHC)\sin(THC+90^o)\hat{y}+\cos(THC+90^o)\hat{z}$$

$$\hat{y}_p = \cos(PHC+90^o)\hat{x}+\sin(PHC+90^o)\hat{y}$$

$$\hat{z}_p = \cos(PHC)\sin(THC)\hat{x}+\sin(PHC)\sin(THC)\hat{y}+\cos(THC)\hat{z}$$

where $0 \leq THC \leq 180^o$ and $0 \leq PHC \leq 360^o$. In its present form it should be noted that the user may not be able to define the x_p-axis at the starting location that he desired. In addition, the rotation of the pattern may be in the opposite sense using this approach. However, these problems can be easily overcome with properly written plot routines.

1. READ: THC, PHC, THETA

   a) THC,PHC: These are real variables. They are input in degrees and define the axis of rotation about which a conical pattern will be computed.

   b) THETA: This is a real variable. It is input in degrees and used to define the conical angle about the axis of rotation for the desired pattern.

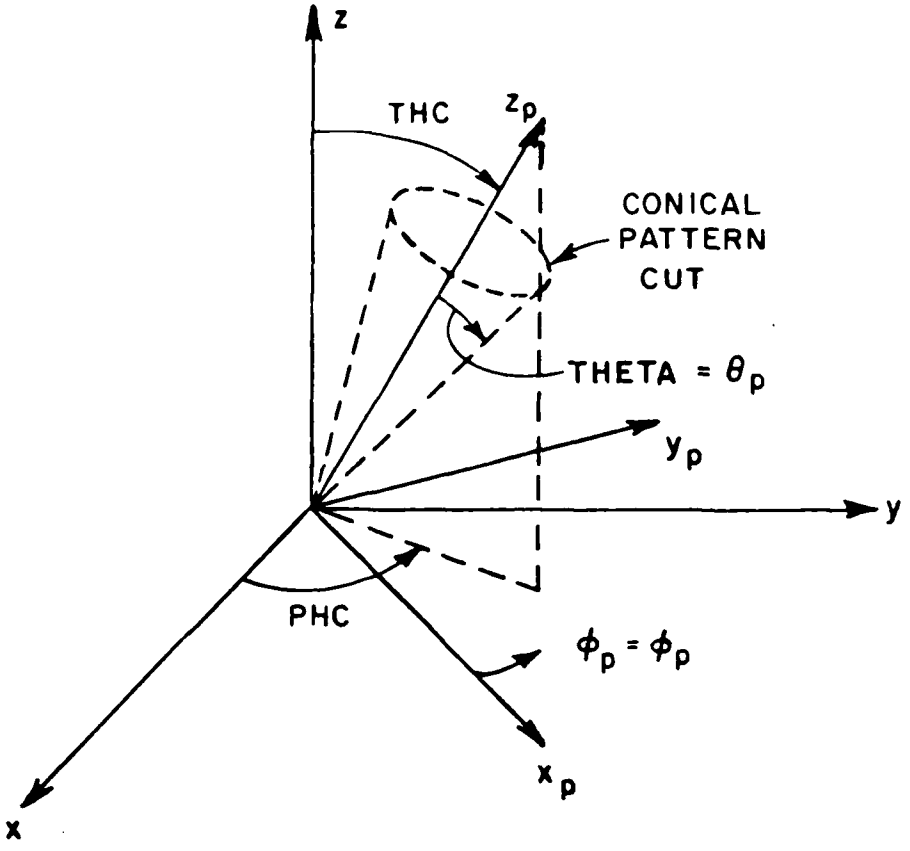

Figure 1. Definition of pattern axis.

2. READ: IPS, IPF, IPD

a) IPS,IPF,IPD: These are integer variables used to define angles in degrees. They are, respectively, the beginning, ending, and incremental values of the phi pattern angle.

As a result of the input given by the two previous read statements, the operator has completely defined the desired conical pattern to be computed during execution of the program.

3. READ: R, FRQG

a) R: This is a real variable which is used to define the range in linear units from the origin to the reciever. If the pattern is to be taken in the far field of the structure, one must be very careful how he inputs the range. This point is discussed in detail in the next section.

b) FRQG: This is a real variable which is used to define the frequency in gigahertz.

D. COMMAND RT:

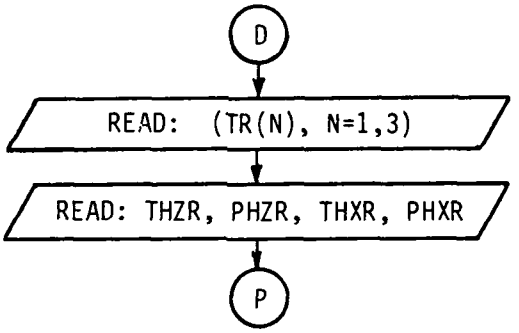

This command enables the user to translate and/or rotate the coordinate system used to define the input data in order to simplify the specification of the plate geometry. The geometry is illustrated in Figure 2.

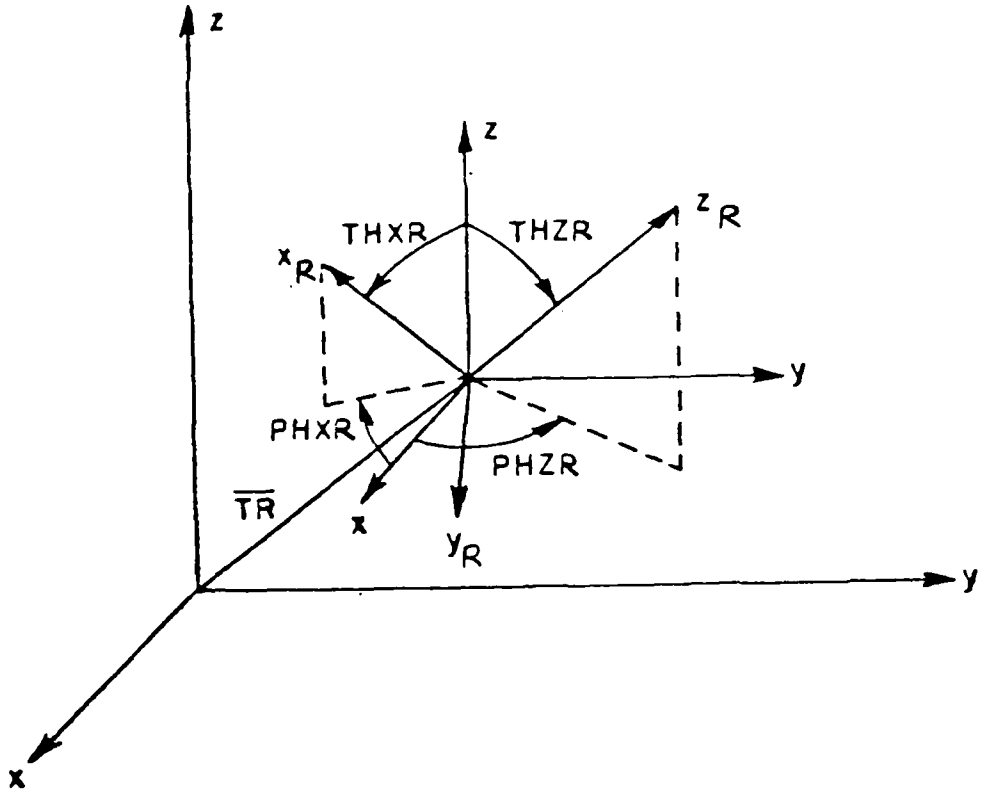

Figure 2. Definition of rotate-translate coordinate system geometry.

1. READ: (TR(N), N=1,3)

   a) TR(N): This is a dimensioned real variable. It is used to specify the origin of the new coordinate system to be used to input the data for the plate structures. It is input on a single line with the real numbers being the x,y,z coordinates of the new origin which corresponds to N=1,2,3 respectively.

2. READ: THZR, PHZR, THXR, PHXR

a) THZR,PHZR: These are real variables. They are input in degrees as spherical angles that define the z_R-axis of the new coordinate system as if it was a radial vector in the reference coordinate system.

b) THXR,PHXR: These are real variables. They are input in degrees as spherical angles that define the x_R-axis of the new coordinate system as if it was a radial vector in the reference coordinate system.

The new x_R-axis and z_R-axis must be defined orthogonal to each other. The new y_R-axis is found from the cross product of the x_R and z_R axes. All the subsequent inputs will be made relative to this new coordinate system, which is shown as (x_R, y_R, z_R) unless command "RT:" is called again and redefined.

E. COMMAND PG:

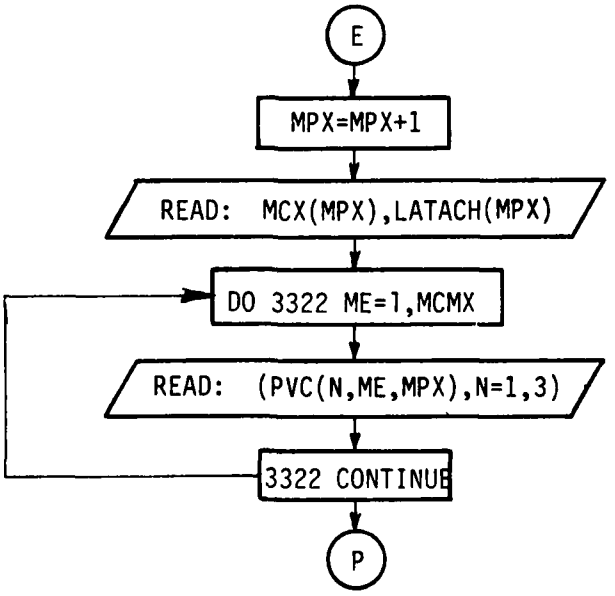

This command enables the user to define the geometry of the flat plate structures to be considered. The geometry is illustrated in Figure 3. It can be called repeatedly up to 25 times.

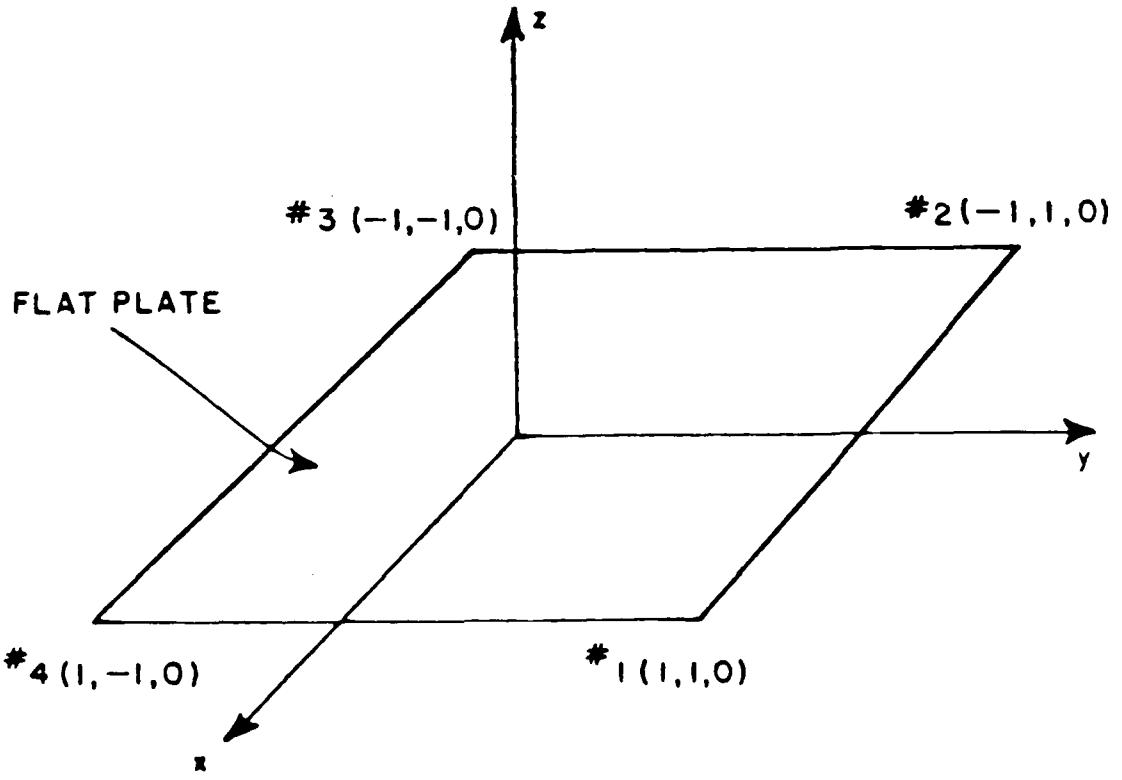

Figure 3. Definition of flat plate geometry.

1. READ: MCX(MPX), LATACH(MPX)

   a) MCX(MPX): This is a dimensioned integer variable. It is used to define the number of corners (or edges) on the MPXth plate. Presently, $1 \leq MCX(MPX) \leq 6$ with $1 \leq MPX \leq 25$

b) LATACH(MPX): This is a logical variable defined by T or F. It is used to indicate if the MPXth plate is attached to the fuselage (T) or not (F). Note that all attached plates should be defined within the first six plates. The first and last corners of attached plates should be specified on or near the fuselage.

2. READ: (PVC(N,ME,MPX),N=1,3)

As stated earlier the locations of the corners of the flat plates are input in terms of the x, y, z coordinates in the specified cartesian coordinate system.

a) PVC(N,ME,MPX): This is a triply dimensioned real variable. It is used to specify the location of the MEth corner of the MPXth plate. It is input on a single line with the real numbers being the x,y,z coordinates of the corner which correspond to N=1, 2,3, respectively, in the array. For example, the array will contain the following for plate #1 and corner #2 located at x=2., y=4., z=6.:

PVC(1,2,1) = 2.
PVC(2,2,1) = 4.
PVC(3,2,1) = 6.

This data is input as: 2.,4.,6.

Considering the flat plate structure given in Figure 3, the input data is given by

```
 1., 1., 0          : corner #1
-1., 1., 0.         : corner #2
-1.,-1., 0.         : corner #3      plate #1
 1.,-1., 0.         : corner #4
```

Presently: $1 \leq MPX \leq 25$

$1 \leq ME \leq 6$

$1 \leq N \leq 3$

(See Chapter IV for further details in defining the corner points.)

F. COMMAND SG:

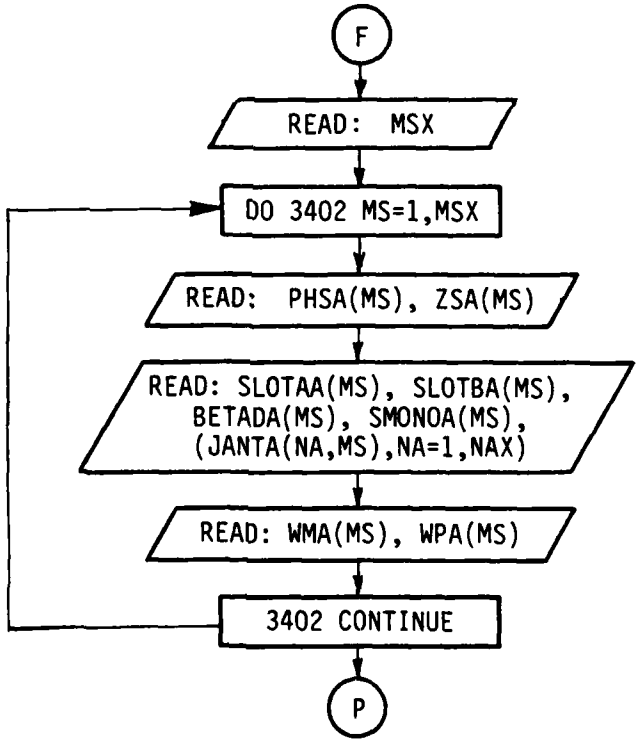

This command enables the user to specify the location and type of antenna to be used. The geometry is illustrated in Figure 4.

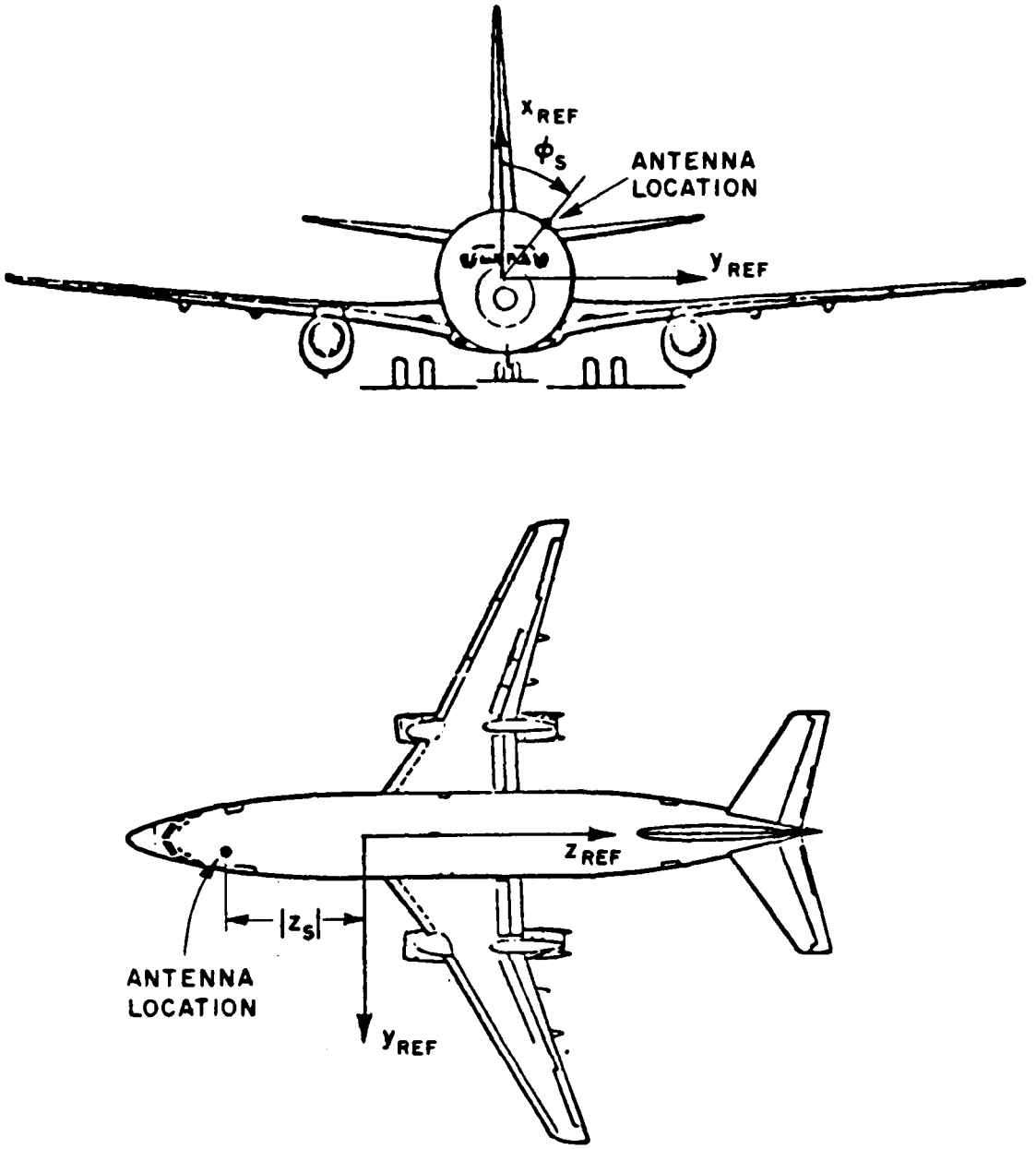

Figure 4. Definition of the source location for computer code. Note that PHSA = ϕ_s and ZSA = - $|Z_s|$ in the above drawings.

1. READ: MSX

   a) MSX: This is an integer variable which defines the maximum number of elemental radiators to be considered during execution of the program. Presently, $1 \leq MSX \leq 10$.

2. READ: PHSA(MS), ZSA(MS)

   a) PHSA(MS),ZSA(MS): These are real variables used to specify the phi-angle (in degrees) and z location of MSth antenna. (Refer to Figure 4) Note: $-90^{o} \leq PHSA \leq 90^{o}$.

3. READ: SLOTAA(MS), SLOTBA(MS), BETADA(MS), SMONOA(MS), (JANTA(NA,MS), NA=1,NAX)

   a) SLOTAA(MS), SLOTBA(MS): These are real variables used to specify the narrow (parallel with E field) and broad (perpendicular to E field) dimensions of the slot in wavelengths.

   b) BETADA(MS): This is a real variable used to specify the angle (in degrees) of the slot relative to the fuselage axis. If BETADA=0., then the slot is axial. If BETADA=90., then the slot is circumferential.

   c) SMONOA(MS): This is a real variable used to specify the length of monopole in wavelengths. Note that SMONOA should not exceed a quarter wavelength.

d) JANTA(1,MS): This is an integer variable used to specify the type of antenna considered in computation:

$$\text{JANTA} = \begin{cases} 1 \rightarrow \text{arbitrarily oriented slot} \\ 2 \rightarrow \text{circumferential slot} \\ 3 \rightarrow \text{radial monopole.} \end{cases}$$

4. READ: WMA(MS), WPA(MS)

a) WMA(MS), WPA(MS): These are real variables used to specify the magnitude and phase (in degrees) of excitation on the MSth antenna. If an array is used, then the excitation including the coupling effect on the radiators may be obtained using a thin-wire code as shown in the results section.

G. COMMAND RS:

This command enables the user to reset the input data to the default case. There is no input data associated with this command.

H. COMMAND DD:

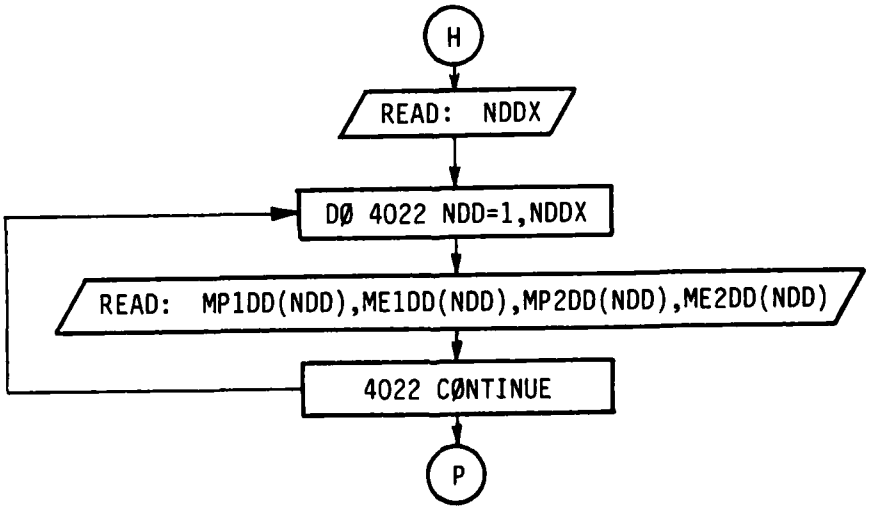

1. READ: NDDX

   a) NDDX: This is an integer variable that specifies the total number of double diffraction terms desired. Presently, $0 \leq NDDX \leq 10$.

2. READ: MP1DD(NDD), ME1DD(NDD), MP2DD(NDD), ME2DD(NDD)

   a) MP1DD(NDD), ME1DD(NDD): These are integer dimensioned arrays used to specify the plate and edge number from which the first diffraction occurs.

   b) MP2DD(NDD), ME2DD(NDD): These are integer dimensioned array used to specify the plate and edge number from which a second diffraction occurs.

I. COMMAND FG:

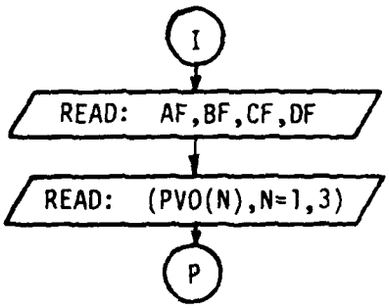

This command enables the user to model the fuselage by a composite elliptic cylinder.

1. READ: AF, BF, CF, DF

a) AF, BF, CF, DF: These are real variables that specify the semi-major and semi-minor axes of the composite elliptic cylinder used to model the fuselage as shown in Figure 5. Note how this figure compared with Figure 4.

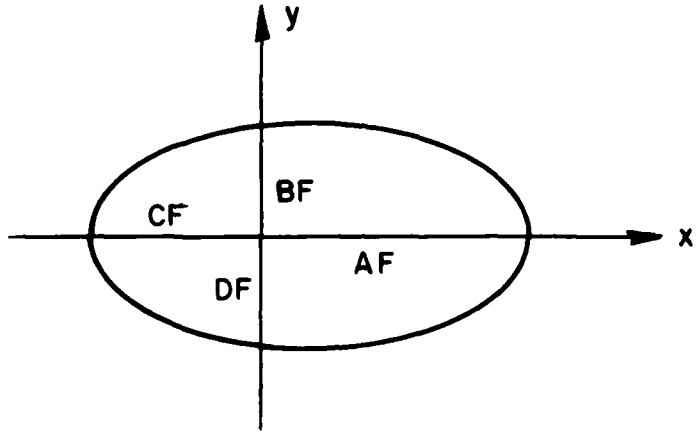

Figure 5. Definition of fuselage geometry.

2. READ: (PVO(N), N=1,3)

(a) PVO(N); This is a real dimensioned array that defines the location of the origin about which the pattern is taken, i.e., PVO(N) = (x,y,z). Note that the conical pattern will be taken about this origin.

J. COMMAND IG:

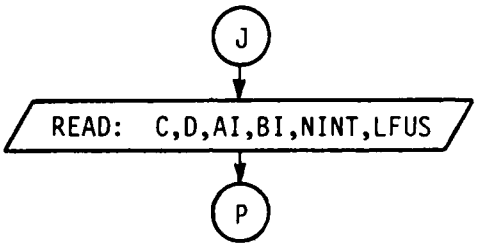

This command enables the user to define the jet intake geometry. The geometry is illustrated in Figure 6.

1. READ: C,D,AI,BI,NINT,LFUS

a) C: This is a real variable which defines the radius of the fuselage.

b) D: This is a real variable which defines the radial distance from the fuselage origin to the intake center.

c) AI,BI: These are real variables that define the semi-major and semi-minor dimensions of the jet intakes.

d) NINT: This is an integer variable that defines the number of jet intakes used in computation. It is assumed that the intakes are uniformly positioned around the fuselage.

e) LFUS: This is a logical variable defined by T or F to specify whether the antenna system is mounted on the fuselage (T) or intake (F).

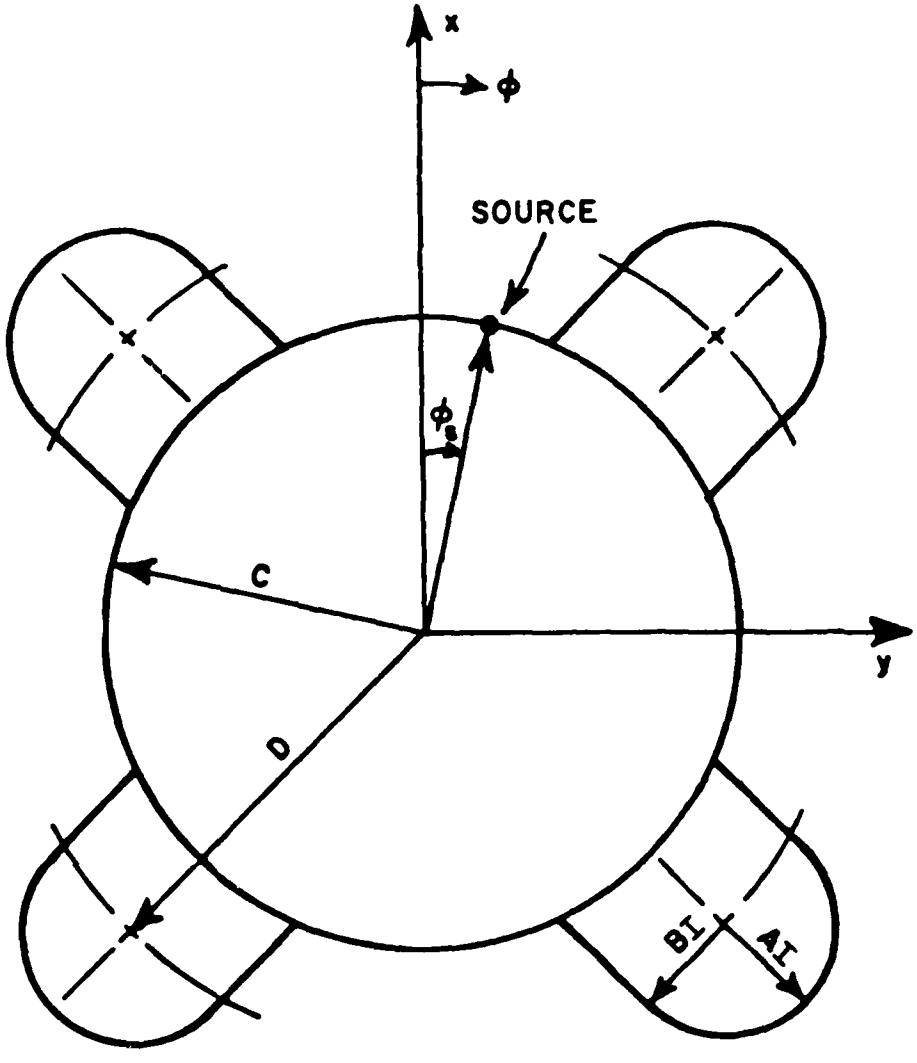

Figure 6. Definition of intake geometry.

K. COMMAND LS:

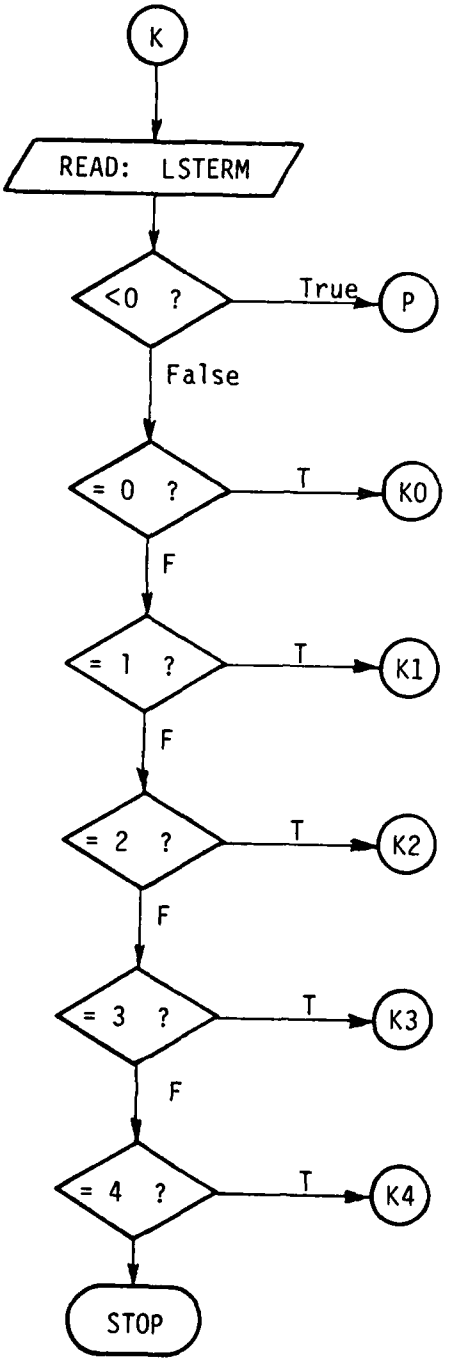
K
READ: LSTERM
<0 ?
True
P
False
= 0 ?
T
K0
F
= 1 ?
T
K1
F
= 2 ?
T
K2
F
= 3 ?
T
K3
F
= 4 ?
T
K4
STOP

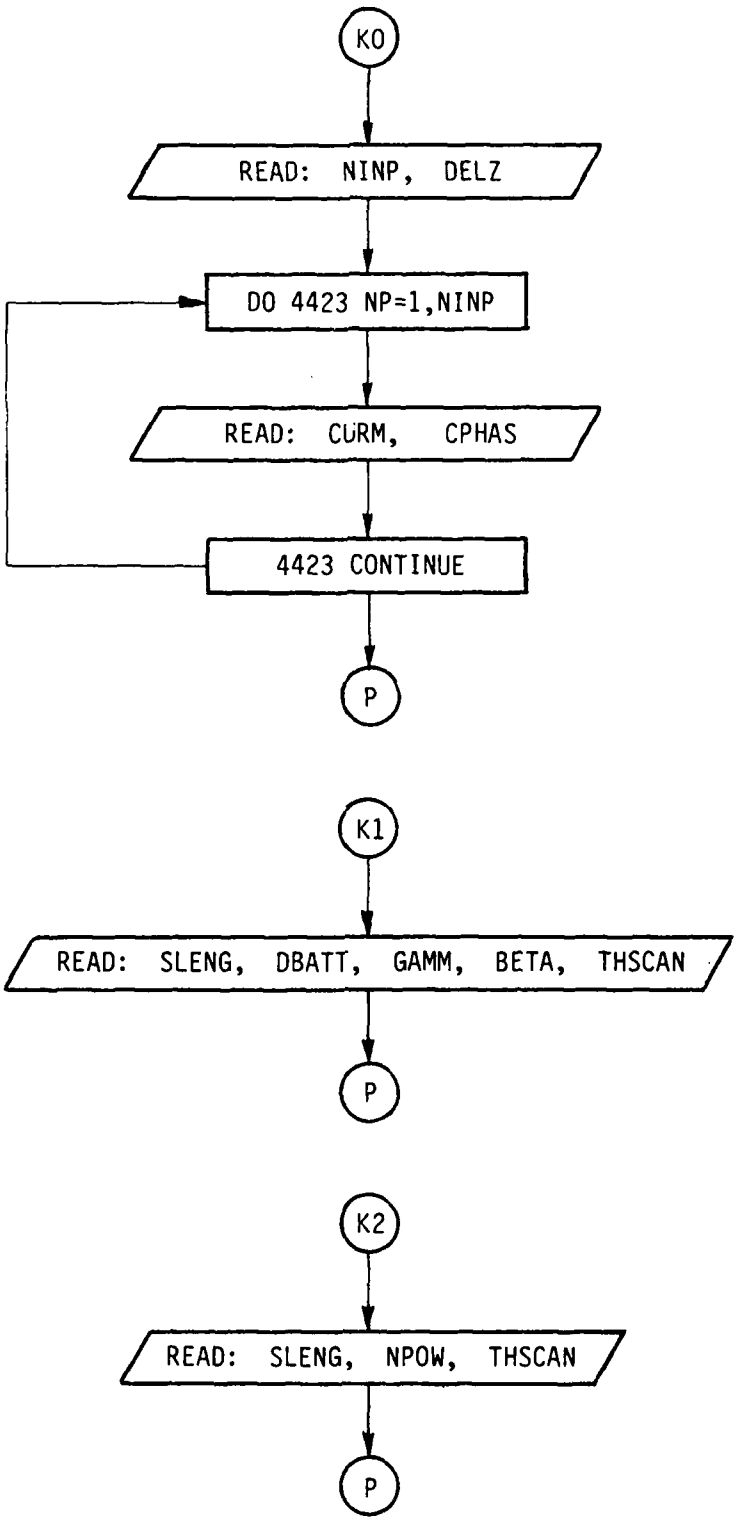
KO
READ: NINP, DELZ
DO 4423 NP=1,NINP
READ: CURM, CPHAS
4423 CONTINUE
P
K1
READ: SLENG, DBATT, GAMM, BETA, THSCAN
P
K2
READ: SLENG, NPOW, THSCAN
P

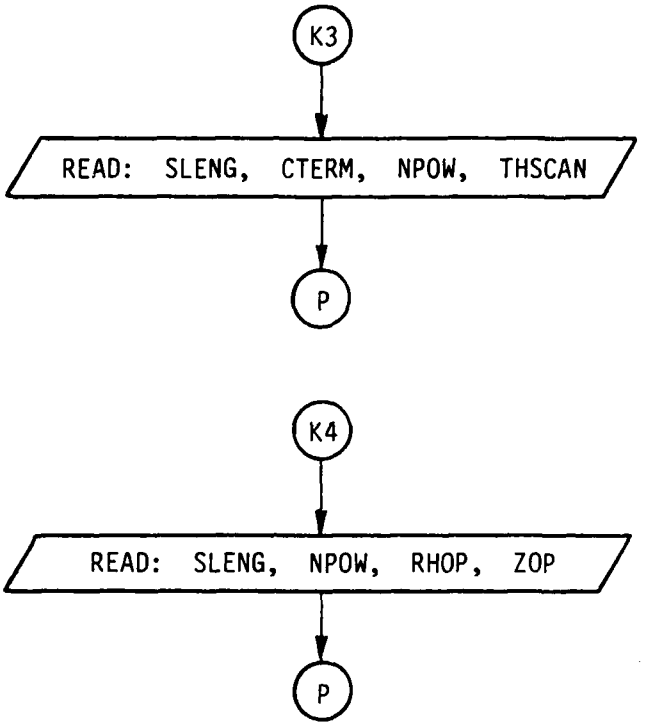
K3
READ: SLENG, CTERM, NPOW, THSCAN
P
K4
READ: SLENG, NPOW, RHOP, ZOP
P

This command enables the user to specify a line source distribution along the z-axis. It is used in an array pattern multiplication analysis. This command applies only when one has a uniform geometry along the axis of the fuselage.

1. READ: LSTERM

a) LSTERM: This is an integer variable that indicates the type of line source distribution treated. The current distribution and, therefore, the following inputs vary according to the following table.

LSTERM=0: $I(z) = \sum_{N=1}^{NINP} |I|_N \, e^{j\phi_N} \, \delta(z-(N-\frac{1}{2})\Delta z)$

2. READ: NINP,DELZ

3. READ: CURM,CPHAS

LSTERM=1: $I(z) = \left[e^{-\alpha z} + \Gamma e^{-j\beta} e^{-\alpha(2L-z)}\right] e^{-jkz\cos\theta_s}$

2. READ: SLENG,DBATT,GAMM,BETA,THSCAN

LSTERM=2: $I(z) = \left\{1 - \left[\frac{2(z-L/2)}{L}\right]^2\right\}^N e^{-jkz\cos\theta_s}$

2: READ: SLENG, NPOW,THSCAN

LSTERM=3: $I(z) = \left[\left(\cos\frac{\pi z}{L}\right)^N + C\right] e^{-jkz\cos\theta_s}$

2: READ: SLENG,CTERM,NPOW,THSCAN

LSTERM=4: $I(z) = \left(\cos\frac{\pi z}{L}\right)^N e^{-jk(\rho-\rho_o)}$

where $\rho = \sqrt{\rho_o^2+(z-z_o)^2}$

2. READ: SLENG, NPOW, RHOP, ZOP

The input data is interpreted as follows.

a) NINP: This is an integer variable that defines the number of current samples.

b) DELZ: This is a real variable (Δz) that defines the current sample spacing in wavelengths.

c) CURM, CPHAS: These are real variables that define the magnitude ($|I|_N$) and phase (ϕ_N) of the current elements.

d) SLENG: This is a real variable (L) that defines the length of the linear array, in wavelengths.

e) DBATT: This is a real variable that defines the attenuation (in dB) along the total length (SLENG) of the array. Note that α is related to DBATT.

f) GAMM, BETA: These are real variables (Γ and β) that define the magnitude and phase (in degrees) of the reflection coefficient at the end of the traveling wave antenna (LSTERM=1).

g) THSCAN: This is a real variable that defines the scan angle (in degrees) of the array.

h) NPOW: This is an integer variable (N) that defines the exponent in the previous equations.

i) CTERM: This is a real variable that defines the constant (C) in the previous equations.

j) RHOP, ZOP: These are real variables that define the phase distribution across an aperture. Note that RHOP and ZOP are specified in wavelengths. In terms of the previous definition for the case (LSTERM=4) RHOP=ρ_o and ZOP=Z_o.

L. COMMAND SA:

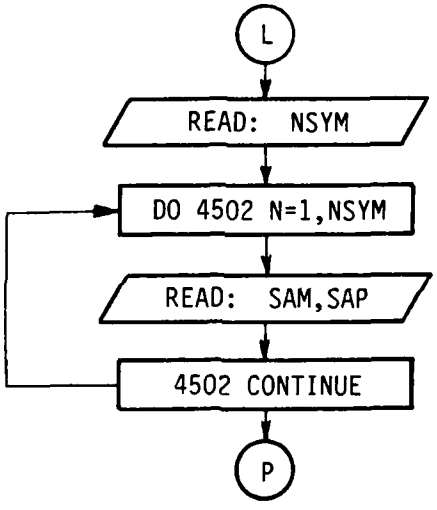

This command enables the user to get a quick array pattern if the structure (geometry, antenna type, and location) has circumferential symmetry. The program is set to take the pattern about the z-axis (longitudinal axis) in one degree steps in this case. This command must be used in conjunction with the IG: command. Otherwise, the program aborts. Presently, this command applies only when $2 \leq$ NINT ≤ 4, where NINT is number of intakes as defined in the "IG:" command.

1. READ: NSYM

a) NSYM: This is an integer variable which defines the number of arrays placed around the circumference. Presently, $2 \leq NSYM \leq 4$. It is used according to the following table:

$$NSYM = \begin{cases} 2 \text{ or } 4 & \text{if NINT} = 4 \\ 3 & \text{if NINT} = 3 \\ 2 & \text{if NINT} = 2 \end{cases}$$

2. READ: SAM,SAP

a) SAM, SAP: These are real variables used to specify the magnitude and phase (in degrees) of the Nth circumferential array element excitation.

M. COMMAND LP:

This command enables the user to obtain a line printer listing of the total fields ($E_{\theta p}$, $E_{\phi p}$). No input is required.

N. COMMAND PP:

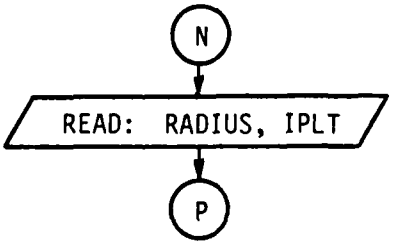

This command enables the user to obtain a pen plot of the total fields ($E_{\theta p}$, $E_{\phi p}$).

1. READ: RADIUS, IPLT

a) RADIUS: This is a real variable that is used to specify the radius of the polar plot.

b) IPLT: This is an integer variable that indicates the type of polar plot desired, such that

$$\text{IPLT} = \begin{cases} 1 \rightarrow \text{field plot} \\ 2 \rightarrow \text{power plot} \\ 3 \rightarrow \text{dB plot} \end{cases}$$

0. COMMAND EX:

This command is used to execute the code so that the total fields may be computed. After execution the code returns for another possible command word.

This concludes the definition of all the input parameters to the program. The program would, then, run the desired data and output the results on unit #6. However as with any sophisticated program, the definition of the input data is not sufficient for one to fully understand the operation of the code. In order to overcome this difficulty the next chapter discusses how the input data are interpreted and used in the program.

IV. INTERPRETATION OF INPUT DATA

This computer code is written to require a minimum amount of user information such that the burden associated with a complex geometry will be organized internal to the computer code. For example, the operator need not instruct the code that two plates are attached to form a convex or concave structure. The code flags this situation by recognizing that two plates have a common set of corners (i.e., a common edge). So if the operator wishes to attach two plates together he needs only define the two plates as though they were isolated. However, the two plates will have two identical corners. All the geometry information associated with plates with common edges is then generated by the code. The present code also will allow a plate to intersect another plate as shown in Figure 7. It is necessary that the corners defining the attachment be positioned a small amount through the plate surface to which it is being connected. These details will be illustrated in the examples of Section VII.

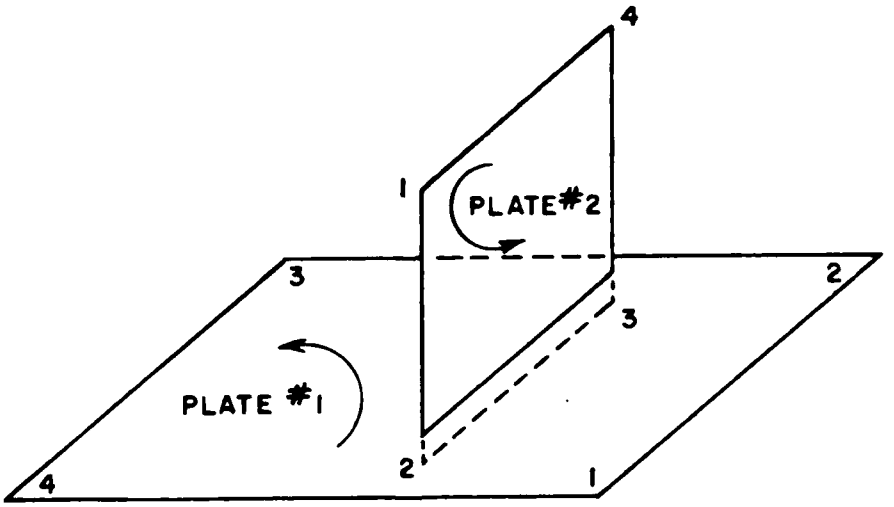

Figure 7. Data format used to define a flat plate intersecting another flat plate.

In defining the plate corners it is necessary to be aware of a subtlety associated with simulating convex or concave structures in which two or more plates are used in the computation. This problem results in that each plate has two sides. If the plates are used to simulate a closed or semi-closed structure, then possibly only one side of the plate will be illuminated by the antenna. Consequently, the operator must define the data in such a way that the code can infer which side of the plate is illuminated by the antenna. This is accomplished by defining the plate according to the right-hand rule. As one's fingers of the right hand follow the edges of the plate around in the order of their definition, his thumb should point toward the illuminated region above the plate. To illustrate this constraint associated with data format, let us consider the definition of a rectangular box. In this case, all the plates of the box must be specified such that they satisfy the right-hand rule with the thumb pointing outward as illustrated in Figure 8. If this rule were not satisfied for a given plate, then the code would assume that the antenna is within the box as far as the scattering from that plate is concerned.

A missile structure is being analyzed as shown in Figure 6. The far field of this structure is classically defined as a range exceeding $2(D+2AI)^2/\lambda$. If this code is used to compute the far field pattern, the user should supply the minimum far field range requirement. This should be done in that excessive ranges can create numerical difficulties within the code. In fact, it is suggested that the user input the range as $(D+2AI)^2/\lambda$ for the far field missile case. In any event if mysterious far field patterns result using this code, one should reduce the range in order to examine the numerical accuracy of the solution.

In the "PG:" command, if LATACH(MPX)=T (i.e., the plate is attached to the fuselage), the program assumes that the first and last

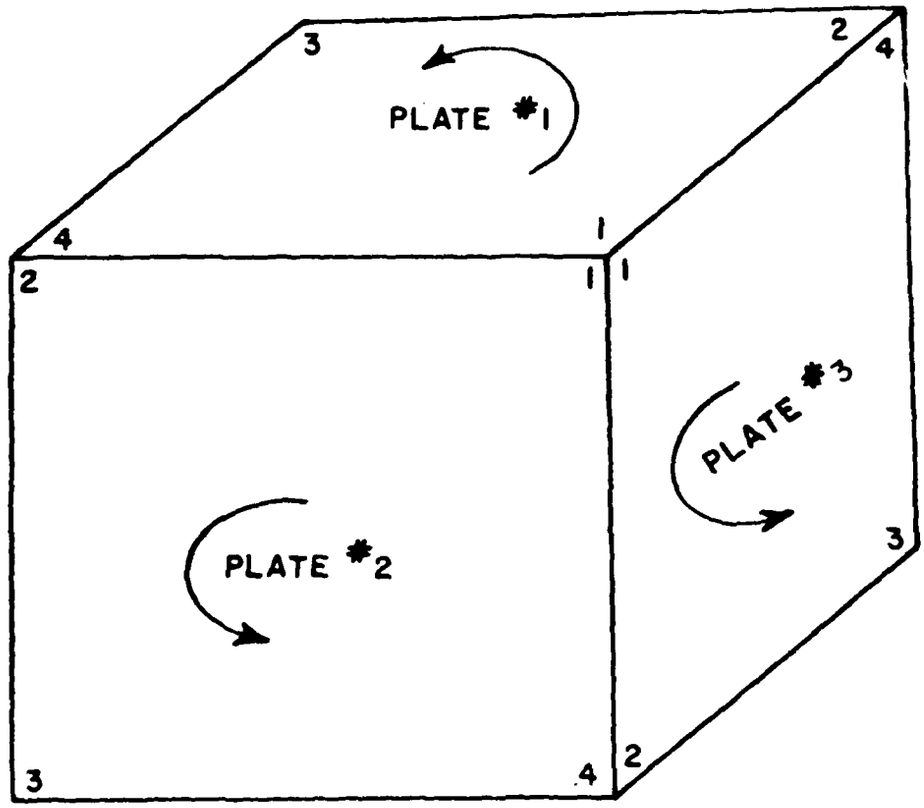

Figure 8. Data format used to define a box structure.

plate corners PVC(N,1,MPX) and PVC(N,MCMX,MPX) are positioned on the fuselage. The user must define the geometry accordingly. However, he need not exactly attach the first and last corner to the fuselage in that the code will extend the edges and reset the first and final corner points on the fuselage as shown in Figure 9.

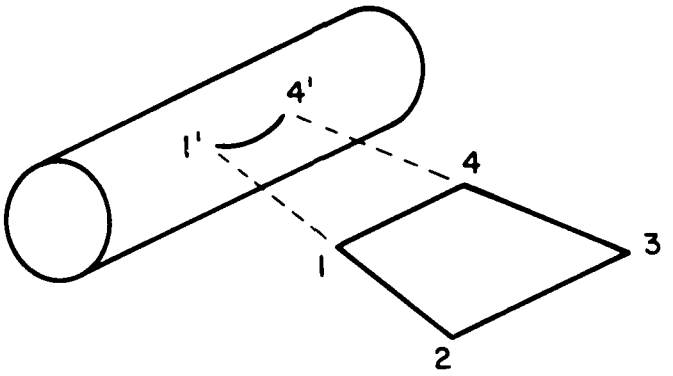

Figure 9. Data format used to define a flat plate intersecting a fuselage.

Using the "SG:" command, it is necessary that $-90^{o} \leq PHSA(MS) \leq 90^{o}$. In case the antenna is placed on the bottom part of the fuselage, the user must redefine the geometry such that $\phi_s(PHSA(MS))$ falls within the required angular range. As shown in Figure 10, the fuselage can be turned upside down by changing AF into CF', BF into DF', etc. to correct this situation.

The ray tracing is always a tedious problem in pattern analysis. It assumes that the higher-order diffraction/reflection fields from the fuselage are small in which case they can be neglected. However, the code automatically simulates fuselage blockage using two additional plates (i.e., one along the x-axis and the other along the y-axis). Thus, even though higher-order interactions between structures and the fuselage are not added in computation, their absence will be apparent in the results.

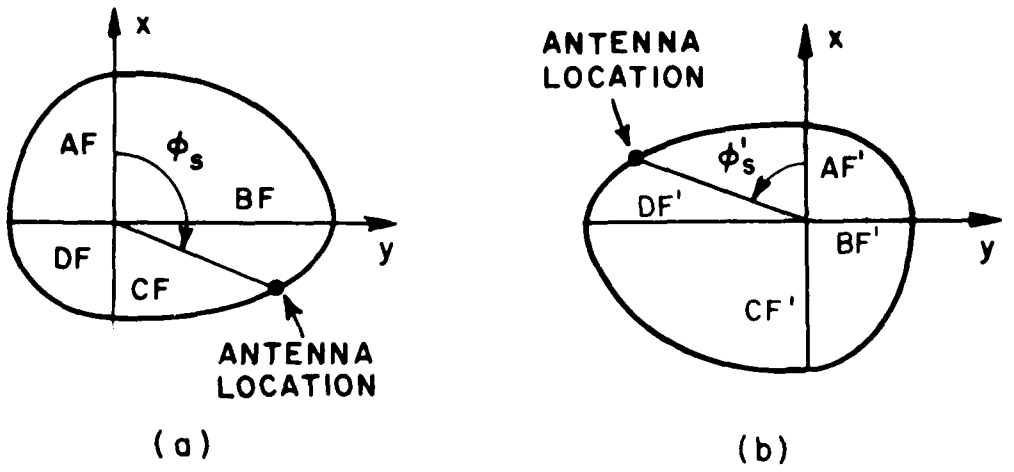

NOTE: AF = CF'
BF = DF'
CF = AF'
DF = BF'

Figure 10. The original (a) and redefined geometry (b) to adapt to the data format in defining the antenna location.

Finally, it must be kept in mind that the antenna should be kept at least a quarter-wavelength away from any diffracting edge. In fact all dimensions should be at least a quarter wavelength.

V. PROGRAM OUTPUT

The basic output from the computer code is a line printer listing of the results. Recall that the results of the program are the $E_{\theta P}$ and $E_{\phi P}$ radiation pattern values. In order to again describe these pattern components, let us consider the various principal plane patterns treated in the previous section. The computer code allows for a rotation of coordinates such that one can take a pattern about an arbitrary axis. This information is input to the code using the spherical angles THC, PHC. The geometry that applies for each of the roll, elevation, and azimuth patterns of the next section is illustrated in Figure 11. Note that the θ_p and ϕ_p angles are defined relative to the rotated pattern coordinates and that they change as THC, PHC is changed. Thus, $E_{\theta P}$ is the theta component of the field (i.e., $E_{\theta P}=\vec{E}\cdot\hat{\theta}_p$) in the pattern coordinate system. Likewise, $E_{\phi P}=\vec{E}\cdot\hat{\phi}_p$. The total radiated electric field is denoted by $\vec{E}$.

In addition to the printed results, one has the option of obtaining a set of polar patterns. If LPLT=T in the input data list, the program will automatically plot the $E_{\theta P}$ and $E_{\phi P}$ polar patterns. These patterns are plotted such that the outer ring corresponds to the pattern maximum in each case. This polar plot routine was used to plot the data presented in the next section.

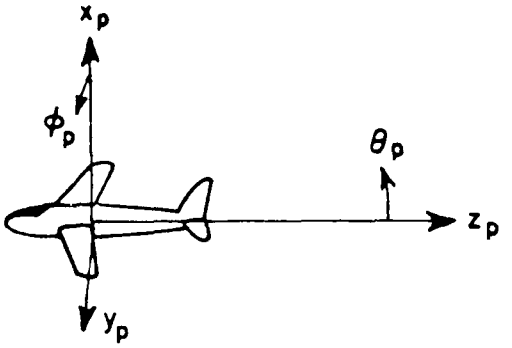

(a) ROLL PLANE COORDINATES (THC=0°, PHC=0°)

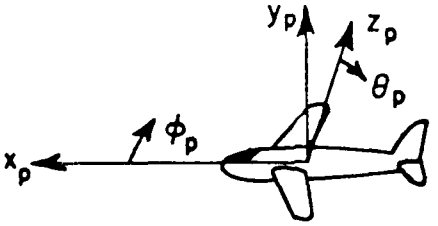

(b) ELEVATION PLANE COORDINATES (THC=90°, PHC = ± 90°)

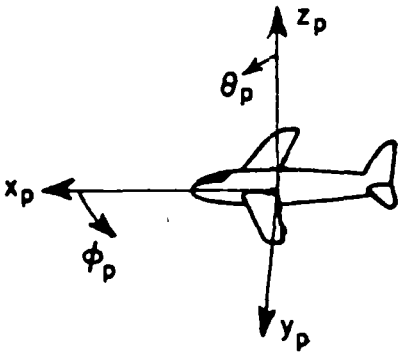

(c) AZIMUTH PLANE COORDINATES (THC=90°, PHC = 0°)

Figure 11a. Illustration of pattern coordinates for the principal plane pattern calculations in roll plane model.

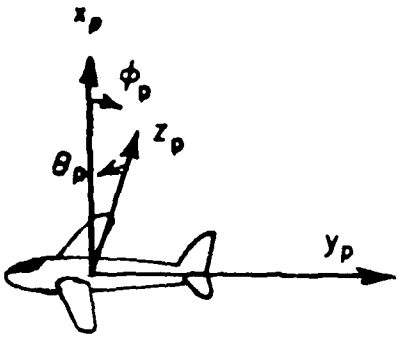

(a) ELEVATION PLANE COORDINATES (THC = 0°, PHC = 0°)

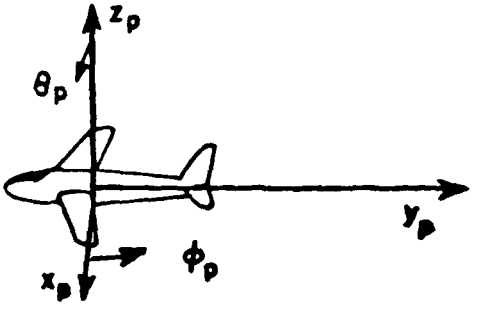

(b) AZIMUTH PLANE COORDINATES (THC = 90°, PHC = 0°)

Figure 11b. Illustration of pattern coordinates for the principal plane pattern calculations in elevation plane model

VI. APPLICATION OF CODE TO SEVERAL SIMPLE EXAMPLES

The following examples are used to illustrate some features of the computer code. Various geometries and input data are used to examine the effect of separate terms. Note that the patterns are plotted in decibels with each division being 10 dB, and the labeling is not included on the plots in some cases.

Example 1:

Consider the roll plane pattern of an axial slot antenna mounted on a cylinder as shown in Figure 12.

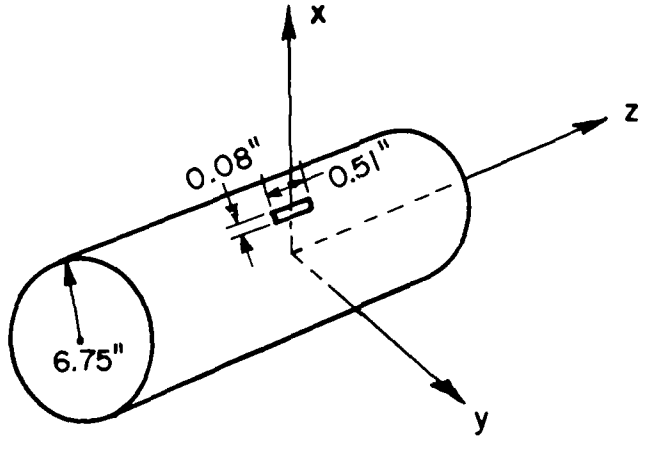

Figure 12. Geometry of an axial slot mounted on a circular cylinder.

The input data is given by

```
UN:
3
SG:
1
0.,0.
0.08,0.51, 0.,0.25,1
1.,0.
```

```
FG:
6.75,6.75,6.75,6.75
0.,0.,0.
PD:
0.,0.,90.
0,360,1
600.,12.
EX:
```

The $E_{\phi P}$ roll plane pattern is plotted in Figure 13. The $E_{\theta P}$ pattern is not plotted because it is of negligible value.

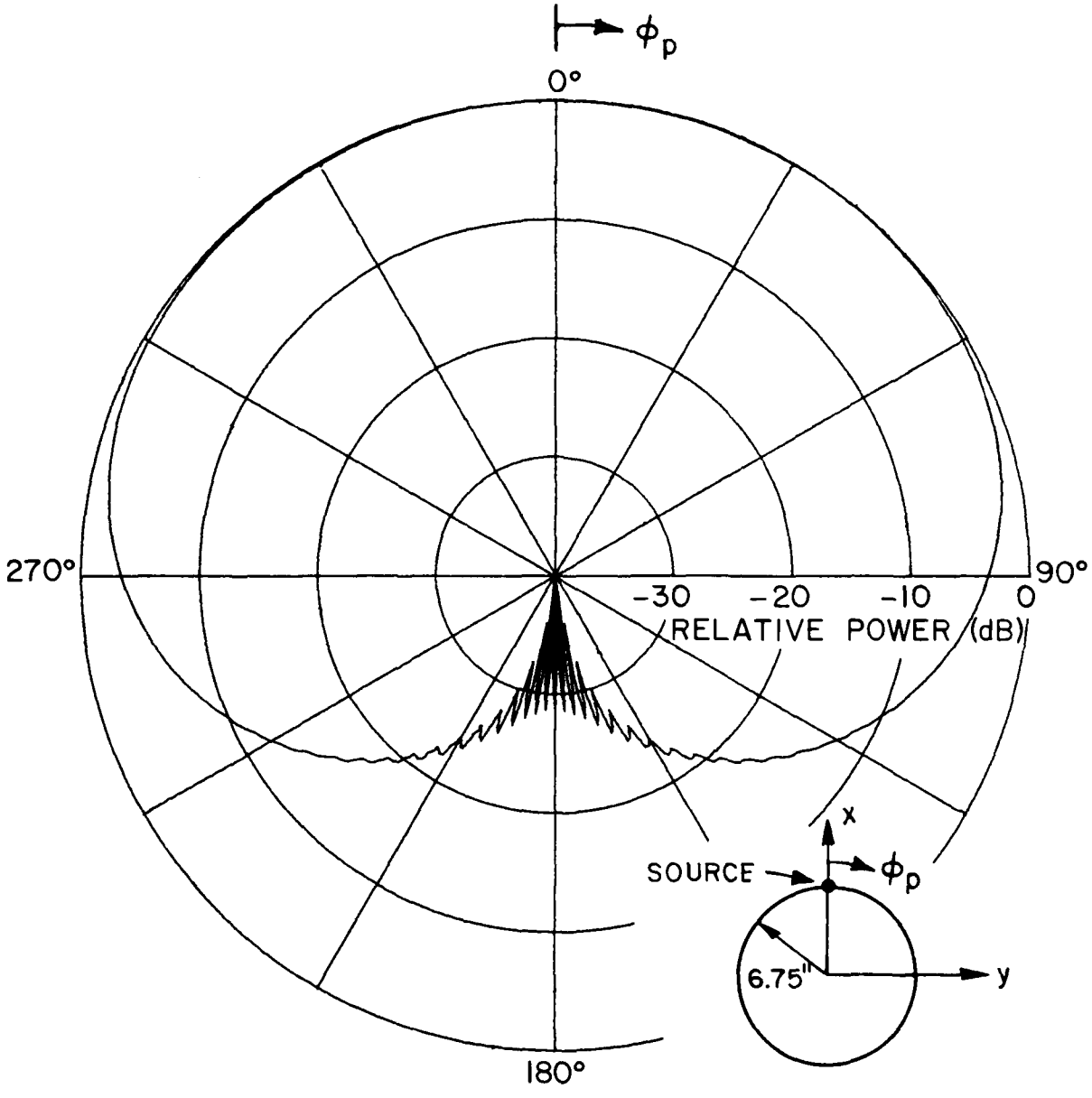

Figure 13. $E_{\phi p}$ roll plane pattern of an axial slot mounted on a circular cylinder at a frequency of 12 GHz.

Example 2:

As shown in Figure 14, consider now the case that 4 intakes are attached to the fuselage with an axial slot antenna mounted on it.

The input data is given by

```
UN:
3
SG:
1
1.32,0.
0.08,0.51,0.,0.25,1
1.,0.
PD:
0.,1.32,90.
0,360,1
600.,12.
IG:
6.75,9.125,2.375,2.375,4,T
EX:
```

The calculated and measured $E_{\phi P}$ roll plane pattern are compared in Figure 14. Note that the source location is adjusted to correspond to the experimental result.

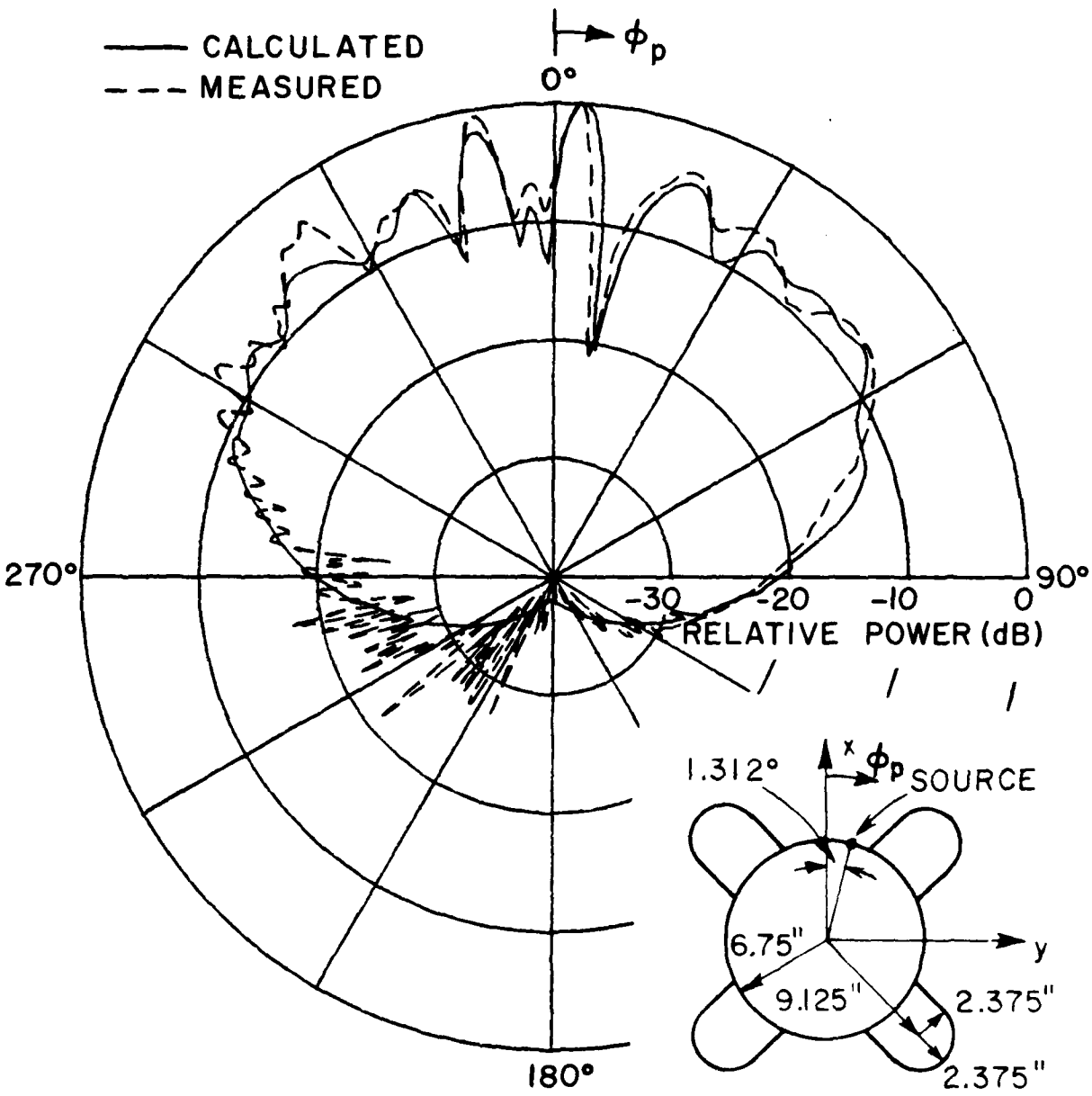

Figure 14. The calculated and measured $E_{\phi p}$ roll plane patterns for a 4-intake case.

Example 3:

Following Example 2, the input data for an elevation plane pattern is given by

```
UN:
3
SG:
1
1.32,0.
0.08,0.51,0.,0.25,1
1.,0.
PD:
90.,91.32,90.
0,360,1
600.,12.
IG:
6.75,9.125,2.375,2.375,4,T
EX:
```

The calculated and measured $E_{\theta P}$ elevation patterns are compared in Figure 15.

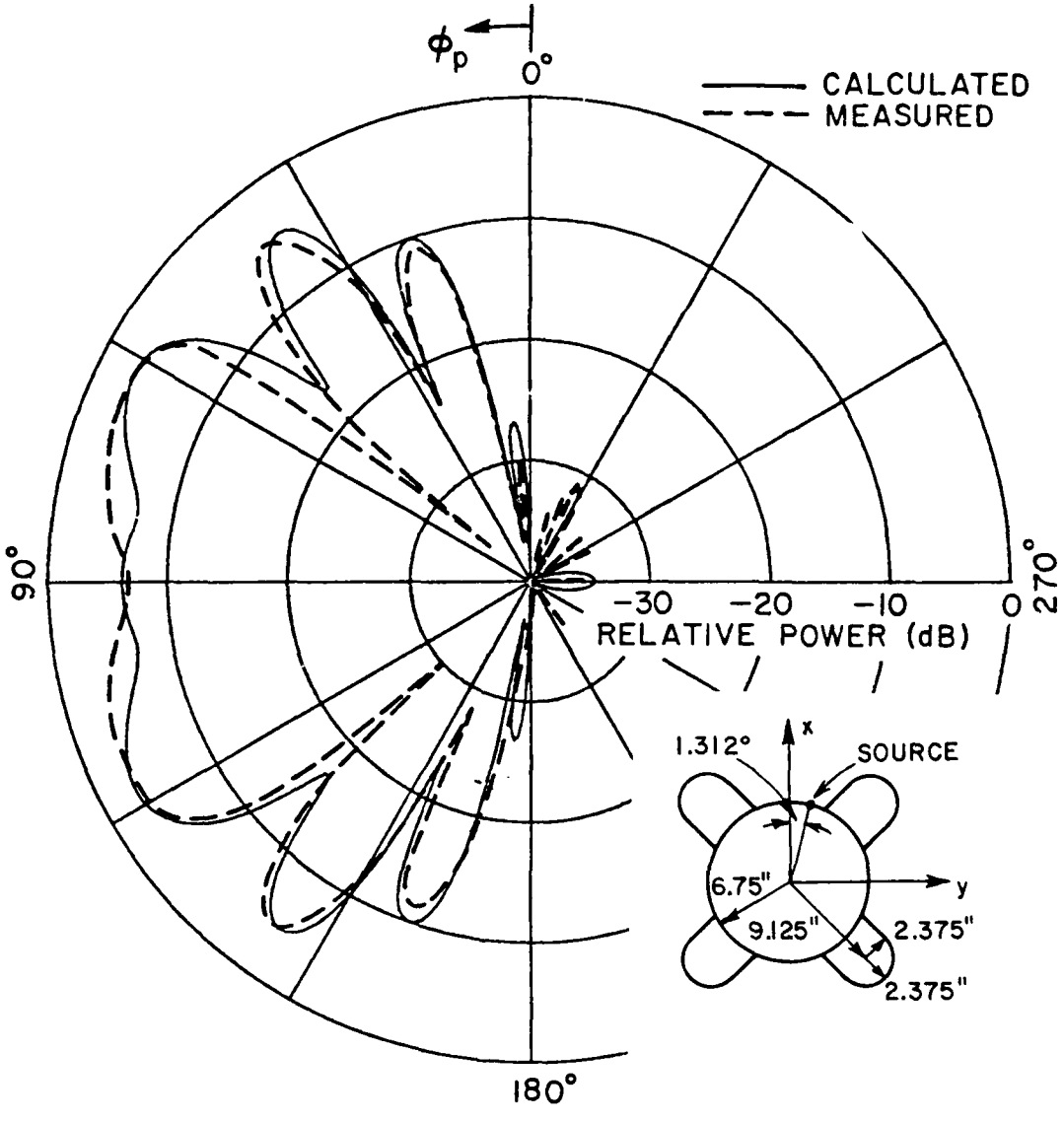

Figure 15. Elevation plane pattern for an axial slot mounted between two air ducts.

Example 4:

Following Example 2, but with an axial slot antenna mounted on the intake instead of the fuselage, as shown in Figure 16, the input data is given by

```
UN:
3
SG:
1
0.08,0.51,0.,0.25,1
1.,0.
PD:
0.,0.,90.
0,360,1
600.,12.
IG:
6.75,9.125,2.375,2.375,4,F
EX:
```

The calculated and measured $E_{\phi P}$ roll plane patterns are compared in Figure 16.

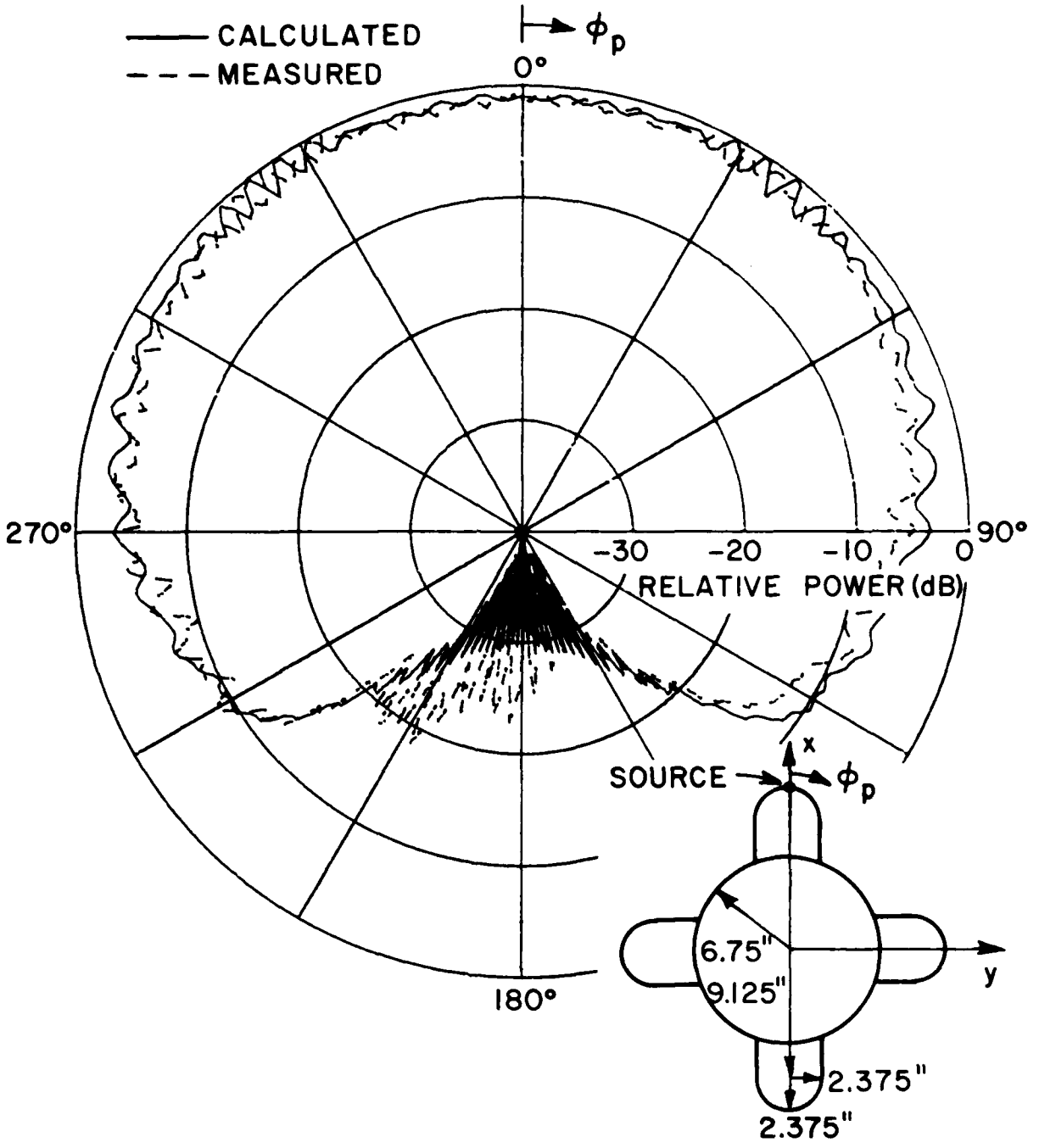

Figure 16. Roll plane radiation pattern for centrally located axial slot mounted on one of the four circular intakes. The pattern was taken at a frequency of 12 GHz.

Example 5:

Following Example 4, the input data for an elevation plane pattern is given by

```
UN:
3
SG:
1
3.76,0.
0.08,0.51,0.,0.25,1
1.,0.
PD:
90.,93.76,90.
0,360,1
600.,12.
IG:
6.75,9.125,2.375,2.375,4,F
EX:
```

The calculated and measured $E_{\theta P}$ elevation plane patterns are compared in Figure 17.

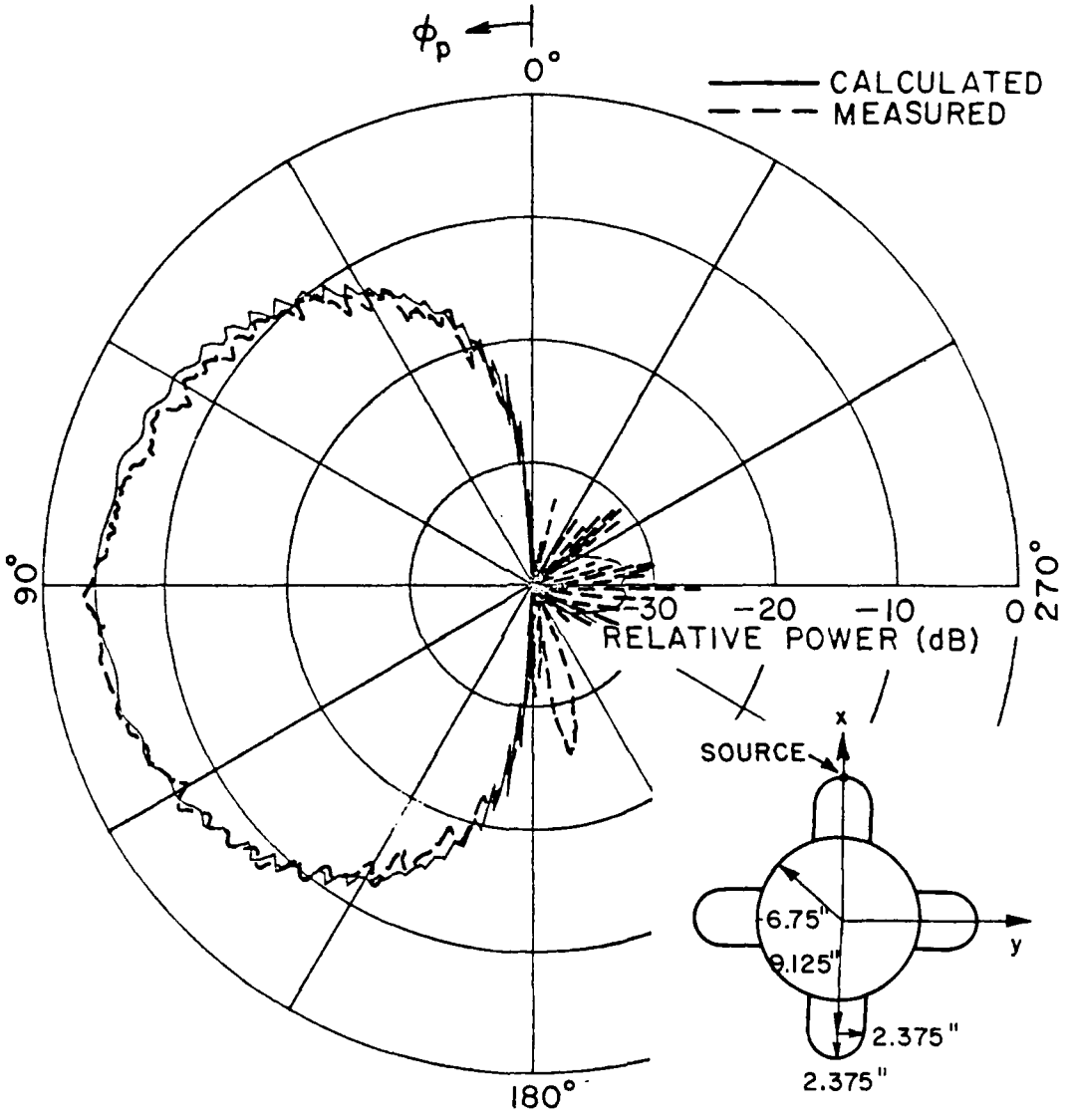

Figure 17. Elevation plane pattern for an axial slot mounted on an air duct.

Example 6:

In order to examine the effect of the separate terms on the total pattern, the "TO:" command can be used. Consider again the geometry in Figure 14 but with ϕ_s=0, the input data for the total and separate field pattern is given by

a) Total field:

```
UN:
3
SG:
1
0.,0.
0.08,0.51,0.,0.25,1
1.,0.
PD:
0.,0.,90.
0,360,1
600.,12.
IG:
6.75,9.125,2.375,2.375,4,T
EX:
```

b) source field:

```
TO:
F,F,F
T,T
T,F,F,F,F,F,F
1,6,1
1,4,1
1,4,1
1,4,1
```

```
1,4,1
1,4,1
1,4,1
UN:
3
SG:
1
0.,0.
0.08,0.51,0.,0.25,1
1.,0.
PD:
0.,0.,90.
0,360,1
600.,12.
IG:
6.75,9.125,2.375,2.375,4,T
EX:
```

The fourth line can be adjusted to yield the reflected or diffracted field, etc. The resulting $E_{\phi P}$ roll plane pattern is plotted in Figure 18.

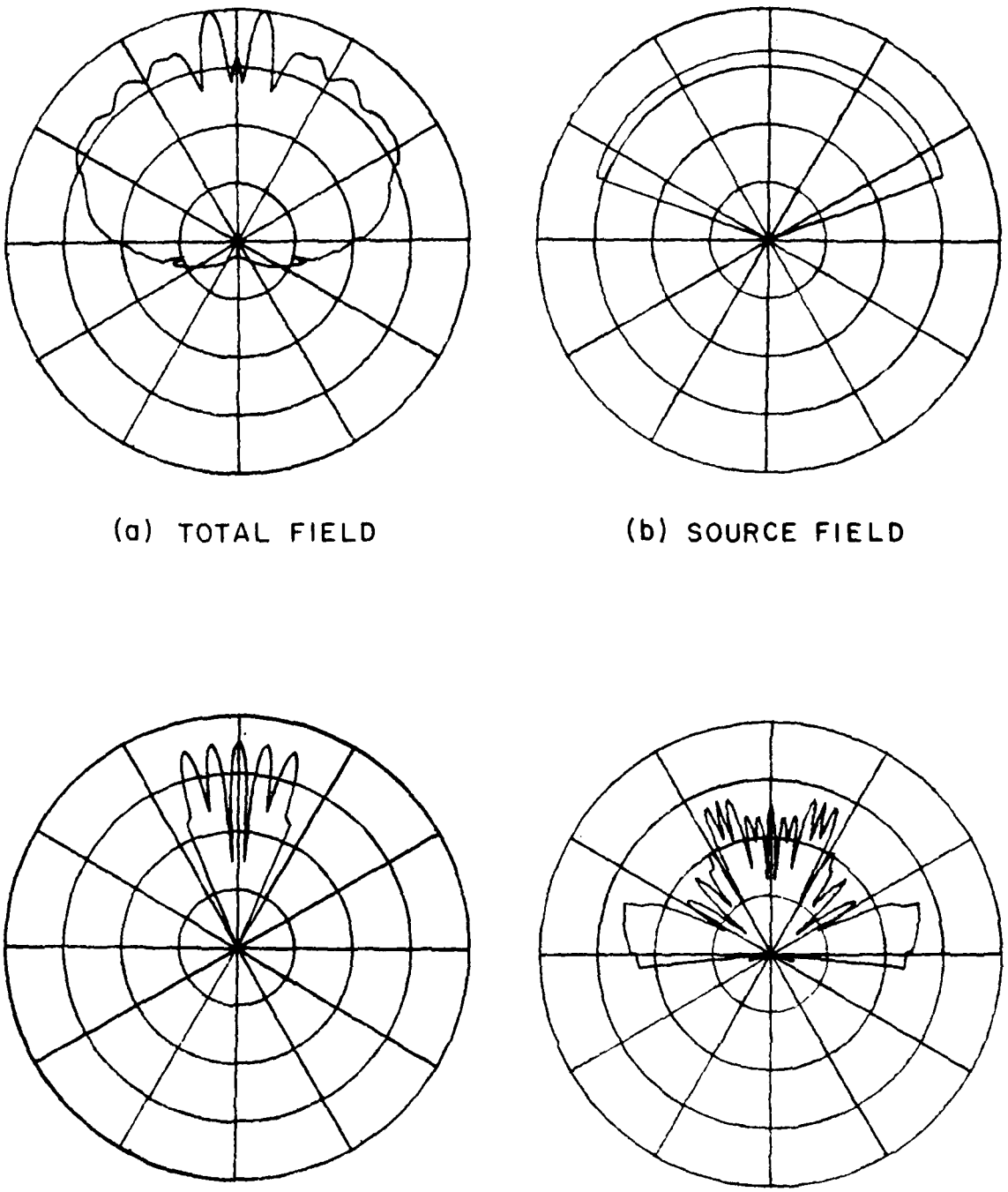

Figure 18. Roll plane patterns for an axial slot located at $\phi_s=0^o$.

VII. APPLICATION OF CODE TO AIRCRAFT SIMULATIONS

A typical aircraft model contains a cylinder and flat plates. Two such configurations are the elevation and roll plane models which can be used to calculate most patterns. The elevation plane model consists of a composite elliptic cylinder chosen to approximate the actual aircraft side-view drawing. Aircraft front-view drawing is for roll plane model. The input parameters used to describe these two aircraft models are given in Figures 10 and 11. Although not shown in Figures 10 and 11, one can simulate various aircraft structures such as stores, pylons, wing tanks, etc. by multiple flat plates.

This code allows for two different methods for defining one plate to be attached to another: 1) edge to edge attachment and 2) edge to surface attachment. Edge to edge attachment, as illustrated in Figure 19, often requires that a plate edge be defined as two or three

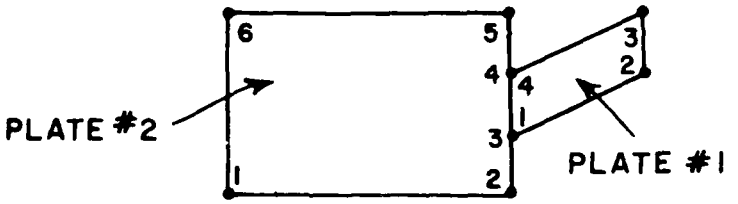

Figure 19. Edge to edge plate attachment.

colinear edges as the program identifies this mode of attachment only by finding two identical pairs of corners. Note that the corners must be consecutive on both plates which means there actually exists an edge between them. In the case of edge to surface attachment, one plate is defined as penetrating a short distance through the surface of the second plate as illustrated in Figure 20. The program then defines the new junction edge and eliminates the smaller portion of plate #1 behind plate #2. Here care must be taken to assure that the new junction edge is completely contained within the bounds of plate

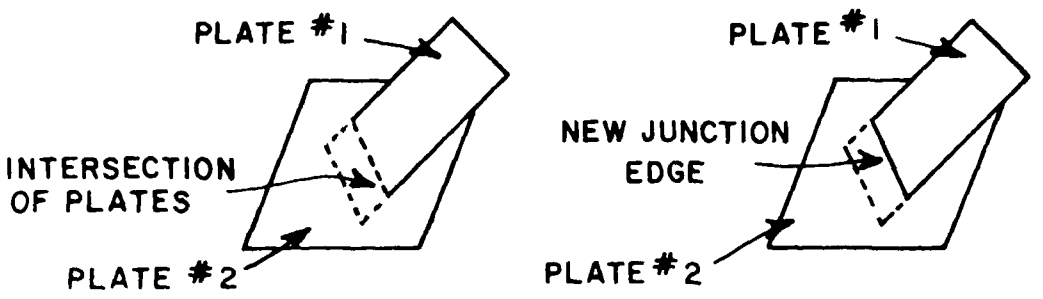

Figure 20. Edge to surface plate attachment.

#2, and no where nearer than a half wavelength or so to an edge of plate #2. Now it will be shown how these two attachment methods are used to simulate aircraft wings.

A roll plane model for a Cessna 402B is shown in Figure 21 with the input file given in Figure 22. This is an illustration of a case in which edge to edge plate attachment is used. Since the engine extends beyond both the forward and rear limits of the wing, it is possible to define the four points at which the engine and wing intersect. Then for the sake of simplicity, the part of the wing beneath the engine is eliminated, which is permissible since the source is mounted such that it will not directly illuminate that area. Note that the sides of the engine, plates #2 and #4 each have six edges.

A case illustrating edge to surface plate attachment is that of the Beechcraft Baron. The roll plane model for this aircraft is shown in Figure 23 and the input file given in Figure 24. Here the engine does not extend behind the rear limit of the wing, necessitating the defining of the rear part of the engine to be mounted flush on the wing. To make such an attachment, the entire junction edge must be contained within the boundaries of the wing. Thus one must use the tab poked slightly through as shown in the three dimensional (3D) view. Note that there is a distinct separation between the front wing edge and the engine according to the rules of edge to surface attachment.

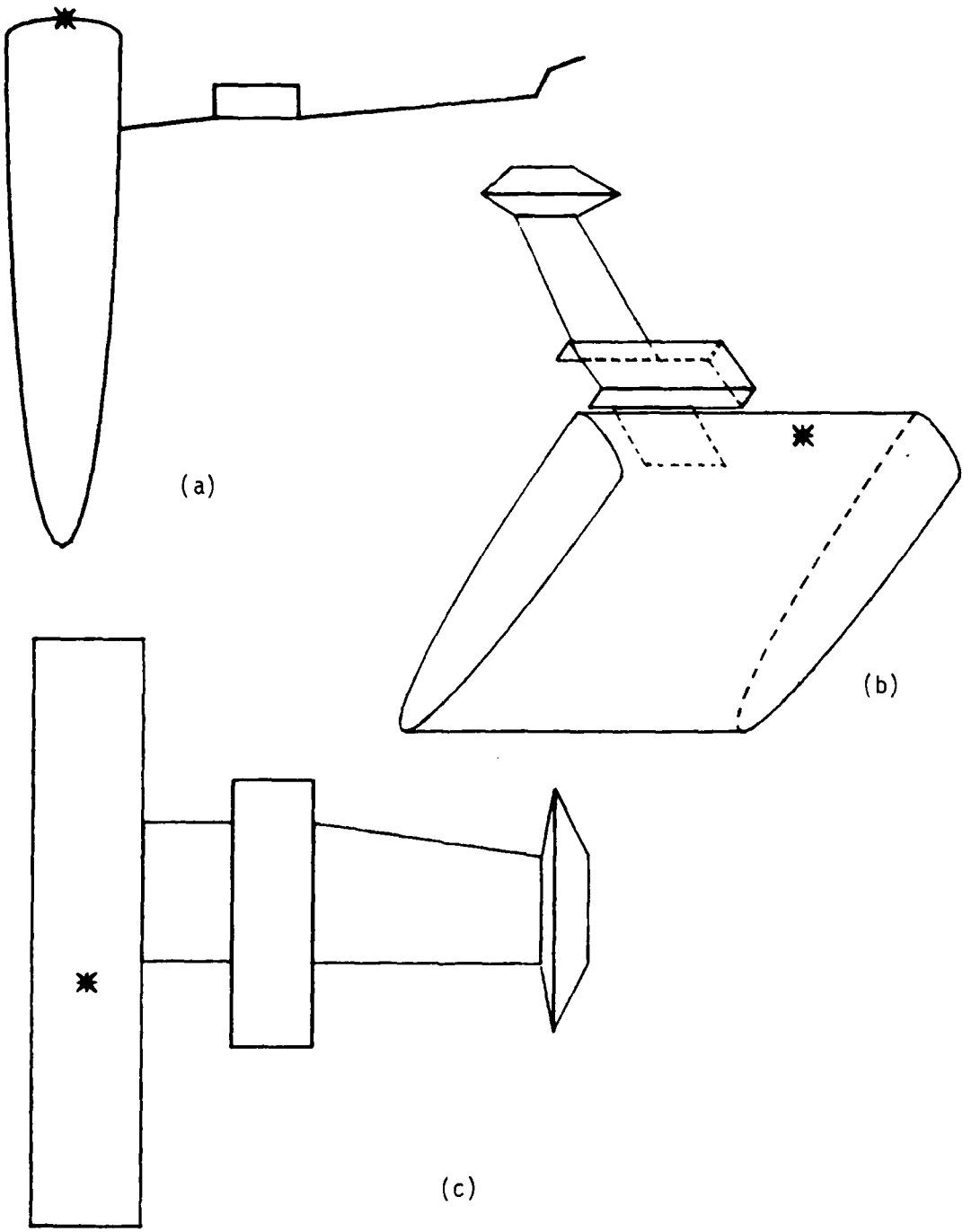

Figure 21. Model of Cessna 402B in which edge to edge attachment is used. Input file shown in Figure 22.
(a) front view (b) 3-D view (c) top view

```
UN: INCHES CESSNA 402B LOC 1  ROLL  W/ FUEL TANKS
3
TO:
F,F,F
F,T
PD:
0.,0.,90.
0,360,1
4200.,5.
PG:LEFT WING (INNER PART)
4,T
-41.8,26.0,0.
-36.8,68.,0.
-36.8,68.,65.
-41.8,26.,65.
PG:LEFT ENGINE (RIGHT SIDE)
6,F
-36.8,68.,0.
-36.8,68.,-40.
-21.8,68.,-40.
-21.8,68.,85.
-36.8,68.,85.
-36.8,68.,65.
PG:LEFT ENGINE(TOP)
4,F
-21.8,68.,-40.
-21.8,106.,-40.
-21.8,106.,85.
-21.8,68.,85.
PG:LEFT ENGINE (LEFT SIDE)
6,F
-36.8,106.,65.
-36.8,106.,85.
-21.8,106.,85.
-21.8,106.,-40.
-36.8,106.,-40.
-36.8,106.,0.
PG:LEFT ENGINE (FRONT)
4,F
-21.8,68.,-40.
-36.8,68.,-40.
-36.8,106.,-40.
-21.8,106.,-40.
PG:LEFT WING(OUTER PART)
4,F
-36.8,106.,0.
-26.8,213.,0.
-26.8,213.,50.
-36.8,106.,65.
PG:LEFT FUEL TANK PLATE #1
4,F
-26.8,213.,0.
-14.8,219.,-32.
-14.8,219.,82.
-26.8,213.,50.
PG:LEFT FUEL TANK PLATE #2
4,F
-14.8,219.,-32.
-8.8,235.,0.
-8.8,235.,50.
-14.8,219.,82.
SG:
1
0.,-10.
.414,.828,0.,.25,3
1.,0.
FG:
8.2,26.,230.,26.
0.,0.,0.
EX:
```

Figure 22. Input data for Cessna 402B.

(a)

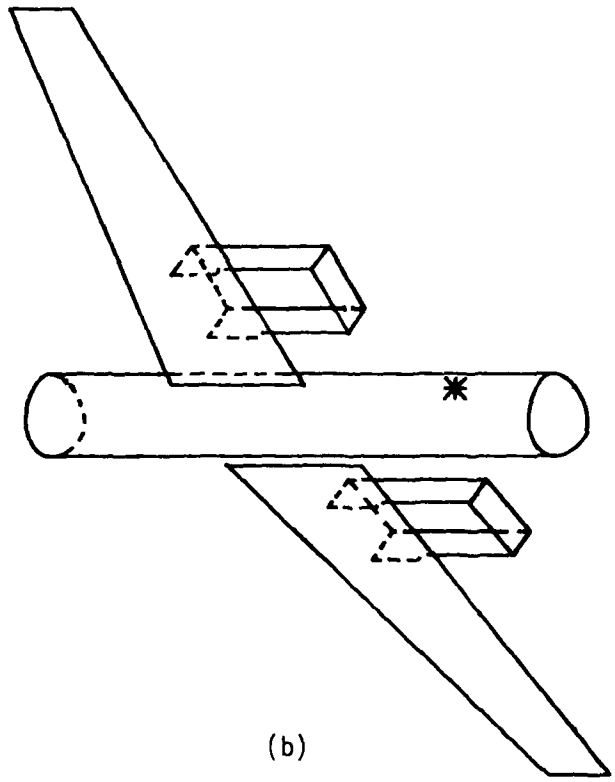

(b)

Figure 23. Model of Beechcraft Baron in which edge to surface attachment is used. Input file shown in Figure 24. (a) front view (b) 3-D view

```
UN: INCHES
3
TO:
F,F,F
F,T
PD:
0.,0.,80.
0,360,1
4200.,5.
PG: LEFT WING
4,T
-10.,23.5,-20.
10.,227.,-10.
10.,227.,27.
-10.,23.5,60.
PG: RIGHT WING
4,T
-10.,-23.5,60.
10.,-227.,27.
10.,-227.,-10.
-10.,-23.5,-20.
PG: LEFT ENGINE (RIGHT SIDE)
6,F
-5.6,50.5,-62.
8.4,50.5,-62.
8.4,50.5,20.
-8.6,50.5,20.
-8.6,50.5,-8.5
-5.6,50.5,-8.5
PG: LEFT ENGINE (TOP)
4,F
8.4,50.5,-62.
11.4,84.5,-62.
11.4,84.5,20.
8.4,50.5,20.
PG: LEFT ENGINE (LEFT SIDE)
6,F
-5.6,84.5,20.
11.4,84.5,20.
11.4,84.5,-62.
-2.6,84.5,-62.
-2.6,84.5,-7.
-5.6,84.5,-7.
PG: LEFT ENGINE (FRONT)
4,F
-2.6,84.5,-62.
11.4,84.5,-62.
8.4,50.5,-62.
-5.6,50.5,-62.
PG: RIGHT ENGINE (LEFT SIDE)
6,F
-5.6,-50.5,-62.
-5.6,-50.5,-8.5
-8.6,-50.5,-8.5
-8.6,-50.5,20.
8.4,-50.5,20.
8.4,-50.5,-62.0
PG: RIGHT ENGINE (TOP)
4,F
8.4,-50.5,-62.
8.4,-50.5,20.
11.4,-84.5,20.
11.4,-84.5,-62.
PG: RIGHT ENGINE (RIGHT SIDE)
6,F
-5.6,-84.5,20.
-5.6,-84.5,-7.
-2.6,-84.5,-7.
-2.6,-84.5,-62.
11.4,-84.5,-62.
11.4,-84.5,20.
PG: RIGHT ENGINE (FRONT)
4,F
-2.6,-84.5,-62.
-5.6,-50.5,-62.
8.4,-50.5,-62.
11.4,-84.5,-62.
SG:
1
0.,-77.
.414,.828,0.,.25,3
1.,0.
FG:
11.7,17.5,22.6,17.5
0.,0.,0.
EX:
```

Figure 24. Input data for Beechcraft Baron.

Example 7:

Consider a crossed-slot mounted on the fuselage of a KC-135 aircraft. The computer model of the KC-135 is illustrated in Figures 25 and 26. The input data is given by:

```
UN: CHANGE TO INCHES
3
FG:KC-135 AIRCRAFT STUDY
3.,3.,3.,3.
0.,0.,0.
SG: CROSSED-SLOT FORWARD OF WINGS
2
45.,8.34
0.,0.5,0.,0.25,1
1.,0.
45.,8.34
0.,0.5,90.,0.25,1
1.,90.
PG: LEFT WING
4,T
-1.,3.,12.31
-1.,28.5,36.41
-1.,28.5,40.41
-1.,3.,24.61
PG: RIGHT WING
4,T
-1.,-3.,24.61
-1.,-28.5,40.41
-1.,-28.5,36.41
-1.,-3.,12.31
PD: ROLL PATTERN
0.,0.,,90.
0,360,1
1000.,187.5
EX: EXECUTE PROGRAM
```

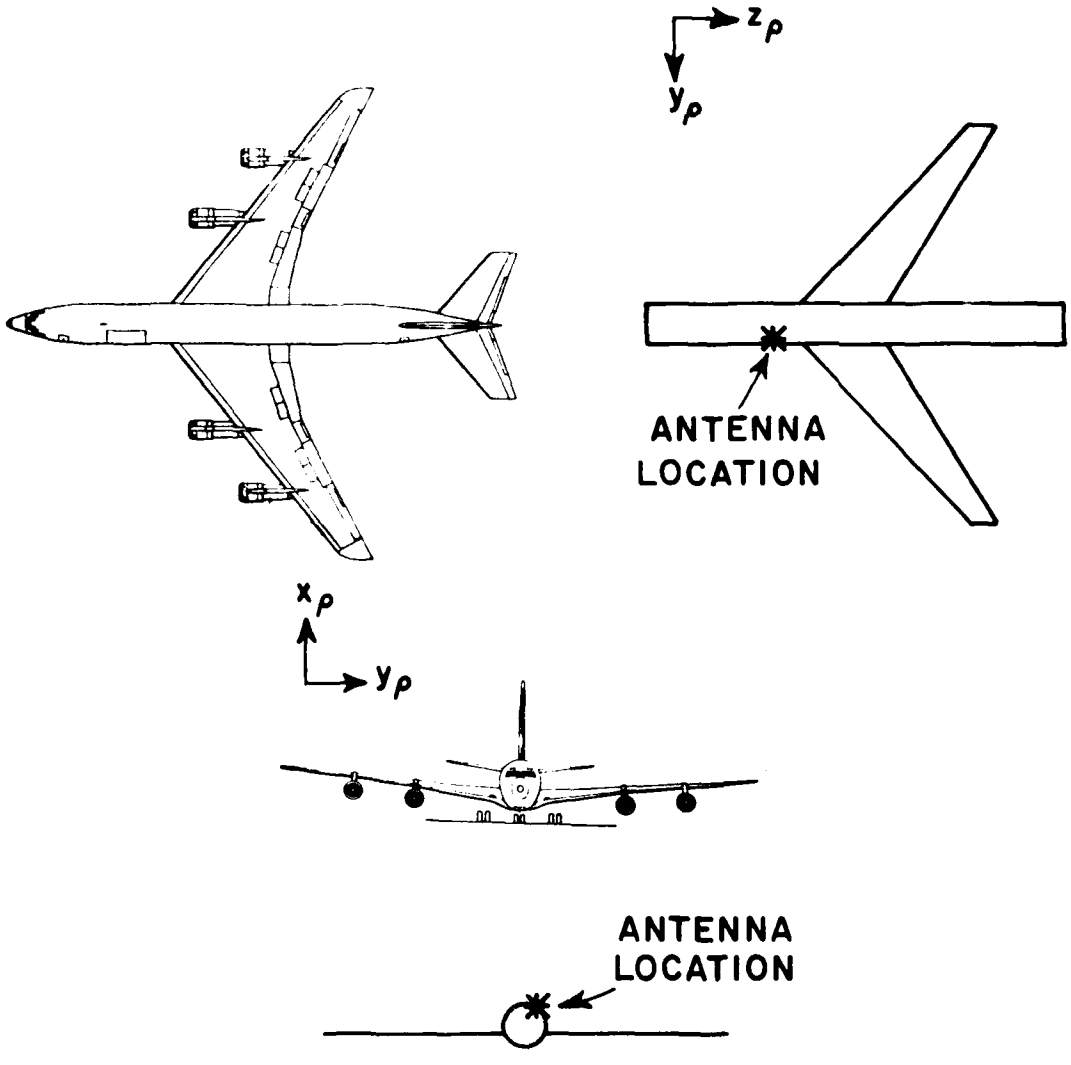

Figure 25. Computer simulated roll plane model for a KC-135. The antenna is located forward of wings (off center).

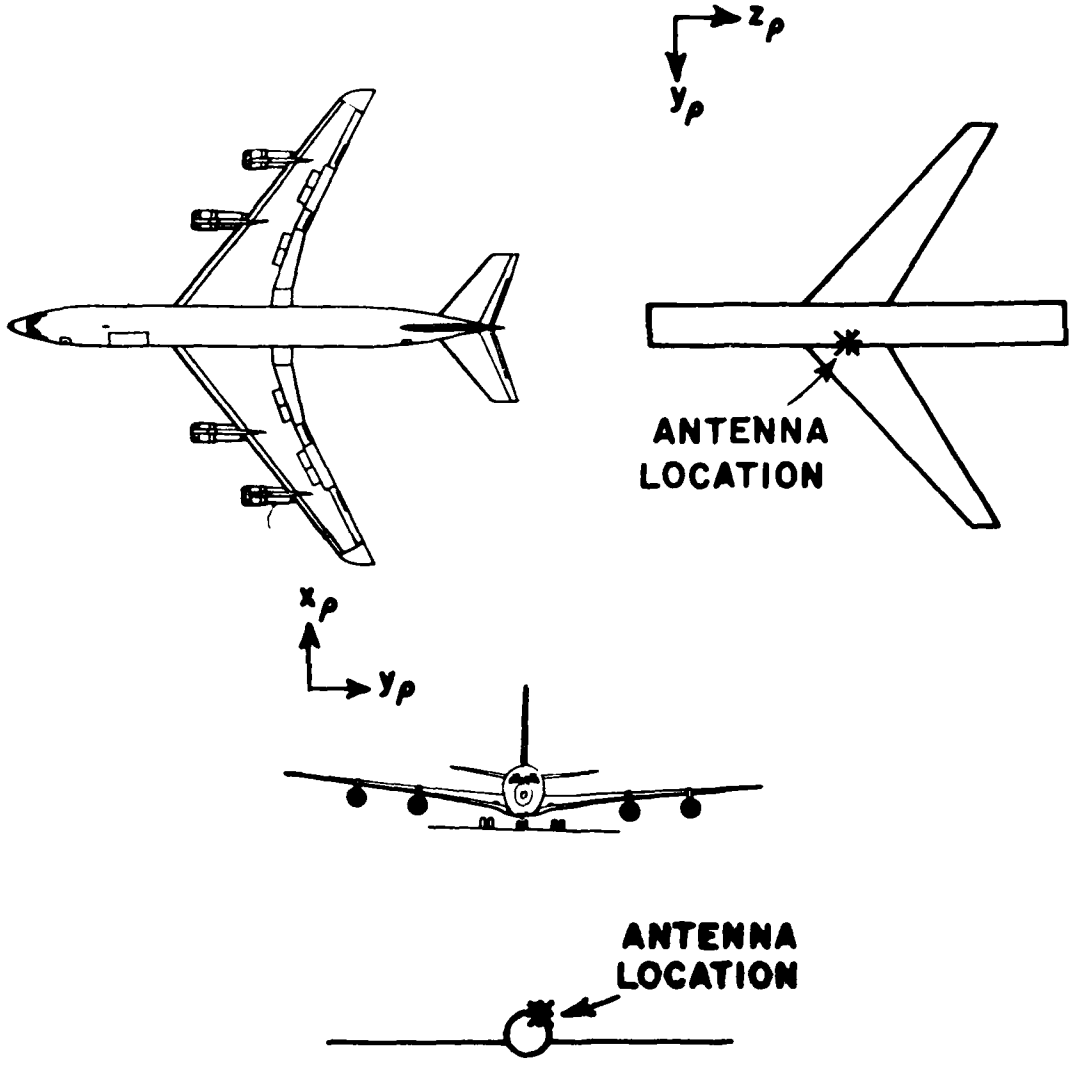

Figure 26. Computer simulated roll plane model for a KC-135. The antenna is located over wings (off center).

The $E_{\phi p}$, $E_{\theta p}$ radiation patterns in the roll plane model for the forward and over wing locations are given in Figure 27 and Figure 28, respectively.

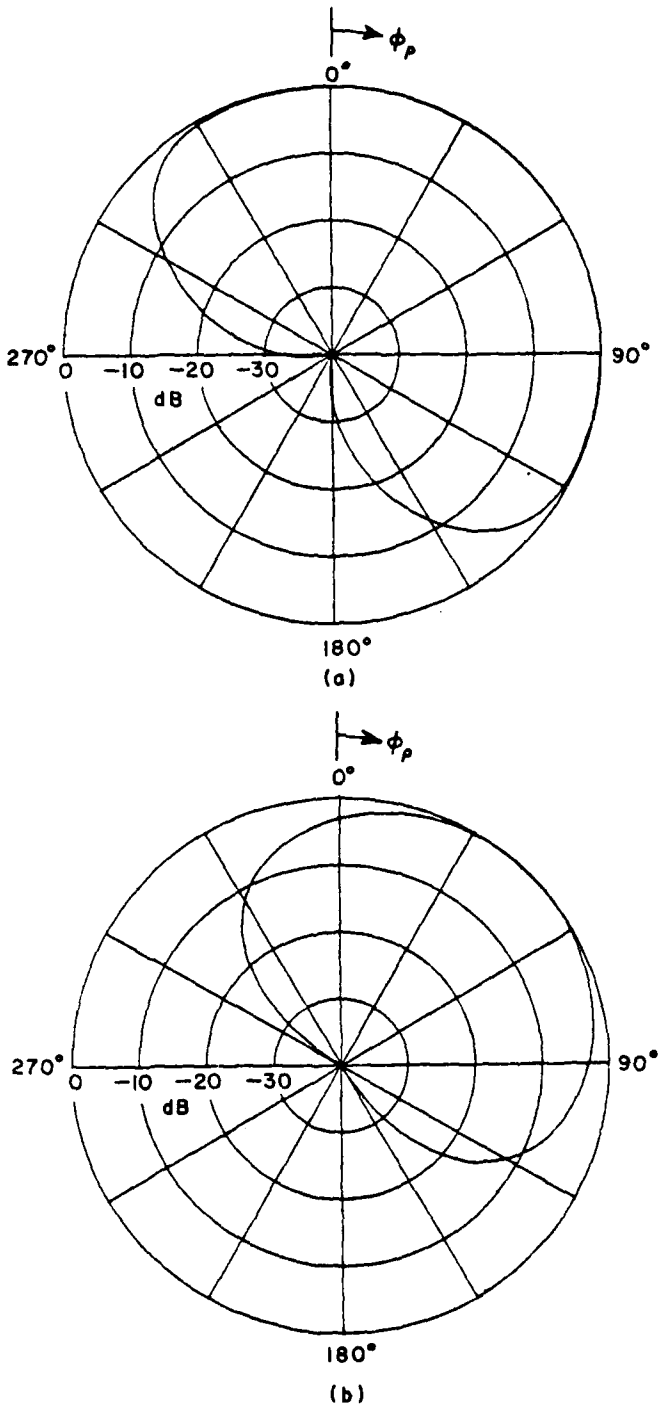

Figure 27. Roll plane pattern of KC-135 with crossed-slot mounted in the forward location. (a) $E_{\phi p}$, (b) $E_{\theta p}$.

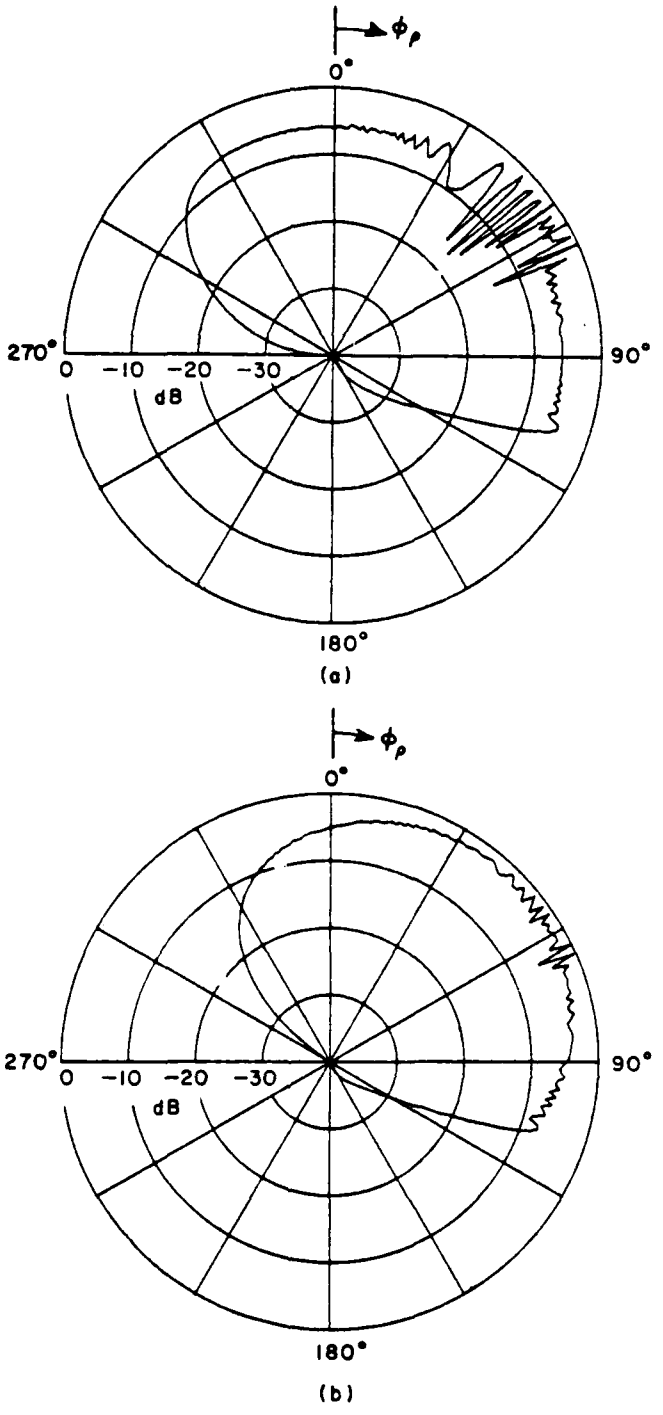

Figure 28. Roll plane pattern of KC-135 with crossed-slot mounted over the wings. (a) $E_{\phi p}$, (b) $E_{\theta p}$.

Example 8:

Consider a monopole mounted on the fuselage of a C-141 aircraft. The computer model of the C-141 is illustrated in Figure 29. The input data is given by:

```
UN: CONVERT TO FEET
2
FG: C-141 AIRCRAFT ROLL PLANE MODEL
7.37,7.37,7.37,7.37
0.,0.,0.
PG: WING
5,T
6.0,7.37,11.0
6.0,78.6,45.44
6.0,78.6,55.26
6.0,30.7,43.
6.0,7.37,41.5
PG: WING
5,T
6.0,-7.37,41.5
6.0,-30.7,43.
6.0,-78.6,55.26
6.0,-78.6,45.44
6.0,-7.37,11.
SG: MONOPOLE
1
0.,18.4
0.,0.5,0.,0.25,3
1.,0.
PD: AZIMUTH CONICAL PATTERN
90.0,0.0,50.0
0,360,1
1000.0,2.52
EX:
```

```
UN: CONVERT TO FEET
2
FG: C-141 AIRCRAFT ELEVATION PLANE MODEL
7.37,27.65,7.37,104.5
0.,0.,0.
PG: VERTICAL STABILIZER
4,T
0.,-104.45,1.93084
24.58,-111.21,1.
24.58,-95.85,0.
11.67,-84.79,0.
PG: VERTICAL STABILIZER
4,T
11.67,-84.79,0.
24.58,-95.85,0.
24.58,-111.21,-1.
0.,-104.45,-1.93084
PG: T-TAIL
4,F
24.58,-111.21,1.
24.58,-116.62,25.3
24.58,-110.45,25.3
24.58,-95.85,0.
PG: T-TAIL
4,F
24.58,-95.85,0.
24.58,-110.45,-25.3
24.58,-116.62,-25.3
24.58,-111.21,-1.
PD: ELEVATION AND THETA CLOSE TO 90 CONICAL PATTERN
90.,0.,70.
0,360,1
1000.,2.52
SG: MONOPOLE
1
-66.,0.
0.2,0.5,0.,0.25,3
1.,0.
DD: DOUBLE TERMS
4
3,3,3,1
3,3,3,4
4,1,4,3
4,1,4,4
EX: EXECUTE PROGRAM
```

The elevation plane model is used to get azimuthal conical patterns (θ_p=60°, 70°, 80°, 90°) and elevation pattern (T-tail effect).
Note that the roll plane model is used to compute the azimuthal conical patterns (θ_p=10°, 20°, 30°, 40°, 50°, 100°, 110°). The radiation patterns are

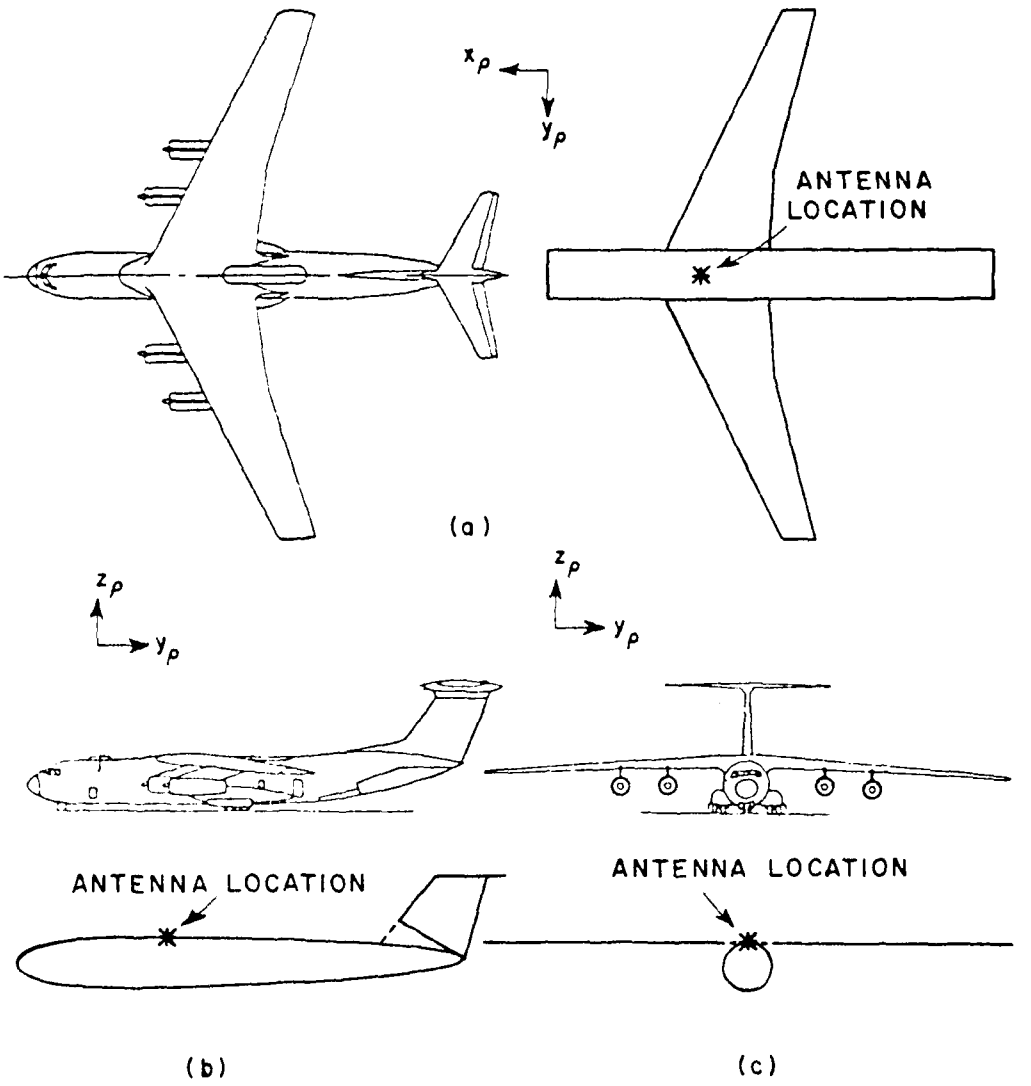

Figure 29. Computer simulated model for the C-141 aircraft. (a) roll plane model, (b) elevation plane model, (c) roll plane model.

compared with measured results made on a $\frac{1}{10}$ scale model of a C-141 at General Dynamics (San Diego, California) in Figures 30, 31, 32 and 33. The T-tail effect on the elevation pattern is illustrated in Figure 34.

Figure 30. Scale model (1/10) of C-141 aircraft at General Dynamics (San Diego, California).

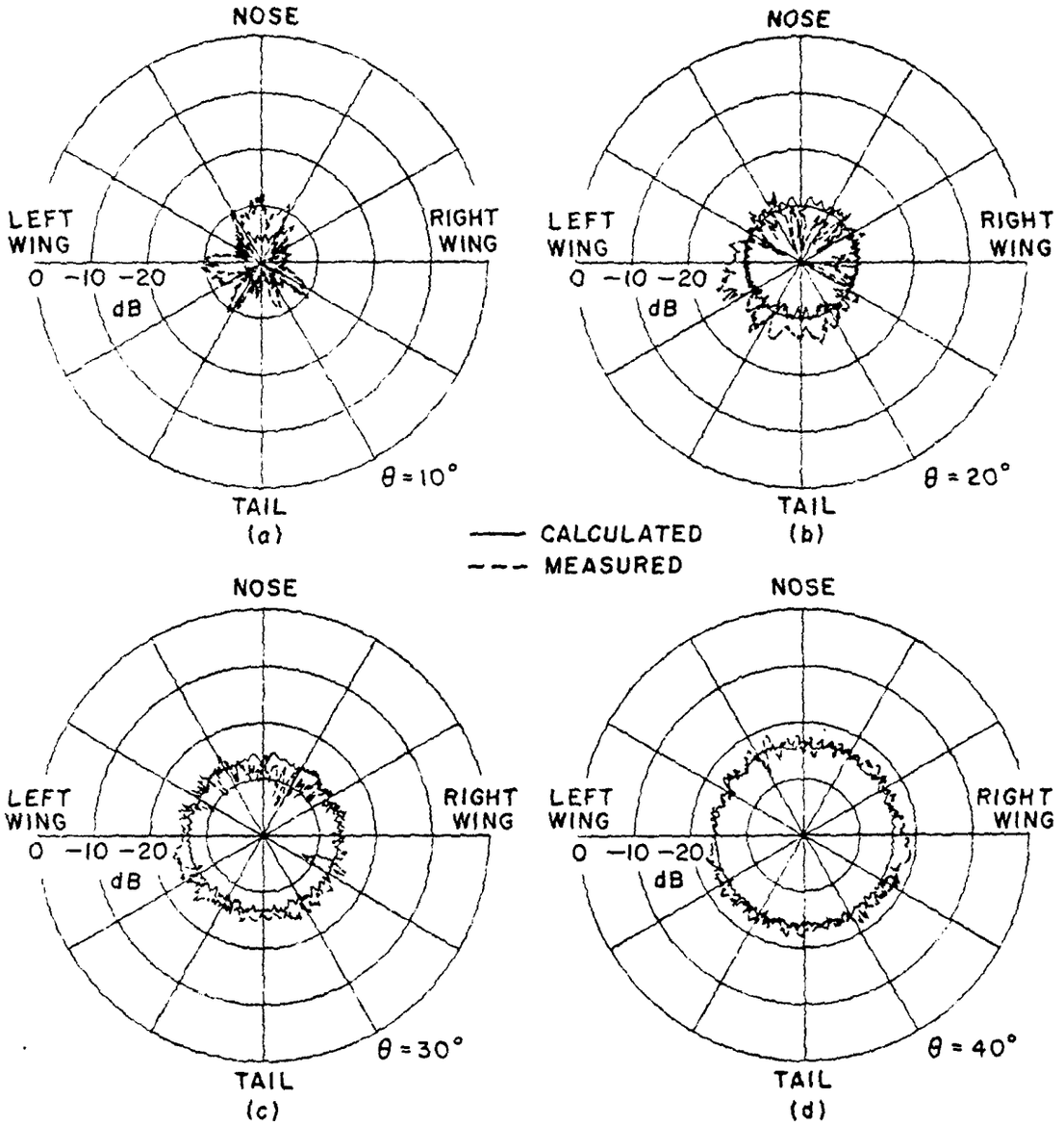

Figure 31. Comparison of measured (dash line) and calculated (solid line) results of azimuthal conical pattern at (a) $\theta_b=10^0$, (b) $\theta_b=20^0$, (c) $\theta_b=30^0$, (d) $\theta_b=40^0$.

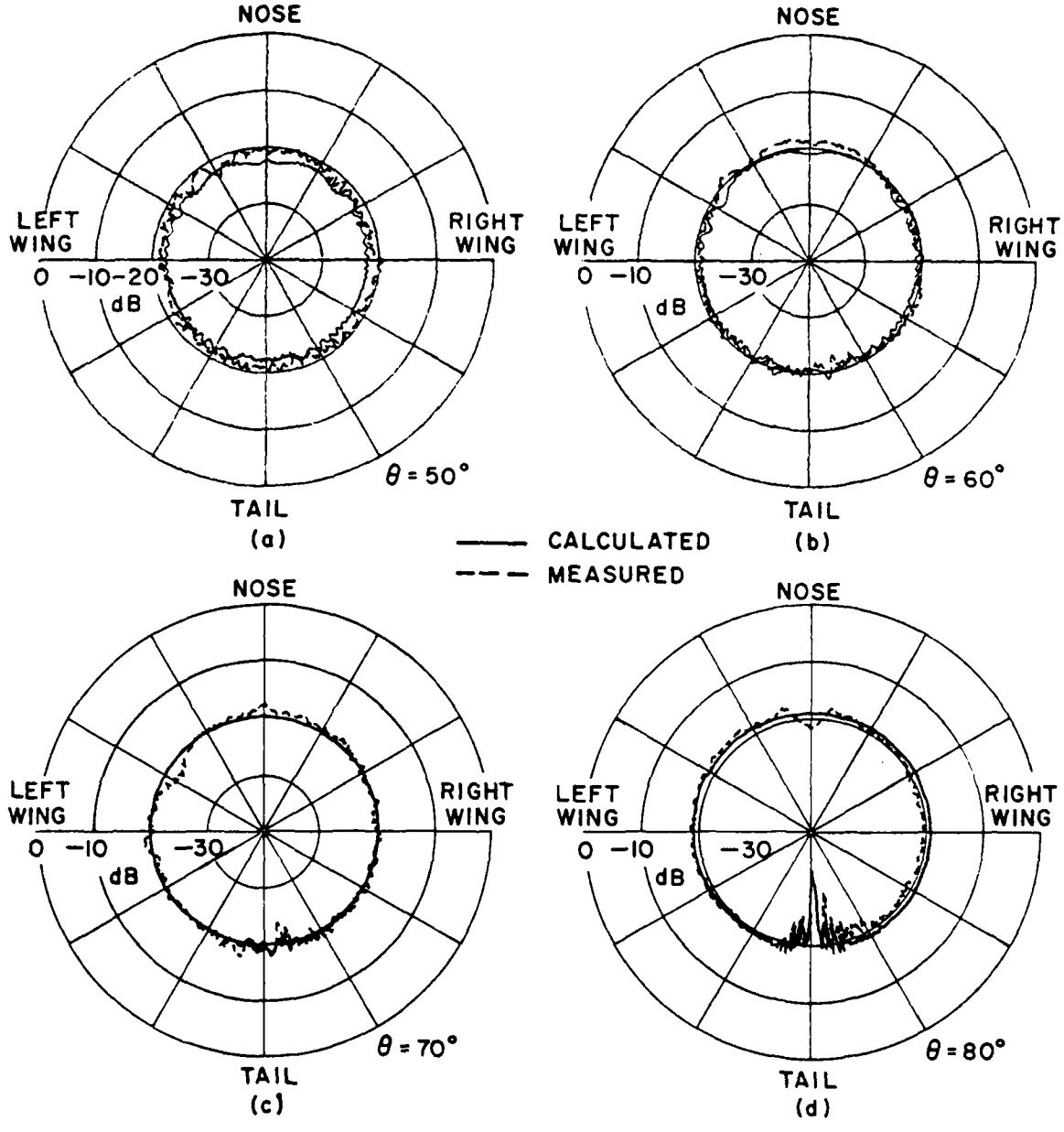

Figure 32. Comparison of measured (dash line) and calculated (solid line) results of azimuthal conical pattern. (a) $\theta_p=50^0$, (b) $\theta_p=60^0$, (c) $\theta_p=70^0$, (d) $\theta_p=80^0$.

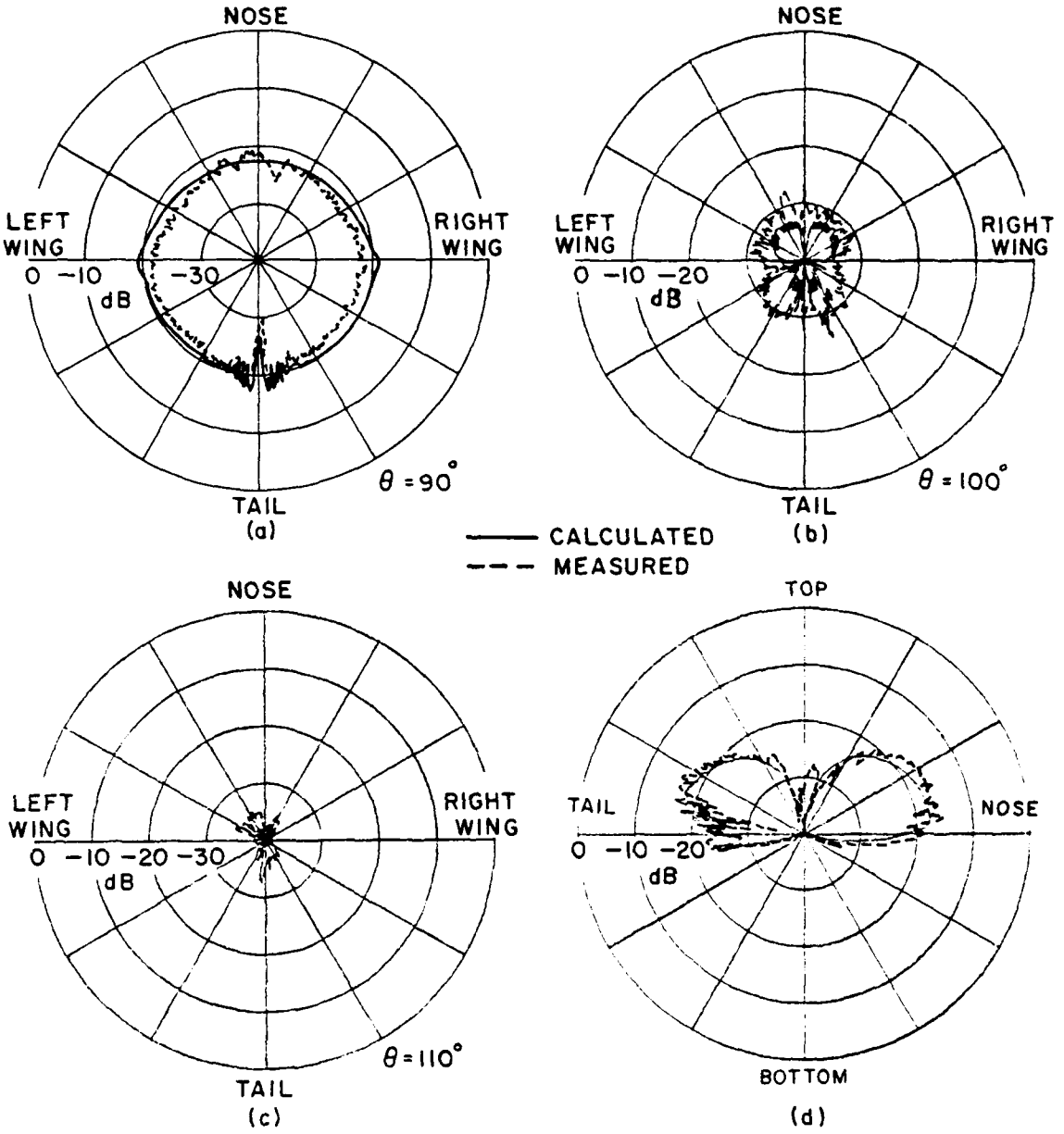

Figure 33. Comparison of measured (dash line) and calculated (solid line) results of azimuthal conical pattern. (a) $\theta_p = 90^0$, (b) $\theta_p = 100^0$, (c) $\theta_p = 110^0$, (d) elevation pattern.

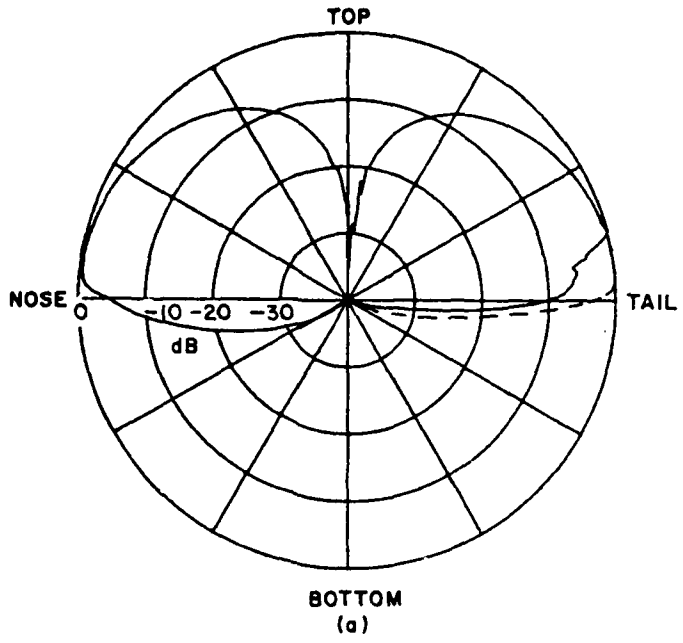

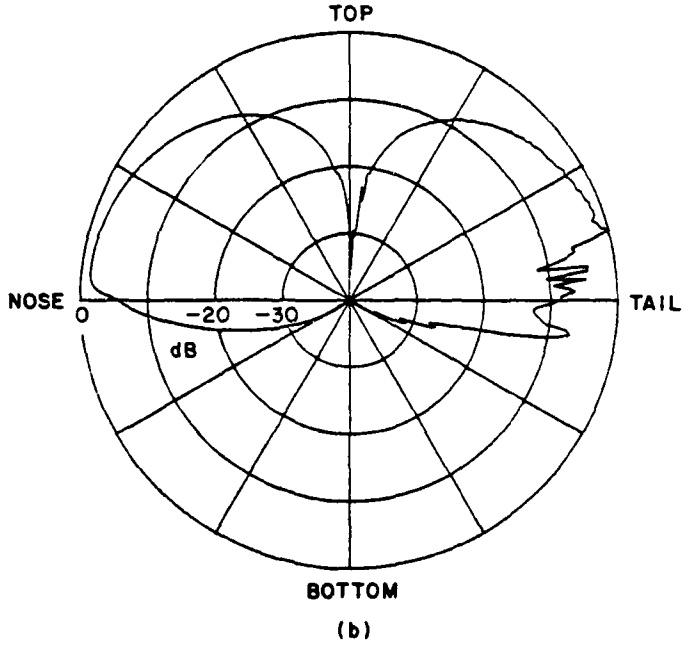

Figure 34. Calculated elevation pattern (a) without T-tail and vertical stabilizer (dash line), without T-tail but with vertical stabilizer (solid line). (b) with T-tail and vertical stabilizer.

Example 9:

Consider a monopole mounted on the bottom fuselage of a F-4 aircraft. The computer model of the F-4 is illustrated in Figure 35. Note that the pattern coordinate system (with subscript p) has been turned upside down on purpose. If the antenna is mounted on the belly of an aircraft, then one needs to turn the aircraft upside down. This is done to insure that one defines the geometry associated with the bottom of the aircraft different from the top, in that most aircraft, especially military aircraft, have a definite shape change from top to bottom. In that the F-4 was turned upside down, there will exist a coordinate system difference between the true aircraft and our model. In fact for the $\theta_p=75^o$ pattern computed here, the actual pattern angle from the vertical is 180^o-75^o or 105^o. With this difference in mind the input data is given by:

```
UN: INCHES F-4 AIRCRAFT
3
TD:
F,F,F
F,T
PD: AZIMUTH CONICAL PATTERN
90.0,0.,75.
0,360,5
5000.,.375
FG: F-4 AIRCRAFT ROLL PLANE MODEL
20.,20.,20.,20.
0.,0.,0.
SG: MONOPOLE
1
0.,0.
.414,.828,0.,.25,3
1.,0.
PG:  ATTACHED PLATE
6,T
19.,-9.,-150.
30.,-13.,-150.
40.,-6.,-150.
40.,6.,-150.
30.,13.,-150.
19.,9.,-150.
PG:  ATTACHED PLATE
6,T
```

```
13.,18.,-344.
13.,230.,-375.
13.,230.,-327.
13.,50.,-138.
13.,50.,-75.
13.,18.,-75.
PG:  ATTACHED PLATE
6,T
13.,-18.,-75.
13.,-50.,-75.
13.,-50.,-138.
13.,-230.,-327.
13.,-230.,-375.
13.,-18.,-344.
PG:  ATTACHED PLATE
4,T
13.,18.,-75.
13.,50.,-75.
-37.,50.,-75.
-37.,18.,-75.
PG:  ATTACHED PLATE
4,T
-37.,-18.,-75.
-37.,-50.,-75.
13.,-50.,-75.
13.,-18.,-75.
PG:
4,F
41.,72.,-91.
15.,72.,-91.
15.,72.,-163.
41.,72.,-163.
PG:
4,F
41.,-72.,-163.
15.,-72.,-163.
15.,-72.,-91.
41.,-72.,-91.
PG:
4,F
51.,127.,-131.
15.,127.,-131.
15.,127.,-356.
51.,127.,-356.
PG:
4,F
51.,-127.,-356.
15.,-127.,-356.
15.,-127.,-131.
51.,-127.,-131.
EX:
```

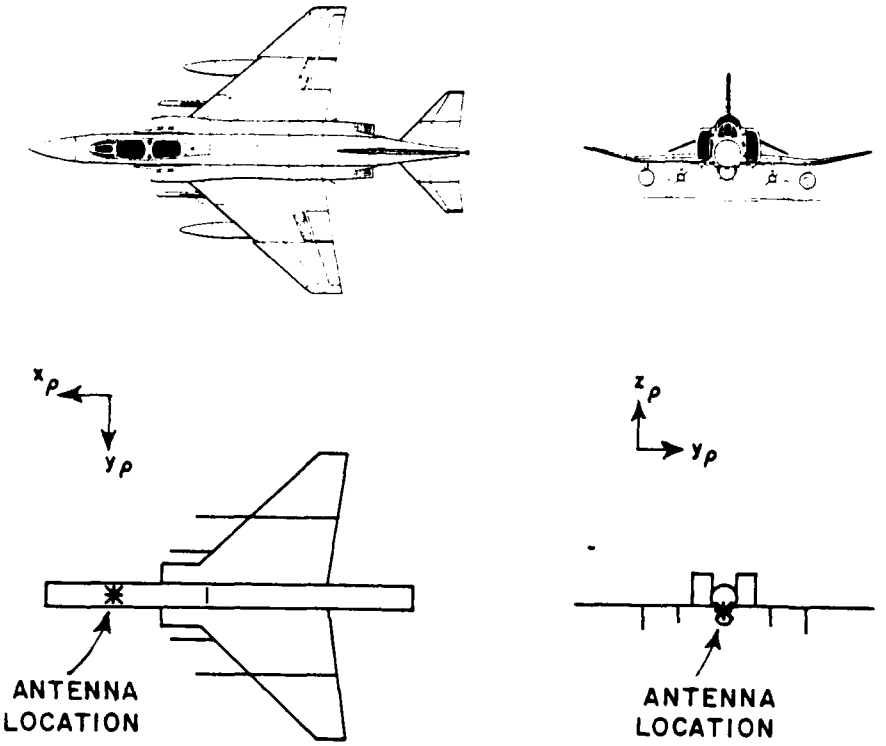

Figure 35. Computer simulated model for the F-4 aircraft (roll plane only).

Figures 36, 37, 38, 39 and 40 indicate the $E_{\theta p}$ pattern contributions associated with different portions of the aircraft structure. One may gain a better feeling for the model through using this kind of process in complex shape pattern computations. The final computed $E_{\theta p}$ pattern is compared with a measured result obtained at the RADC Newport antenna range in Figure 41.

The F-4 is obviously a complex airframe with many structures attached to the basic frame. If an antenna system is to be developed for such an aircraft, the antenna designer needs to know how the various structures associated with the airframe affect the resulting patterns. Simply using measured data this is not always available in that a detailed complete model is usually experimentally examined. However using this code, the antenna designer can examine the effects of various structures as done here for the F-4 and later for the A-10.

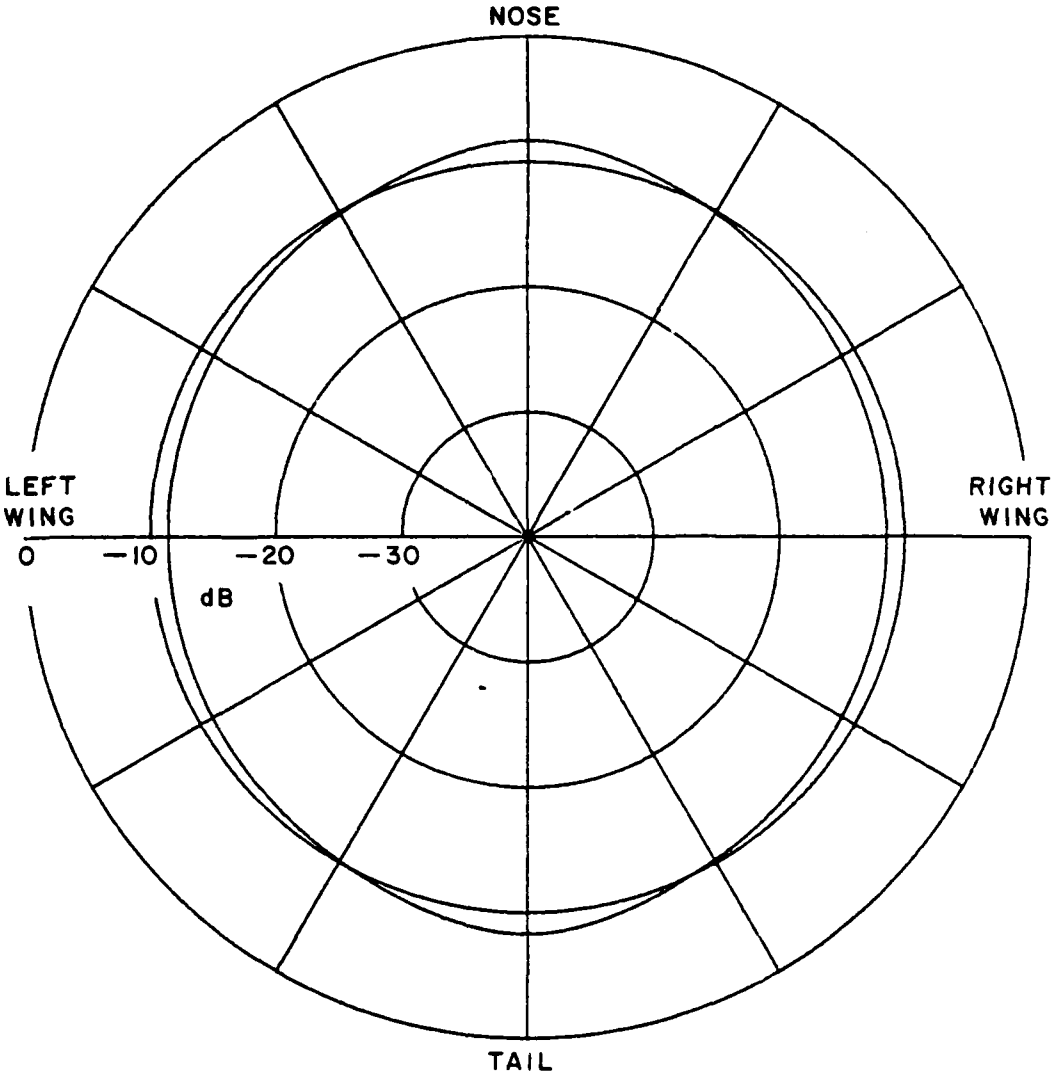

Figure 36. Calculated F-4 azimuthal conical pattern for cylinder only model at $\theta_p = 105^o$ frequency = 375 MHz.

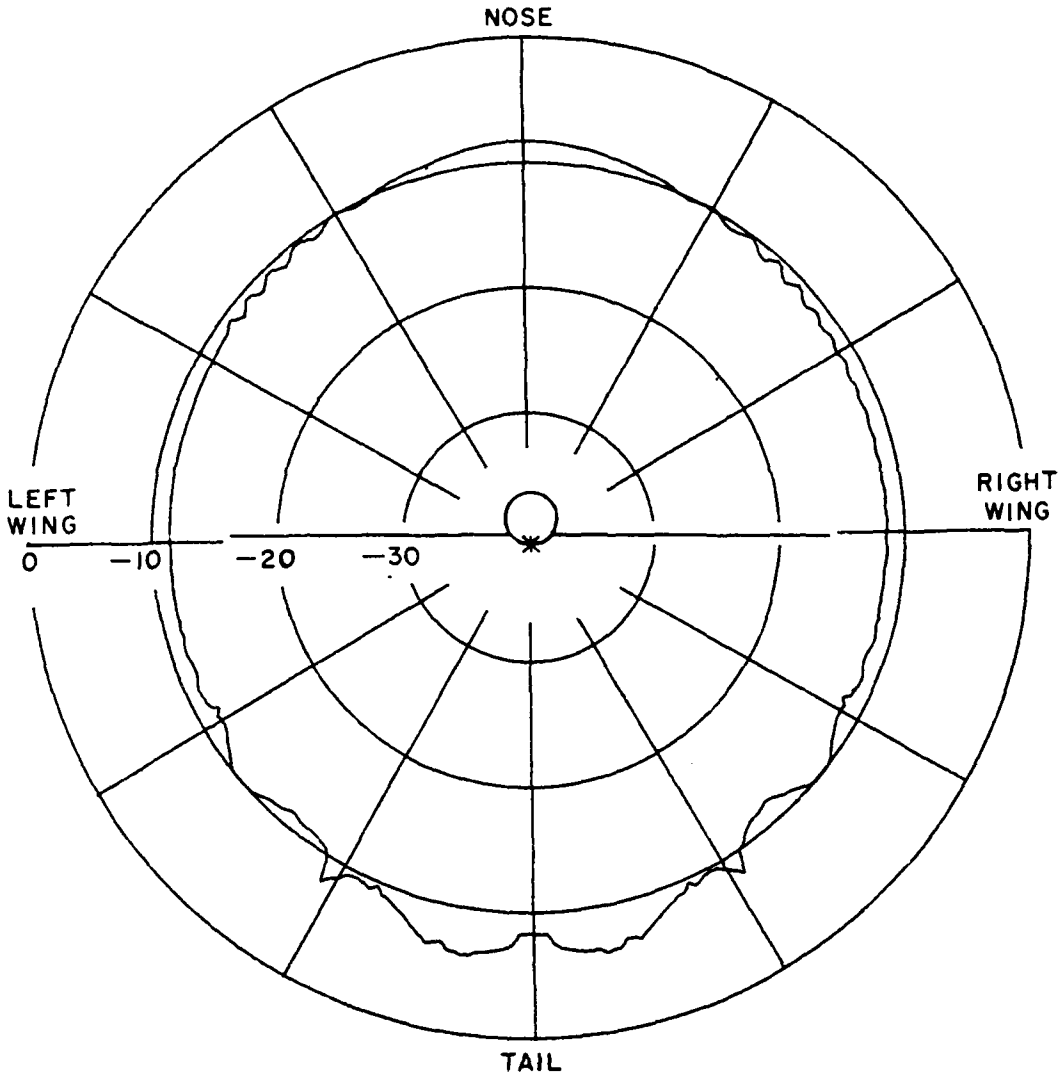

Figure 37. Calculated F-4 azimuthal conical pattern for cylinder and two wings model at $\theta_p = 105^0$, Frequency = 375 MHz.

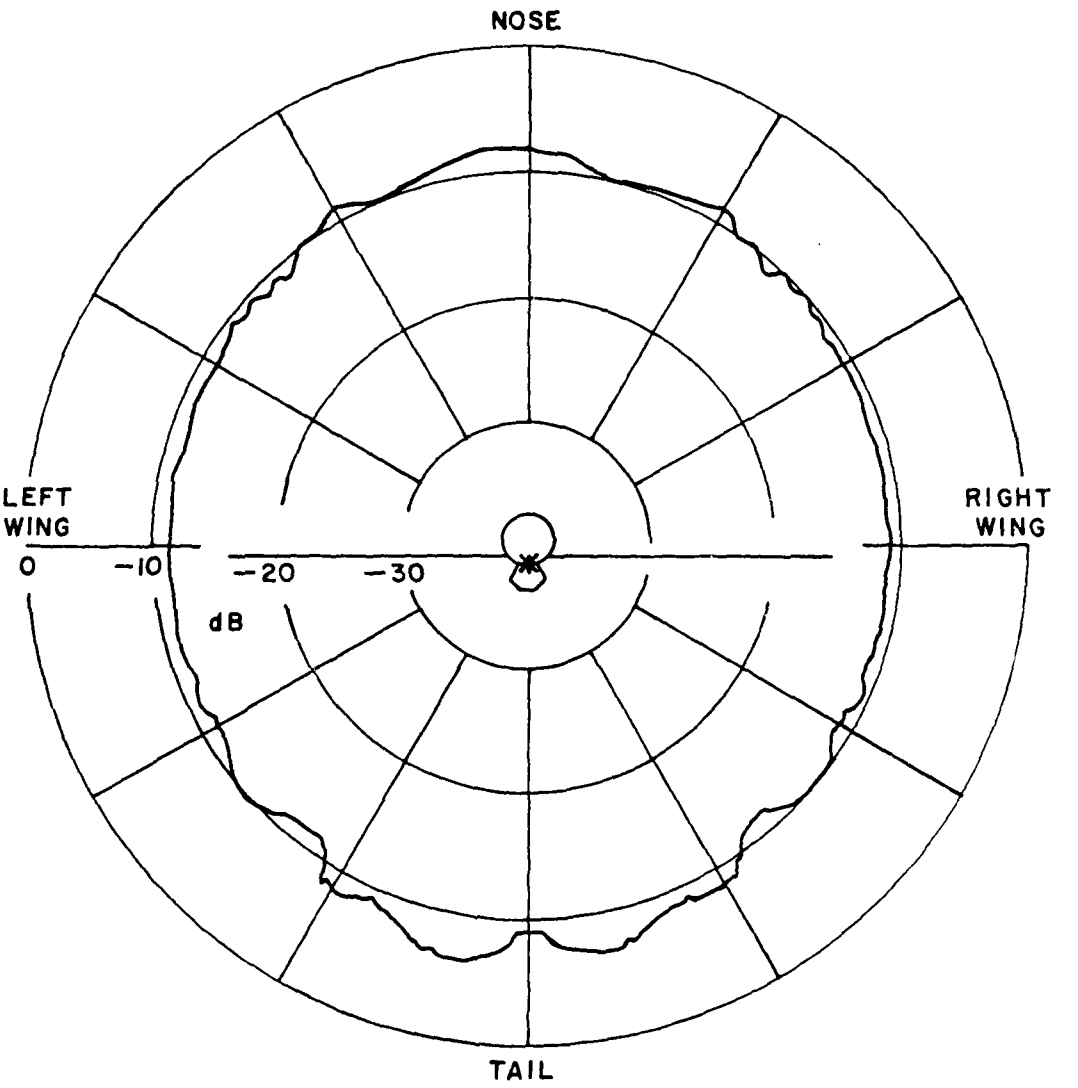

Figure 38. Calculated F-4 azimuthal conical pattern for cylinder, two wings and blockage underneath the fuselage model at $\theta_p = 105^0$, frequency = 375 MHz.

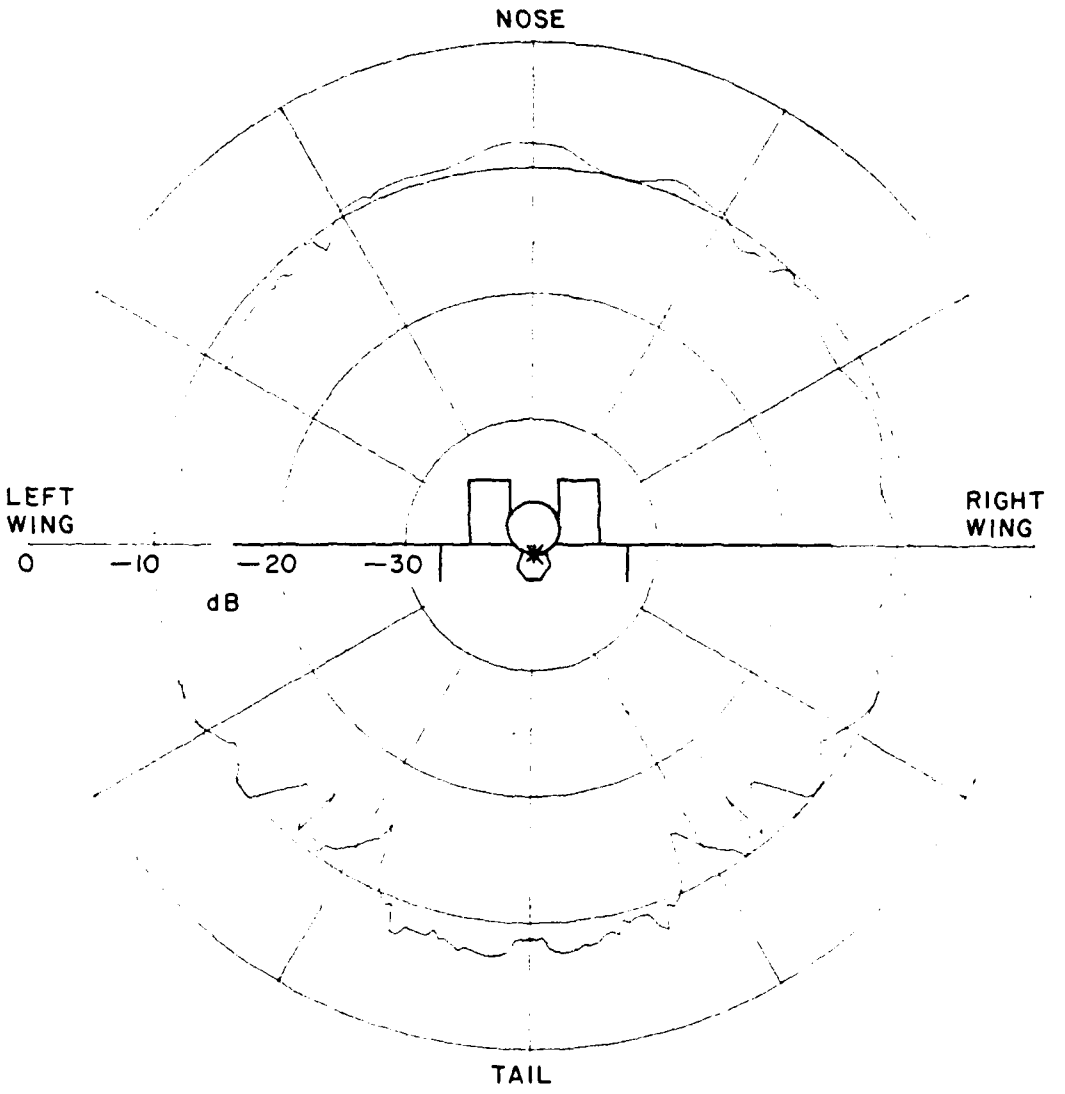

Figure 39. Calculated F-4 azimuthal conical pattern with more structure on cylinder model at $\theta_p = 105^0$, frequency = 375 MHz.

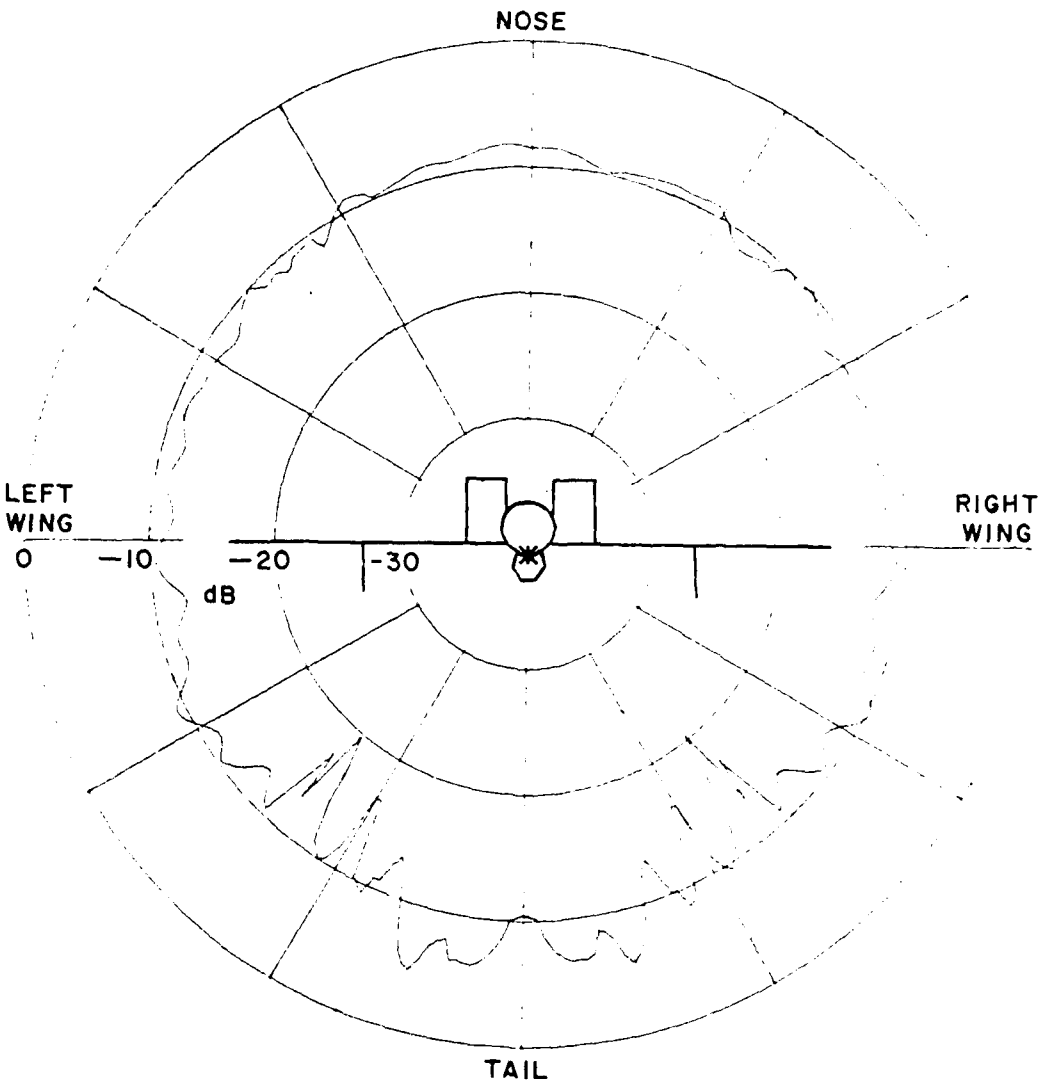

Figure 40. Calculated F-4 azimuthal conical pattern with more structure on cylinder model at $\theta_p = 105^0$, frequency = 375 MHz.

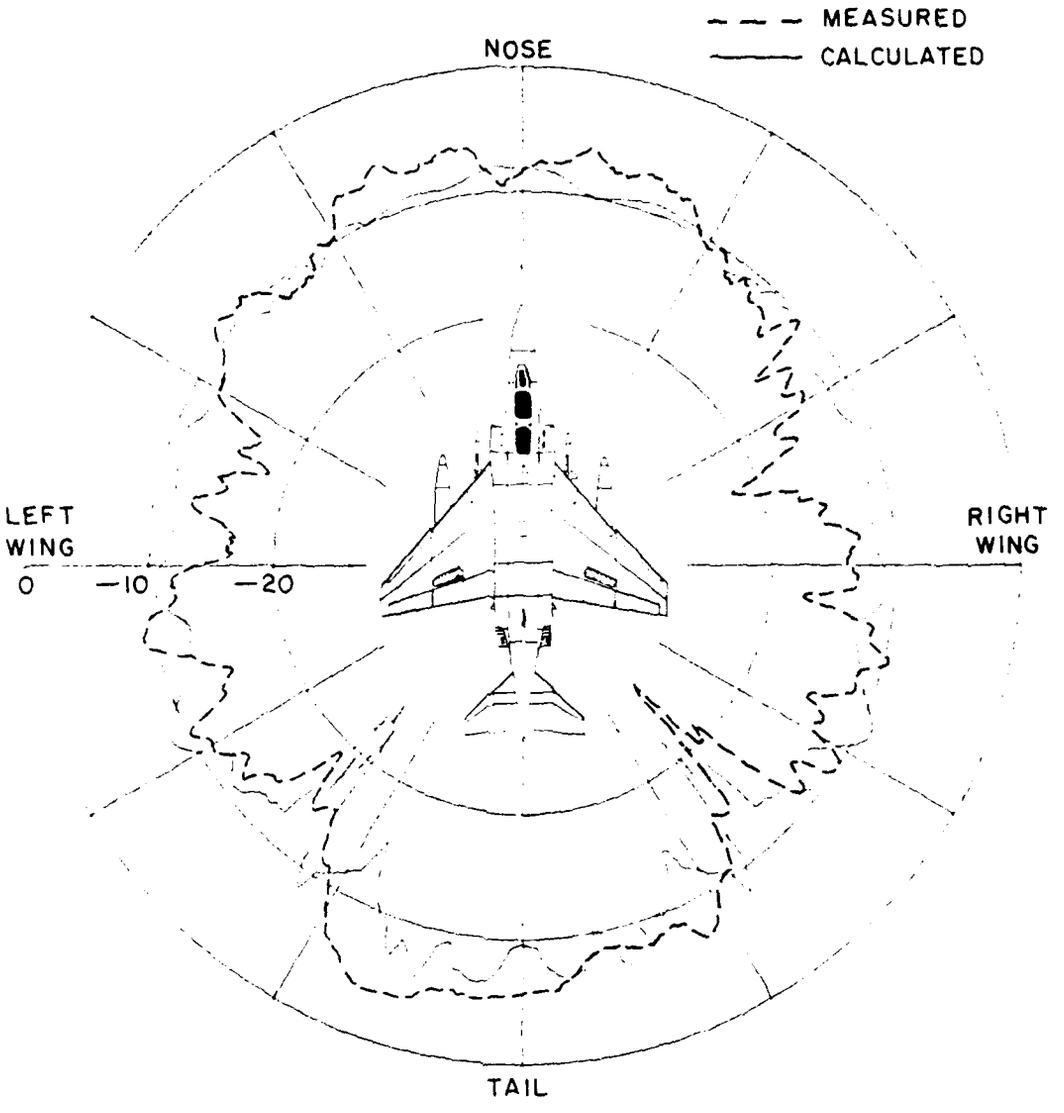

Figure 41. Comparison of measured (dash line) and calculated (solid line) final results of azimuthal conical pattern at $\theta_p = 105^0$, frequency = 375 MHz.

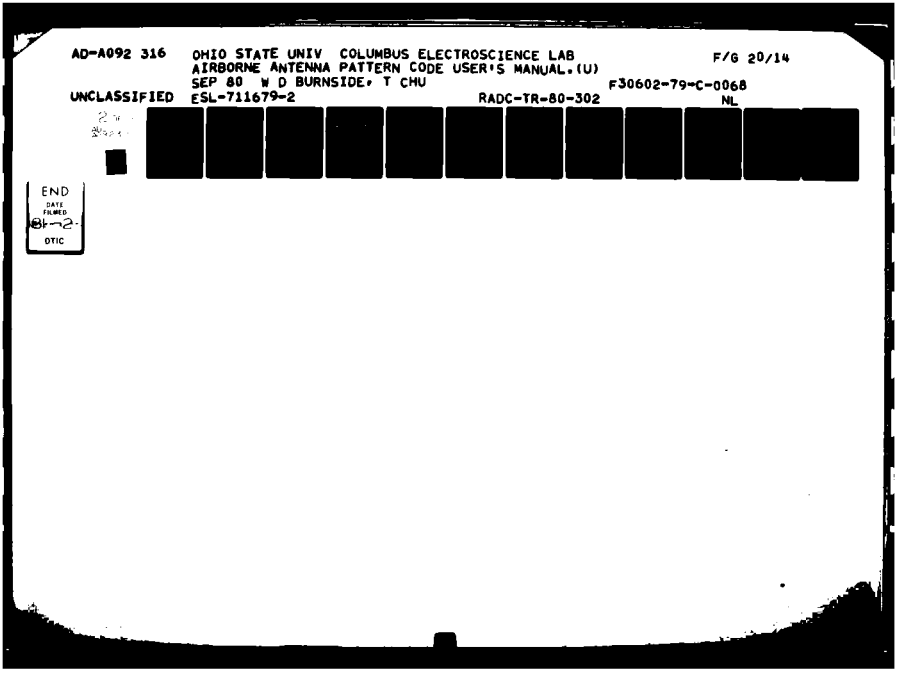
AD-A092 316
OHIO STATE UNIV COLUMBUS ELECTROSCIENCE LAB
AIRBORNE ANTENNA PATTERN CODE USER'S MANUAL.(U)
F/G 20/14
SEP 80 W D BURNSIDE, T CHU
F30602-79-C-0068
UNCLASSIFIED
ESL-711679-2
RADC-TR-80-302
NL
END
DATE FILMED
8-82
DTIC

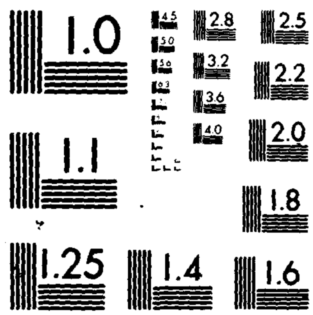

MICROCOPY RESOLUTION TEST CHART
NATIONAL BUREAU OF STANDARDS-1963-A

Example 10:

Consider four monopoles mounted on the belly of an A-10 aircraft. The computer model of the A-10 is illustrated in Figure 42. The input data is given by:

```
TO:
F,F,F
F,T
UN: INCHES A-10 AIRCRAFT
3
PB: AZIMUTH CONICAL PATTERN
90.0,0.0,75.0
0,360,1
6000.0,17.576
PB:  ATTACHED PLATE
4,T
0.0,0.425,-4.62
0.0,1.58,-4.62
0.0,1.58,-2.69
0.0,0.425,-2.69
PB:  ATTACHED PLATE
4,T
0.,-0.425,-2.69
0.,-1.58,-2.69
0.,-1.58,-4.62
0.,-0.425,-4.62
PB:
4,F
0.54,1.58,-4.62
0.54,1.58,-2.69
0.0,1.58,-2.69
0.0,1.58,-4.62
PB:
4,F
0.54,1.58,-4.62
0.54,1.86,-4.62
0.54,1.86,-2.69
0.54,1.58,-2.69
PB:
4,F
0.54,1.86,-2.69
0.54,1.86,-4.62
0.0,1.86,-4.62
0.0,1.86,-2.69
```

```
PG:
4,F
0.0,1.86,-4.62
-0.5,5.6,-4.39
-0.5,5.6,-3.11
0.0,1.86,-2.69
PG:
3,F
0.18,1.715,-2.02
0.0,1.58,-2.69
0.54,1.58,-2.69
PG:
3,F
0.18,1.715,-2.02
0.54,1.58,-2.69
0.54,1.86,-2.69
PG:
3,F
0.18,1.715,-2.02
0.0,1.86,-2.69
0.0,1.58,-2.69
PG:
3,F
0.18,1.715,-2.02
0.54,1.86,-2.69
0.0,1.86,-2.69
PG:
4,F
0.0,1.58,-2.69
0.0,1.86,-2.69
0.0,1.86,-4.62
0.0,1.58,-4.62
PG:
4,F
0.0,-1.58,-4.62
0.0,-1.58,-2.69
0.54,-1.58,-2.69
0.54,-1.58,-4.62
PG:
4,F
0.54,-1.58,-2.69
0.54,-1.86,-2.69
0.54,-1.86,-4.62
0.54,-1.58,-4.62
PG:
4,F
0.0,-1.86,-2.69
0.0,-1.86,-4.62
0.54,-1.86,-4.62
0.54,-1.86,-2.69
```

```
PS:
4,F
0.0,-1.86,-2.69
-0.5,-5.6,-3.11
-0.5,-5.6,-4.39
0.0,-1.86,-4.62
PS:
3,F
0.18,-1.715,-2.02
0.54,-1.58,-2.69
0.0,-1.58,-2.69
PS:
3,F
0.18,-1.715,-2.02
0.54,-1.86,-2.69
0.54,-1.58,-2.69
PS:
3,F
0.18,-1.715,-2.02
0.0,-1.58,-2.69
0.0,-1.86,-2.69
PS:
3,F
0.18,-1.715,-2.02
0.0,-1.86,-2.69
0.54,-1.86,-2.69
PS:
4,F
0.0,-1.58,-4.62
0.0,-1.86,-4.62
0.0,-1.86,-2.69
0.0,-1.58,-2.69
SS: MONOPOLE ARRAY WITH COUPLING EFFECT INCLUDED ON RELATIVE CURRENT VALUE
4
0.0,-0.824
0.0,0.0,0.0,0.25,3
0.272,14.0
0.0,-1.16
0.0,0.0,0.0,0.25,3
1.0,-3.0
73.67,-1.328
0.,0.0,0.0,0.25,3
0.272,14.0
-73.67,-1.328
0.0,0.0,0.0,0.25,3
0.272,14.0
FS: A-10 AIRCRAFT ROLL PLANE MODEL
0.117,0.425,3.07,0.425
0.0,0.0,0.0
EX:
```

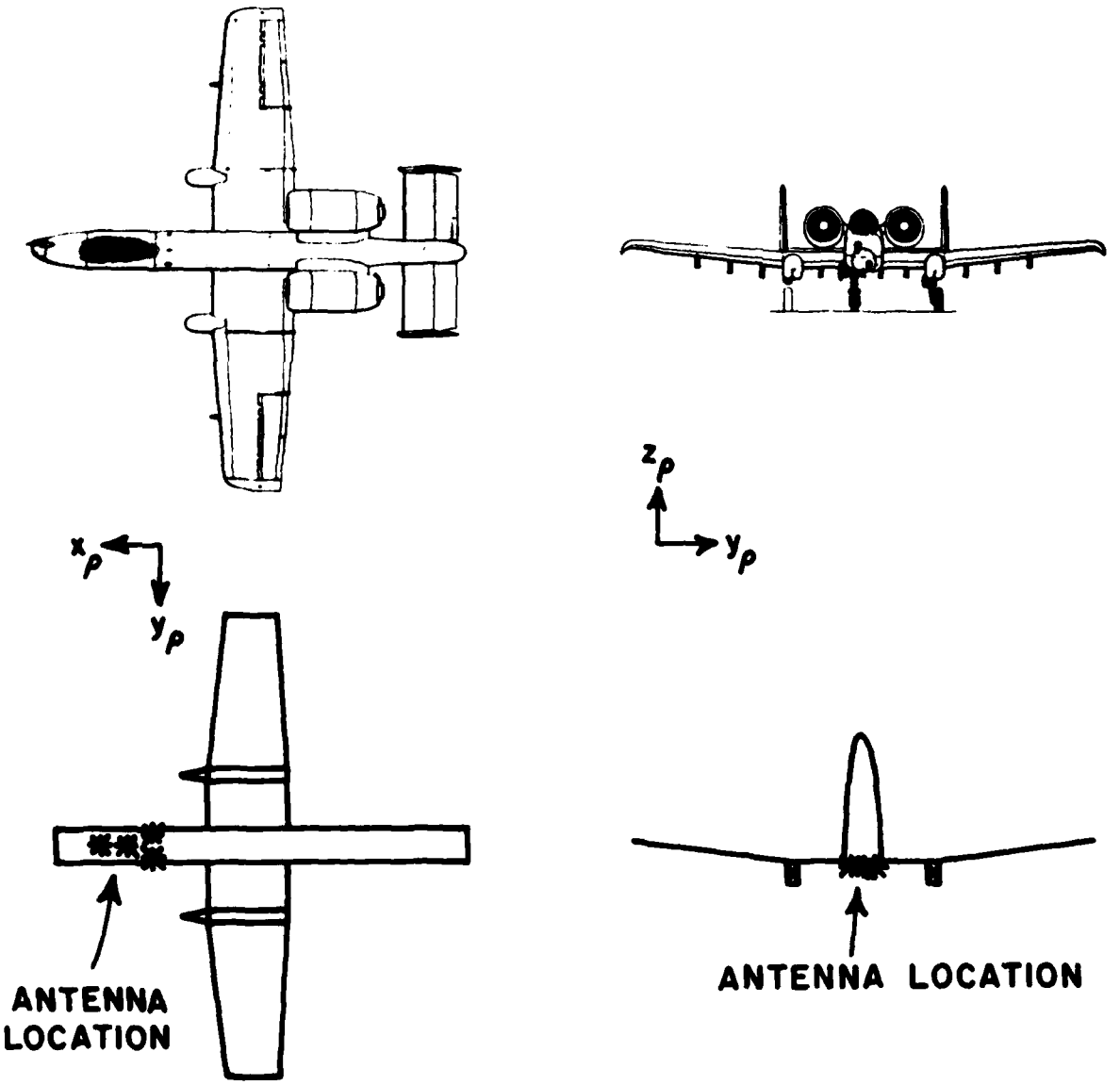

Figure 42. Computer simulated model for the A-10 aircraft (roll plane model only).

Note that four monopoles are spaced a half wavelength apart. Mutual coupling between the antennas is significant for this spacing and cannot be neglected in the pattern computations. This problem can be solved for this geometry using a thin wire moment method code to treat the four closely spaced loaded-dipoles (50 ohms at center of each dipole). The relative current distributions on the four monopoles are approximately the same as dipoles in free space if curvature of the surface where monopoles are mounted is smooth (image theory then holds here for engineering purposes). Figures 43, 44 and 45 indicate the $E_{\theta p}$ pattern contribution from different portions of the aircraft structure. The final computed $E_{\theta p}$ pattern is compared with a measured result obtained at the RADC Newport site in Figure 46.

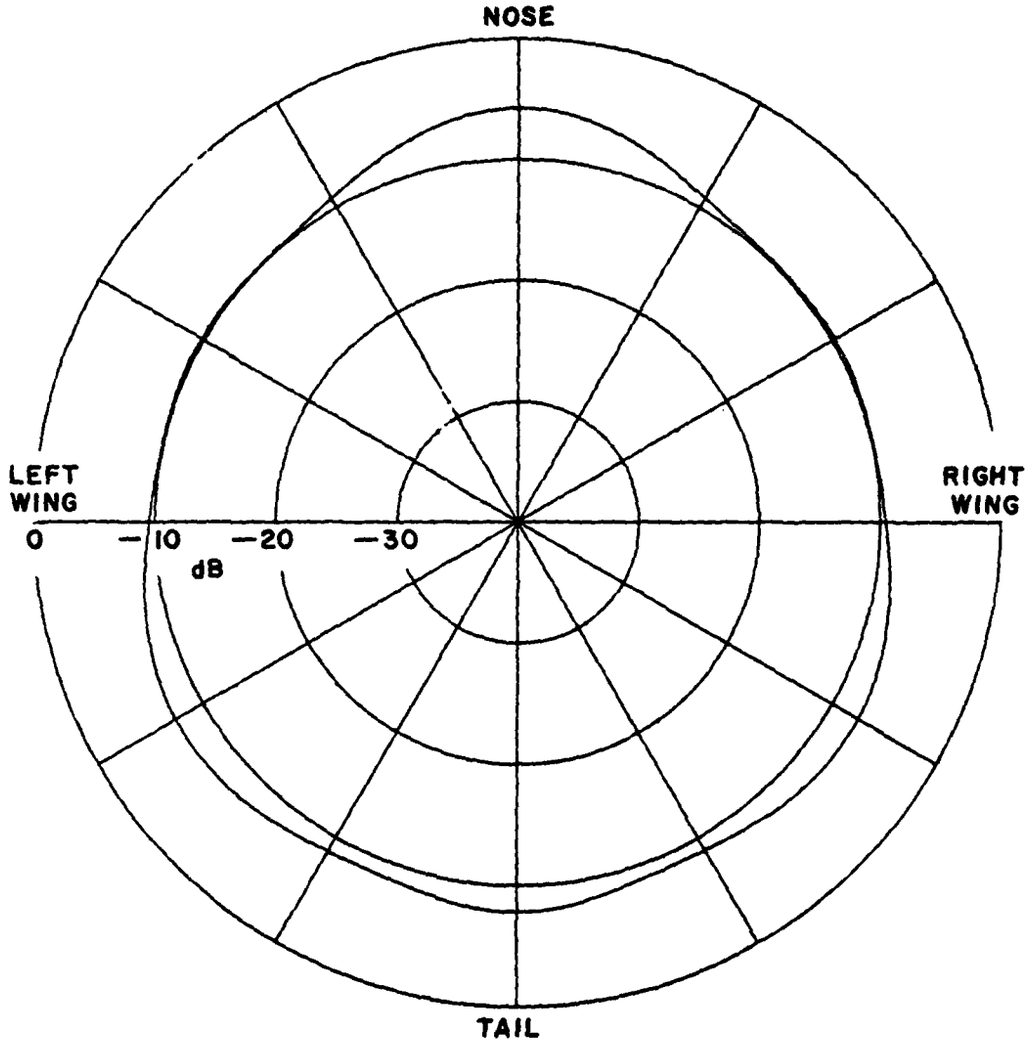

Figure 43. Calculated A-10 azimuthal conical pattern for cylinder only model at θ_p=105°, frequency = 300 MHz.

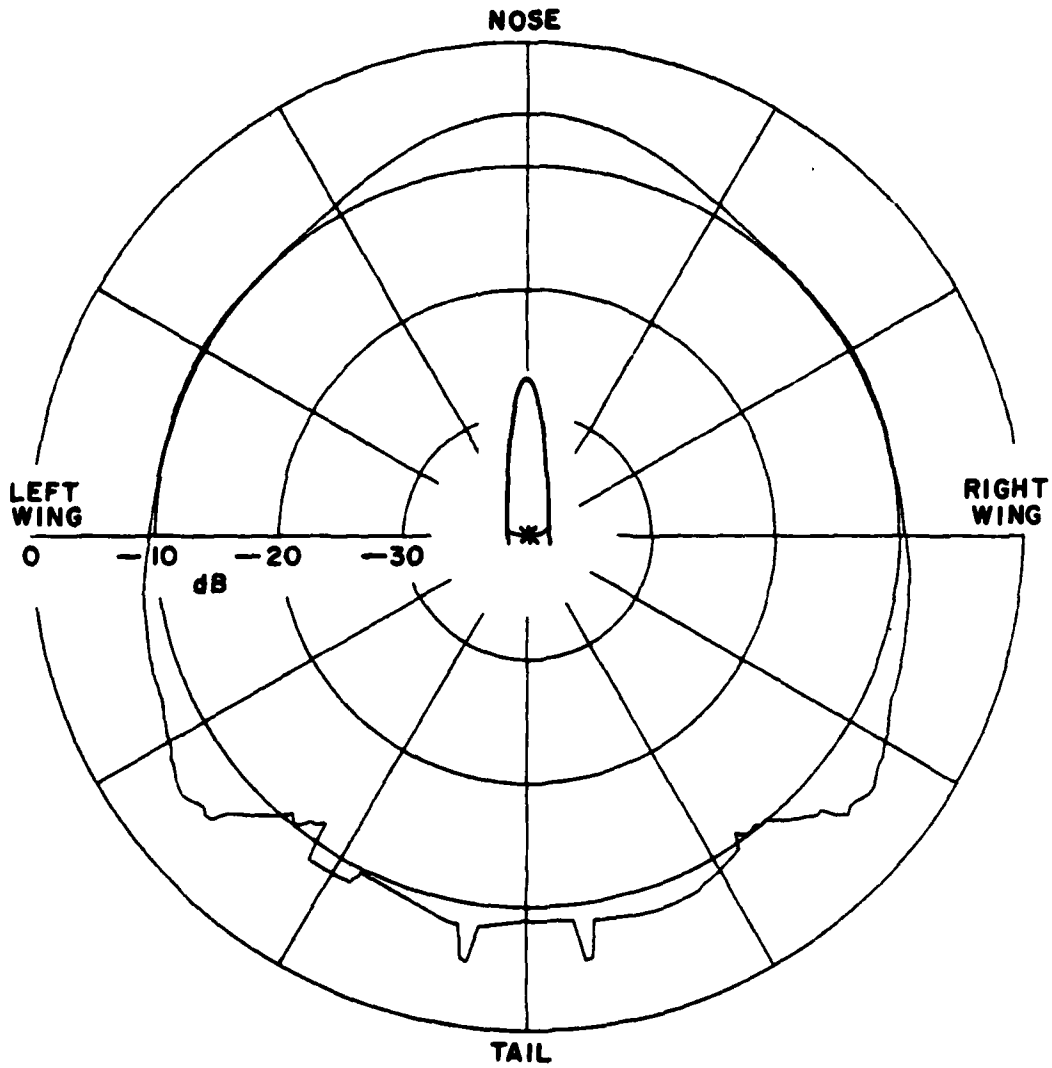

Figure 44. Calculated A-10 azimuthal conical pattern for cylinder and two flat plates model at $\theta_p = 105^0$, frequency = 300 MHz.

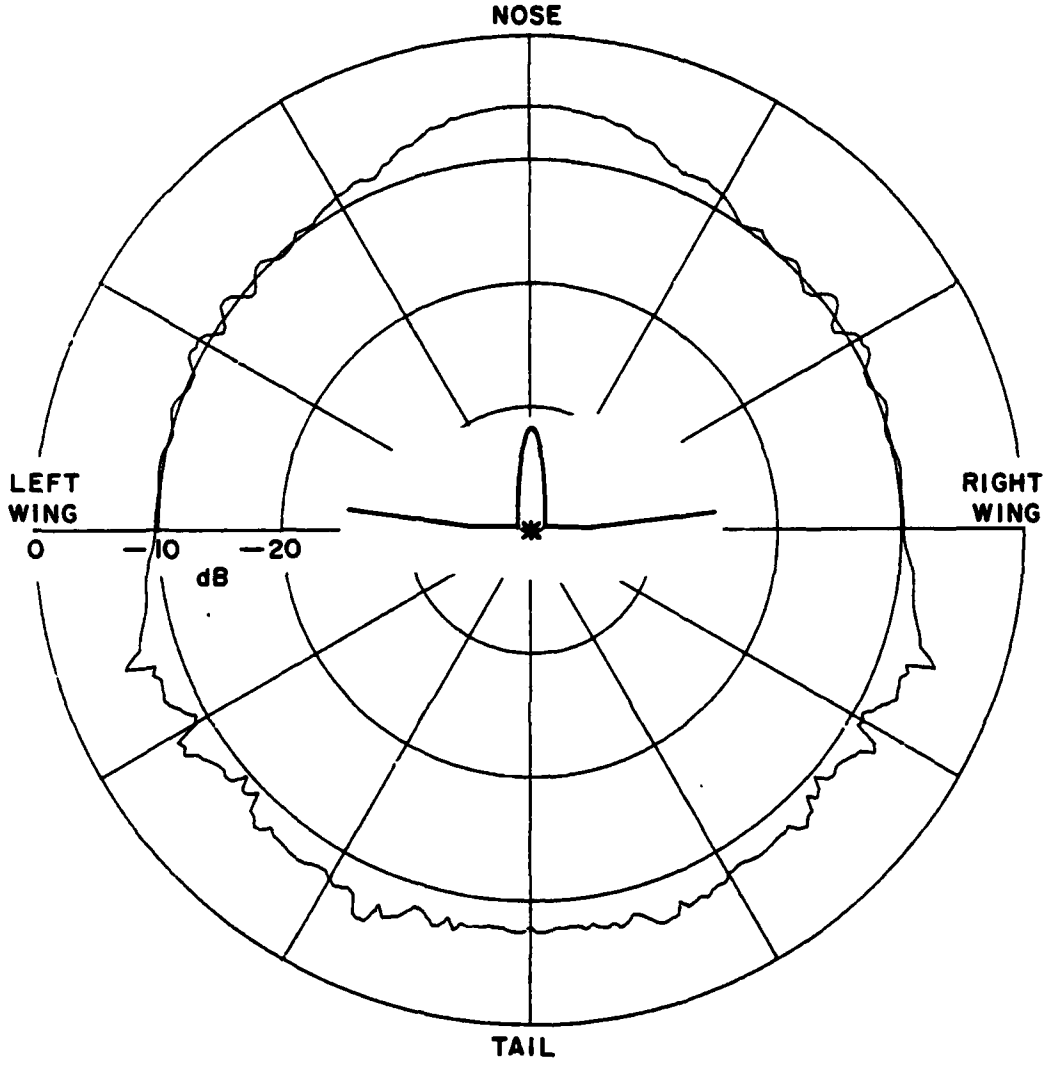

Figure 45. Calculated A-10 azimuthal conical pattern for cylinder and two wings model at $\theta_p=105^0$, frequency = 300 MHz.

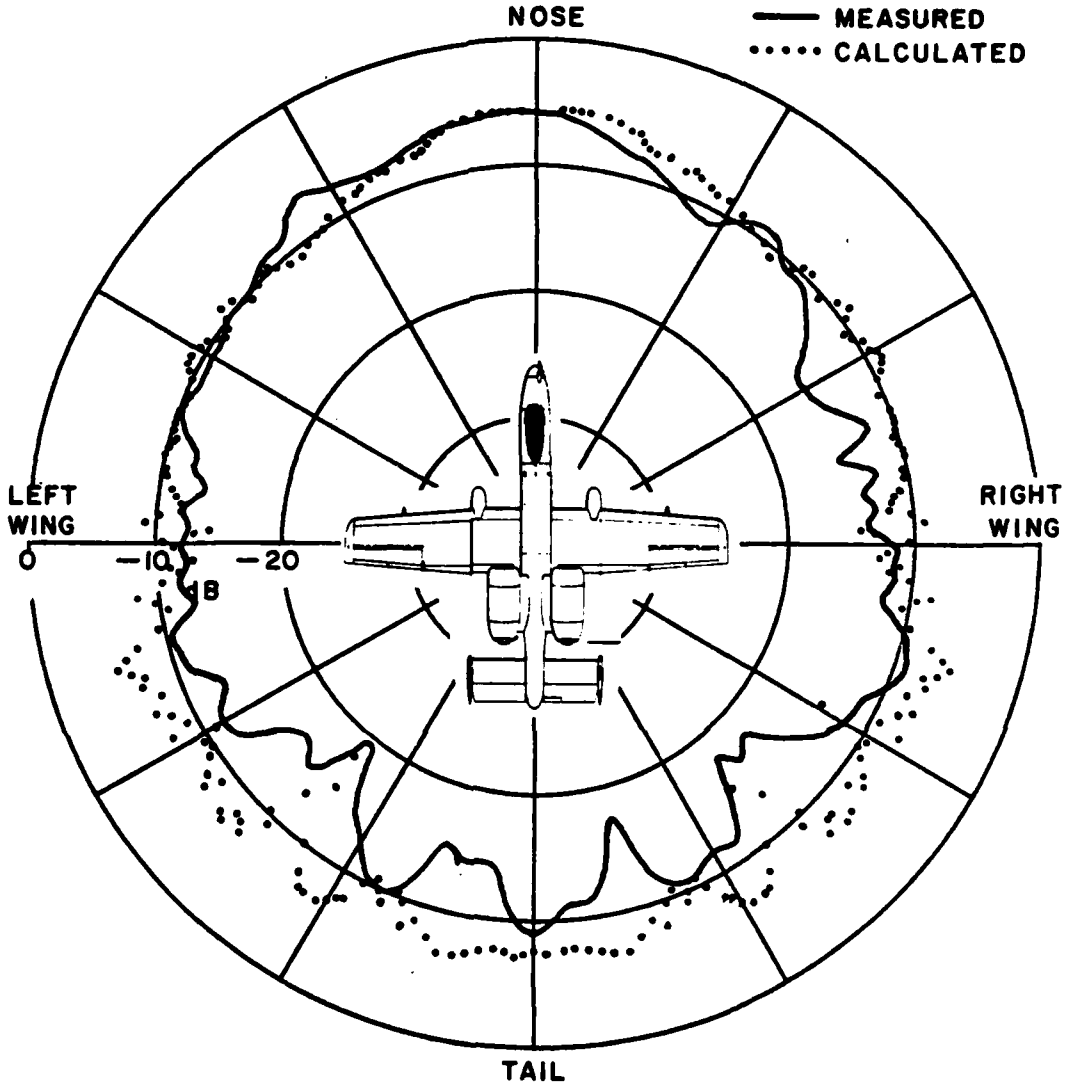

Figure 46. Comparison of measured (solid line) and calculated (dotted line) final results of azimuthal conical pattern at $\theta_p = 105^0$, frequency = 300 MHz.

REFERENCES

1. R. G. Kouyoumjian and P. H. Pathak, "A Uniform Geometrical Theory of Diffraction for an Edge in a Perfectly-Conducting Surface," Proc. IEEE, Vol. 62, November 1974, pp. 1448-1461.

2. R. G. Kouyoumjian, "The Geometrical Theory of Diffraction and Its Applications," Numerical and Asymptotic Techniques in Electromagnetics, edited by R. Mittra, Spring-Verlag, New York, 1975.

3. W. D. Burnside, M. C. Gilreath, R. J. Marhefka, and C. L. Yu, "A Study of KC-135 Aircraft Antenna Patterns," IEEE Trans. on Antennas and Propagation, Vol. AP-23, No. 3, May 1975, pp. 309-316.

4. R. J. Marhefka, "Analysis of Aircraft Wing-Mounted Antenna Patterns," Report 2902-25, June 1976, The Ohio State University ElectroScience Laboratory, Department of Electrical Engineering; prepared under Grant No. NGL 36-008-138 for National Aeronautics and Space Administration.

5. W. D. Burnside, N. Wang and E. L. Pelton, "Near Field Pattern Computations for Airborne Antennas," Report 784685-4, June 1978, The Ohio State University ElectroScience Laboratory, Department of Electrical Engineering; prepared under Contract N00019-77-C-0299 for Naval Air Systems Command. (AD/A057244)

6. W. D. Burnside, E. L. Pelton, N. Wang, "Analysis of Aircraft Simulations Using an Elliptic Cylinder and Multiple Plate," Report 711305-1, April 1979, The Ohio State University ElectroScience Laboratory, Department of Electrical Engineering; prepared under Contract N00019-78-C-0524 for Naval Air Systems Command.

7. W. D. Burnside, R. G. Kouyoumjian, R. J. Marhefka, R. C. Rudduck, and C. H. Walter, "Asymptotic High Frequency Techniques for UHF and Above Antennas," Annual Report 4508-6, August 1977, The Ohio State University ElectroScience Laboratory, Department of Electrical Engineering; prepared under Contract N000123-76-C-1371 for Naval Regional Procurement Office.

8. W. D. Burnside, "User's Manual Flat Plate Program," Report 4508-4, May 1977, The Ohio State University ElectroScience Laboratory, Department of Electrical Engineering; prepared under Contract N00123-76-C-1371 for Naval Regional Procurement Office, Long Beach, California.

9. R. J. Marhefka, "User's Manual for Plates and Cylinder Computer Code," Report 4508-8, March 1978, The Ohio State University Electro-Science Laboratory, Department of Electrical Engineering; prepared under Contract N00123-76-C-1371 for Naval Regional Procurement Office, Long Beach, California.

10. J. H. Richmond, "Radiation and Scattering by Thin-wire Structures in the Complex Frequency Domain," Report 2902-10, July 1973, The Ohio State University ElectroScience Laboratory, Department of Electrical Engineering; prepared under Grant No. NGL 36-008-138 for National Aeronautics and Space Administration.

MISSION
of
Rome Air Development Center

RADC plans and executes research, development, test and selected acquisition programs in support of Command, Control Communications and Intelligence (C^3I) activities. Technical and engineering support within areas of technical competence is provided to ESD Program Offices (POs) and other ESD elements. The principal technical mission areas are communications, electromagnetic guidance and control, surveillance of ground and aerospace objects, intelligence data collection and handling, information system technology, ionospheric propagation, solid state sciences, microwave physics and electronic reliability, maintainability and compatibility.

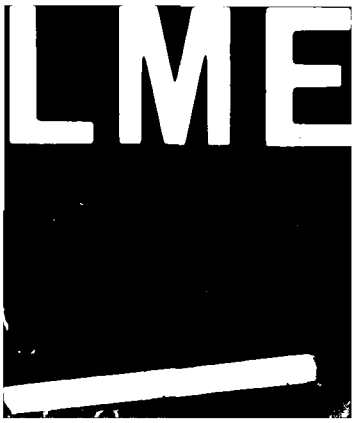
LME